DYNAMIC CUTBACK OPTIMIZATION

A Thesis
Presented to
The Academic Faculty

by

Shankar Jayaraman

In Partial Fulfillment
of the Requirements for the Degree
Master of Science in the
School of Aerospace Engineering

Georgia Institute of Technology
May 2010

DYNAMIC CUTBACK OPTIMIZATION

Approved by:

Dr. Dimitri Mavris, Advisor
Professor
School of Aerospace Engineering
Georgia Institute of Technology

Dr. Jimmy C. M. Tai
Senior Research Engineer
Aerospace Systems Design Lab
School of Aerospace Engineering
Georgia Institute of Technology

Dr. Muni Majjigi
Consulting Engineer, Acoustics
GE Aviation

Dr. Michelle Kirby
Senior Research Engineer
Aerospace Systems Design Lab
School of Aerospace Engineering
Georgia Institute of Technology

Date Approved: 26 March 2010

ACKNOWLEDGEMENTS

There are many people to whom I owe a lot in the completion of this work. Firstly, I would like to thank my research advisors, Dr. Dimitri Mavris and Dr. Jimmy Tai for giving me this unique opportunity to pursue my Masters thesis via Distance Learning from GE Bangalore, and for providing valuable advice - both technical and process-related - during review meetings held via teleconference. Special thanks to my advisor at GE Aviation, Dr. Muni Majjigi, for helping me formulate the thesis objectives, explaining the impact of this work, and for all the guidance provided throughout the execution of this project. Thanks to Dr. Peter Hollingsworth, earlier at ASDL, Georgia Tech, and Dr. Vivek Sanghi, formerly at GE Aviation, for their guidance during the initial stages of this project. Thank you to Dr. Michelle Kirby for reviewing this thesis writeup.

A big thank you to the Acoustics experts - Greg Szczepkowski, Egbert Geertsema, Mike Martinez, Sreeni Vasulu, and Jose Mathew, for patiently explaining the fundamentals behind noise certification, and for providing great feedback during our weekly and bi-weekly meetings. Without all your help and support, none of this would have been possible. Thanks also to Gaurishanker Soni and Vivek for helping me understand the Acoustic models and for the swift help in troubleshooting any problems I faced.

I would like to thank Jim Geiger for his help and advice in building the takeoff simulation model required for this thesis, and for the great insights he has given me in the field of aircraft performance. Many thanks to my technical leader, Sridhar Pakanati, for guiding me throughout the execution of this effort, and for reviewing the progress of my work on a weekly basis.

Thanks to Vinay Ramanath in helping me select this as my thesis topic, and for the advice and recommendations involving the optimization-related aspects of this work. Thanks to Shamik Chaudhuri, for help in understanding and enhancing the takeoff simulation model,

and to Jorge de Luis, for reviewing the thesis proposal and providing useful pieces of advice. To Randy Cepress, thank you for your sharp questioning and constructive feedback in several review meetings. Thanks also to you and Ron Plybon for agreeing to fund this effort at GE. Thanks to my former manager, Kalyan and present manager, Sasikumar, for their complete support and co-operation, and allowing me to work on the thesis writeup in office. I would also like to thank Phil Viars and Rick Wallace for their useful feedback during review meetings.

Last, but certainly not least, a huge thanks to my family and friends for their patience, understanding, and tons of support from beginning to end.

TABLE OF CONTENTS

LIST OF TABLES

LIST OF FIGURES

NOMENCLATURE

$C(k)$	Tone correction factor
C_L	Lift coefficient
C_{D0}	Drag coefficient at zero lift
C_{L0}	Lift coefficient at zero angle of attack
D	Duration correction factor
D	Total aircraft drag
$Grad_{AEO}$	All-engines-operating climb gradient
$Grad_{OEI}$	One-engine-inoperative climb gradient
L	Total aircraft lift
N	Number of engines
P	Sound power
$PNL(k)$	Instantaneous perceived noise level
$PNLT(k)$	Tone-corrected perceived noise level
$PNLT_M$	Maximum tone-corrected perceived noise level
P_{ref}	Reference sound power
S	Total wing surface area
T	Net thrust
T	Time duration
V	True air speed
V_0	Zero velocity at start of takeoff roll
V_2	Takeoff safety speed
V_3	All-engines screen speed
V_R	Rotation speed
V_x	Component of true air speed along X axis
V_y	Component of true air speed along Y axis
V_{CLIMB}	Climb speed

V_{LOF}	Liftoff speed
W	Aircraft weight
α	Angle of attack
γ	Flight path angle
μ	Coefficient of friction
ϕ_G	Runway slope angle
ϕ_T	Thrust incidence angle
ρ	Air density
d	Time interval
g	Acceleration due to gravity
h	Altitude
$p(d)$	Probability of defect
Δt	Time increment for PNLT calculation

Abbreviations

AEDT	Aviation Environmental Design Tool
AEO	All-engines operating
ANOPP	Aircraft Noise Prediction Program
BPR	Bypass ratio
DOE	Design of Experiments
EDS	Environmental Design Space
EPNL	Effective Perceived Noise Level, EPNdB
FAA	Federal Aviation Administration
FAR	Federal Aviation Regulations
FLOPS	Flight Optimization System
FPA	Flight path angle
GE	General Electric
ICAO	International Civil Aviation Organization
ISA	International Standard Atmosphere

JAR	Joint Aviation Requirements
MDO	Multi-disciplinary optimization
NADP	Noise Abatement Departure Profile
NASA	National Aeronautics and Space Administration
OEI	One engine inoperative
PNL	Perceived noise level, PNdB
PNLT	Tone-corrected Perceived Noise Level, PNLTdB
PREDATER	Preliminary Robust Engine Design Analysis Tool for Evaluating Return
RPM	Revolutions per minute
SPL	Sound pressure level, dB

SUMMARY

Dynamic Cutback is a takeoff noise optimization procedure to minimize noise at the flyover certification point wherein engine thrust is reduced at a pre-determined altitude from the full power takeoff rating to a "cutback" rating. Simplified methods for flyover EPNL prediction used by propulsion designers assume instantaneous thrust reduction and do not take into account the spooling down of the engine during the cutback procedure. This research effort evaluates additional noise benefit that can be gained by modeling the engine spool down behavior.

Another important aspect of the research work is the determination of the optimal conditions for minimum flyover EPNL. An optimization framework is developed that incorporates a takeoff simulation model, a cycle model, and an acoustics model. The optimizer varies the cutback initiation altitude and spool down behavior and finds the optimum point that minimizes certification noise levels. This optimization process is significant during engine sizing in the preliminary and detailed design stages wherein reduced certification noise levels can be traded for a reduced fan diameter. This in turn leads to a reduction in weight, fuel burn, and cost. The optimization process also helps the propulsion engineer make recommendations to the airframer regarding optimal cutback locations in view of International Civil Aviation Organization (ICAO) Annex 16 or FAR Part 36 aircraft noise certification.

The thesis first provides a background to the reader regarding dynamic cutback and its importance in reducing community noise levels. The noise certification process is then described, including how the EPNL is calculated. The role of dynamic cutback optimization is highlighted, both from the preliminary design standpoint, and its usefulness in determining the optimal cutback conditions for noise certification.

In order to verify the hypotheses stated, a process is developed to implement dynamic cutback considering engine spool down. The assumptions in this process are discussed,

followed by a description of the various models that are used in an integrated optimization framework.

Parametric studies were initially carried out for a four-engine commercial aircraft to understand the contribution of each design variable on the flyover EPNL, and also to define the bounds on these variables. Subsequently, a dynamic cutback optimization was performed to determine the global optimum. Several observations are made from the optimization results, including the convergence trend, analysis of the optimum region, and the effect of constraints. Similar studies were performed for a twin-engine configuration to verify if these trends remain the same.

Relative to instantaneous cutback, dynamic cutback simulation showed a reduction of 0.5 and 0.35 EPNdB for a four and two engine aircraft, respectively. Dynamic cutback optimization using a Genetic Algorithm varying cutback initiation altitude, cutback power, and spool down rate found a reduction of 5.51 and 4.52 EPNdB, respectively, compared to a full power takeoff, with ICAO Annex 16 constraints satisfied.

Quite often, in deterministic optimization studies, the optimal design point is found to be close to a constraint boundary. For the dynamic cutback optimization studies, it was found that perturbations in the design variables at the optimum were very likely to lead to an infeasible solution. Therefore, a robust optimization technique was applied to determine the location of the global minimum that remains feasible even if there are perturbations in the design variables.

CHAPTER I

INTRODUCTION

Since the beginning of commercial aviation, aircraft noise has been a major environmental issue. People living in communities near airports continue to be concerned about potential health effects and quality of life issues from noise due to aircraft operations. In fact, the International Civil Aviation Organization (ICAO) defines aircraft noise as "the most significant cause of adverse community reaction related to the operation and expansion of airports both in developed and developing countries." [1] Although today's modern commercial aircraft are 75% quieter than their predecessors 40 years ago, communities around airports are still affected as air traffic densities have been increasing over the years.

The ICAO has led the effort of noise reduction since the 1960's, by introducing different standards that set limits on maximum allowable noise levels for various categories of aircraft at three noise certification positions - flyover, approach, and sideline. The noise certification metric is the EPNL or Effective Perceived Noise Level. Aircraft need to demonstrate compliance with these standards before they receive airworthiness certification for revenue service.

The introduction of the high-bypass turbofan engine in the 1970's saw large reductions in noise. Since then, low noise technology improvements along with continued increase in engine bypass ratio (BPR) continue to provide significant additional reduction of aircraft noise. If this does not happen, increasingly stringent noise restrictions at every level could severely hamper the capacity of the global aviation system to meet the projected increase in air traffic. [2][3]

1.1 Goal and Motivation

Thrust Cutback is a technology by means of which noise levels at the flyover certification position can be significantly minimized. Consequently, both aircraft and engine manufacturers have developed simulation techniques to study this technology, and assess its impact

both during preliminary design and noise certification. Typically, the cutback procedure - which involves a reduction in thrust during the initial takeoff climb - is simulated as an instantaneous thrust reduction. This research work aims to investigate if there is any marginal noise reduction that can be attributed to the spooling down of the engine during the thrust reduction. Coupled with an optimization process that determines the ideal conditions for a cutback to minimize noise levels, this "dynamic cutback" model can help the propulsion or airframe designer in multiple ways.

The dynamic cutback optimization may lead to reduced noise levels that can be traded for a reduced fan diameter or increased fan rpm. The process may be used during the initial stages of certification of a new or derivative aircraft configuration, wherein it may be desired to understand how noise levels vary as a function of cutback altitude, fan speeds, or other parameters. The optimization process may also be used to assess if older aircraft meet present-day noise regulations, and if expensive retrofitting of noise reduction packages can be avoided.

The main goal of this thesis is to develop a dynamic cutback optimization procedure that can be applied to an aircraft-engine configuration to determine the cutback conditions for least noise, and also to quantify the benefits of the spool down effect.

While dynamic cutback optimization procedures do exist currently, these are proprietary in nature. Although the models used in this research work are proprietary, the optimization procedure developed can be applied in existing design environments (in industry and academia) to minimize certification noise levels.

1.2 Research Questions

In order to understand the significance and effect of dynamic cutback for minimizing flyover noise, the following research questions were posed.

Research Question 1: What impact does the modeling of engine spool-down during cutback have on the flyover EPNL?

Research Question 2: Is there a single optimum combination of cutback altitude and spool-down behavior for a given aircraft that results in the minimum possible flyover EPNL,

while also satisfying ICAO Annex 16 Volume 1 airworthiness requirements?

Research Question 3: How sensitive is the flyover EPNL to perturbations in cutback altitude and spool down behavior at the optimal design point?

The first Research Question aims to quantify the noise benefit, if any, which can be gained by modeling the spooling down of the engine during a cutback procedure, as opposed to a cutback procedure with instantaneous power reduction.

The second Research Question investigates if there is a unique optimum point in the design space that adheres to the airworthiness requirements described in ICAO Annex 16 Volume 1.

The third Research Question is concerned with variation in the design variables at the design optimum. The optimal design point obtained using deterministic optimization techniques may not be robust to perturbations in the design variables. Using probabilistic analysis and optimization techniques, the location of the robust minimum point, if any, is sought relative to the deterministic minimum.

1.3 Hypotheses

In an attempt to answer these research questions, the following hypotheses are proposed.

Hypothesis 1: The modeling of engine spool down in a cutback simulation leads to a lower Effective Perceived Noise Level at the flyover certification point.

This hypothesis is based on the fact that the modeling of engine spool down will result in a flight path post-cutback that is relatively higher than the case when spool down is not modeled. This gain in altitude will have the effect of reducing the noise at the flyover certification point. If the flight paths for the full power and cutback regions are pre-defined, then modeling the spool down between these two regions might be beneficial as lower noise is generated because of reduction in fan speed.

Hypothesis 2: There could be more than one combination of optimum cutback altitude and spool down behavior for a given aircraft that results in minimum flyover EPNL, while also satisfying the ICAO Annex 16 Volume 1 airworthiness requirements.

It is known that both cutback altitude and the degree of cutback play an important role in flyover noise reduction. Therefore, a low cutback altitude for a given degree of cutback might have the same effect as for a higher cutback altitude with a greater degree of cutback.

Hypothesis 3: The robust optimum has a higher flyover EPNL than the optimum found using regular optimization techniques.

This hypothesis is based on the general observation in optimization problems that the deterministic minimum either lies on a constraint boundary, or may be located at a region in the design space where perturbations in the design variables can lead to large variations in the response. Either case might be applicable for this study.

1.4 Outline of Chapters

The research work in this document is structured based on distinct chapters. This chapter (Chapter 1) provides the reader a high-level understanding of the significance of the research, and also presents the research questions and hypotheses. Chapter 2 explains the background behind the research work, including certification noise, ICAO and FAR Part 36 regulations governing aircraft noise, and the concept of noise abatement operational procedures. In Chapter 3, the assumptions and overall methodology for the research work are discussed. Chapter 4 explains the process established to estimate flyover noise for a flight path with both instantaneous and dynamic cutback. The optimization framework consisting of flight path and acoustic models is also described. Chapter 5 describes the results obtained from various studies, including optimization and parametric analysis, and provides an interpretation of these results. Finally, Chapter 6 chapter draws conclusions based on the results obtained and delineates future work to be performed.

CHAPTER II

BACKGROUND

With higher density populations surrounding airports throughout the world, and with increasing airport capacities, aircraft noise has become an issue of increasing concern in recent years. Policies governing aircraft noise - from local airport restrictions to international regulations have consequently become more and more stringent. Figure 1 [4] shows the types of noise restrictions for airports across the world.

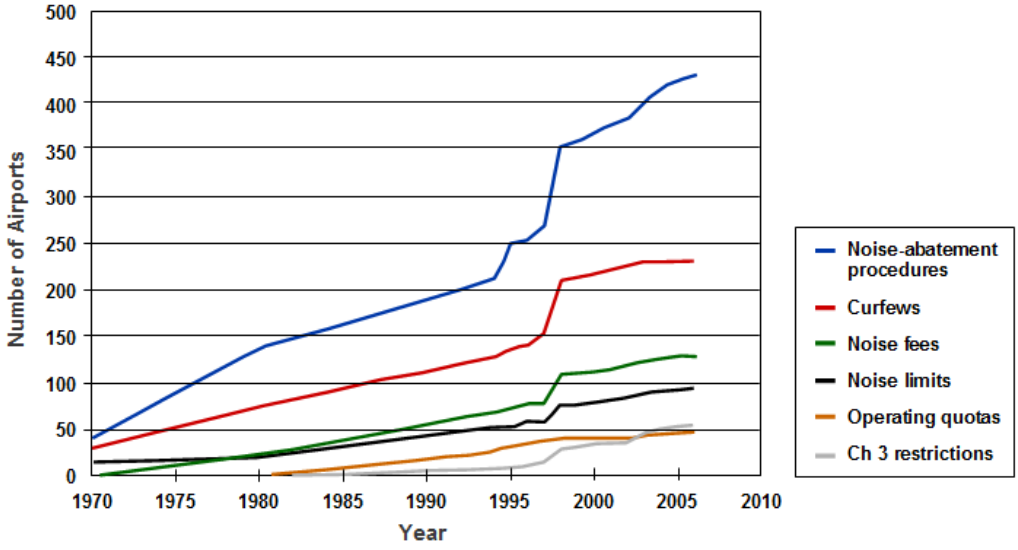

Figure 1: Noise Restrictions Across the World [4]

The International Civil Aviation Organization (ICAO) defines aircraft noise standards in Annex 16 - Environmental Protection, Volume I - Aircraft Noise [5], while practical guidance to certificating authorities on implementation of the technical procedures of Annex 16 is contained in the Environmental Technical Manual on the use of Procedures in the Noise Certification of Aircraft [6]. In the United States, the FAR Part 36 [7] regulations govern aircraft noise certification, while in Europe, it is the JAR 36 that does so. Both the FAR and JAR regulations are very similar to the international ICAO standards, and a comparison between these can be found in [8].

2.1 Noise Certification Standards

The FAA and ICAO define three specific points for noise measurement and certification of aircraft. As shown in Figure 2, two of these points are for takeoff conditions - the "flyover" or "community" reference point which is 21,325 ft from brake release on the extended centerline of the runway, and a "sideline" point which is 1,476 ft away from the runway centerline at a location where the noise level is the highest. The "approach" certification point is located 6,562 ft from touchdown.

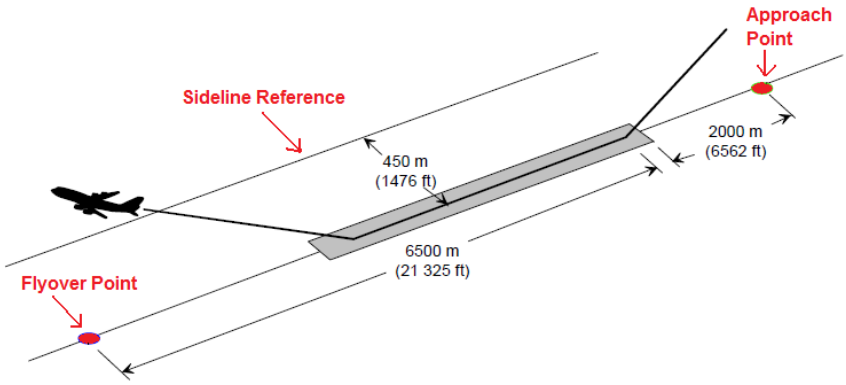

Figure 2: Observer Locations for ICAO/FAR Noise Certification

Aircraft manufacturers have to demonstrate that noise levels at the certification points are within these noise limits while certifying a new airplane. Figure 3 graphically shows the noise limits defined by Chapter 3 standards. The noise certification metric (discussed in Section 2.2) is the Effective Perceived Noise Level (EPNL), measured in units of EPNdB.

Chapter 4 standards (Stage 4 as per FAR Part 36) require that the cumulative sum of the noise levels at the three certification points is lower by at least 10 EPNdB than the sum of the Chapter 3 noise limits. Moreover, the sum of the noise levels at any two measurement locations should be below the sum of the corresponding Chapter 3 limits by 2 EPNdB.

2.2 EPNL and its Calculation

The Effective Perceived Noise Level or EPNL is defined by the ICAO as "a single number evaluator of the subjective effects of aircraft noise on human beings" [5]. For noise certification, the applicant must carry out acoustic measurements under well-defined atmospheric

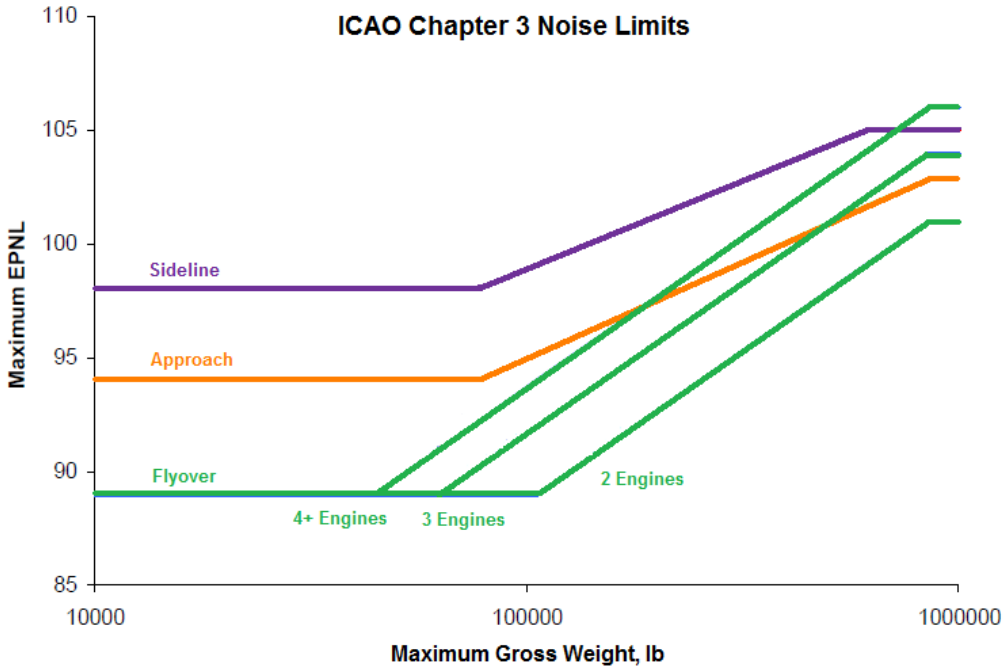

Figure 3: ICAO Chapter 3 Noise Limits

conditions using approved measurement systems at the three certification points, viz. the flyover, sideline, and approach locations. The calculation of this noise certification metric is discussed in brief in this section.

The sound pressure level (SPL) is expressed in decibels above a standard reference level P_{ref} (which is the threshold of human hearing set at 20 μPa).

$SPL = 20\, log_{10}(P/P_{ref})dB$

For aircraft noise certification, three basic properties of sound pressure are considered - the level (in SPL), frequency, and time variation. The SPL is measured in the frequency range from 50 to 10000 Hz. This frequency range is divided into 8 octave bands, and each band is further sub-divided into 3 bands. The SPL measurements are made at the midrange frequency of these 24 "one-third octave" bands. There is a four-step process to convert these SPL values to the single number noise metric - the EPNL, and this is summarized below.

(a) Annoyance Correction: The 24 one-third octave bands of sound pressure levels are converted to perceived noisiness by means of a "noy" table. This is done to account for the annoyance response of the human hearing system as a function of frequency. The

noy values for each band are then combined and converted to instantaneous perceived noise levels, PNL(k).

(b) Tone Correction: A tone correction factor, C(k), is calculated for each spectrum to account for the subjective response to the presence of spectral irregularities. This procedure consists of 10 steps. The tone correction factor is added to the perceived noise level to obtain tone-corrected perceived noise levels, PNLT(k), at each one-half second increment of time.

$$PNLT(k) = PNL(k) + C(k)$$

(c) Duration Correction: A duration correction factor, D, is computed by integration under the curve of tone corrected perceived noise level versus time, according to the formula below.

$$D = 10\,log\left(\frac{1}{T}\sum_{k=0}^{d/\Delta t}\Delta t\; antilog\frac{PNLT(k)}{10}\right) - PNLT_M$$

where t is the length of the equal increments of time for which PNLT(k) is calculated and d is the time interval to the nearest 0.5 seconds during which PNLT(k) remains greater or equal to $PNLT_M$ - 10.

The values T=10 s and del T = 0.5 s are used in the above equation to obtain the equation:

$$D = 10\,log\left(\sum_{k=0}^{2d} antilog\frac{PNLT(k)}{10}\right) - PNLT_M - 13$$

If there is more than one peak value of PNLT(k), the applicable limits must be chosen to yield the largest possible value for the duration time.

(d) Final Objective: The effective perceived noise level, EPNL, is determined by the algebraic sum of the maximum tone corrected perceived noise level and the duration correction factor.

$$EPNL = PNLT_M + D$$

This process is shown pictorially in Figure 4.

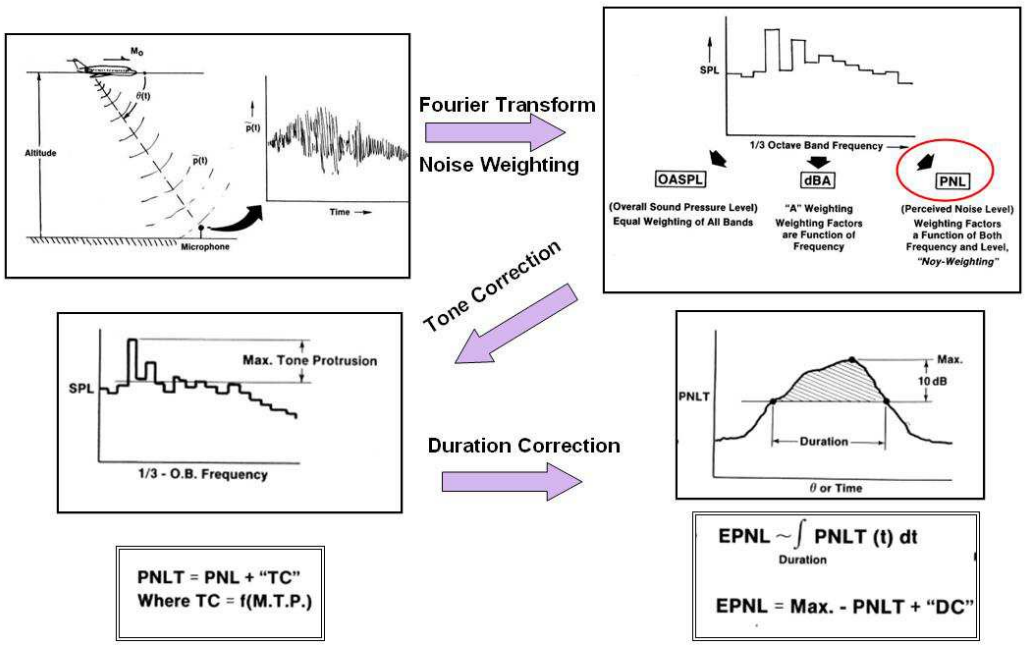

Figure 4: EPNL Calculation Process

2.3 Dynamic Cutback

Dynamic Cutback is a procedure used in noise abatement departures to alleviate the noise impact on communities located close to the airport. In this procedure, engine thrust is reduced at a specific altitude from the full power takeoff rating to a cutback rating for a fixed duration. This procedure is named "dynamic cutback" because of the spooling down of the engine during the thrust reduction. A flight path during takeoff with thrust reduction is shown in Figure 5.

Due to the lower thrust level after cutback, the noise footprint is reduced, which benefits the community directly beneath the flight path. If a noise monitor kept at a fixed location on the ground in line with the flight trajectory were to record the noise from the aircraft performing a cutback procedure, the noise level would vary as shown in Figure 6 [9]. As the aircraft approaches the microphone, the noise level increases. On initiating a cutback, engine thrust reduces which leads to a reduction in noise. But as the aircraft approaches the monitor, noise levels increase due to the decreasing straight-line distance between the aircraft and monitor. Finally, as the aircraft leaves the monitor, noise levels recede.

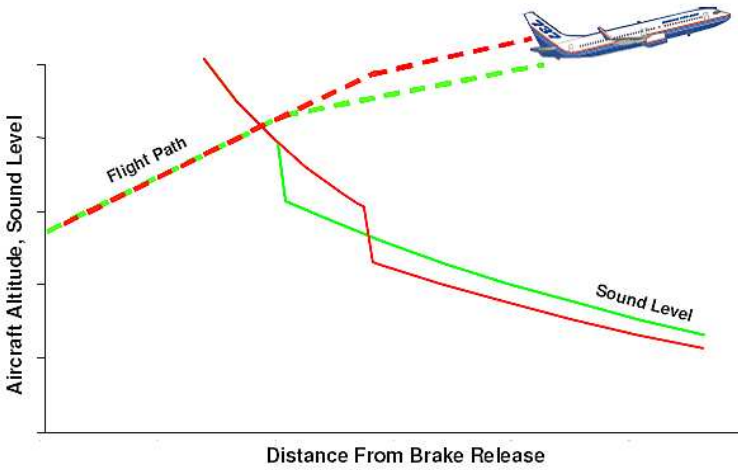

Figure 5: Concept of Dynamic Cutback [4]

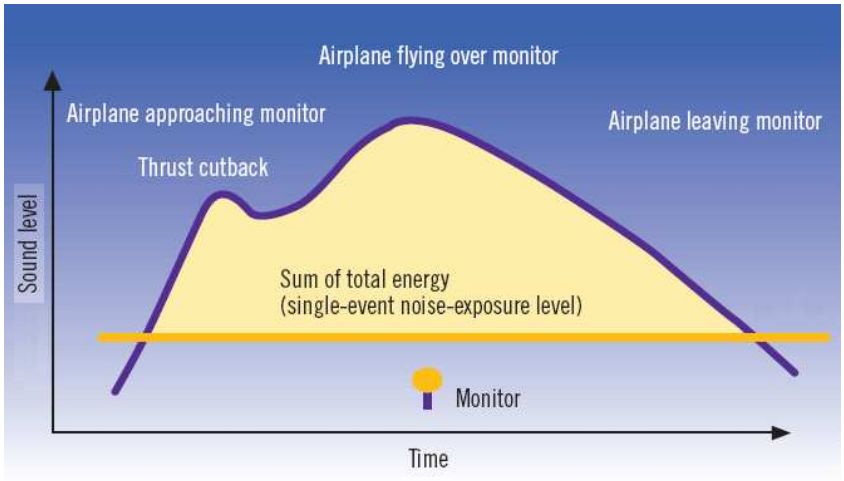

Figure 6: Noise Level Variation in Dynamic Cutback [9]

Antoine and Kroo [10] describe an example to demonstrate the effect of thrust cutback in noise reduction for two different cutback altitudes. This example is shown in Figure 7.

The time-integrated noise that corresponds to the area under the curve is the noise metric used for certification. Although the effect of engine spool down is not seen in this figure, it nonetheless gives an idea as to how noise levels reduce due to cutback.

This thesis focuses on modeling the engine spool down behavior, and developing an optimization process to minimize flyover certification noise levels. The modeling and optimization of dynamic cutback procedures is significant from two key standpoints - first, for

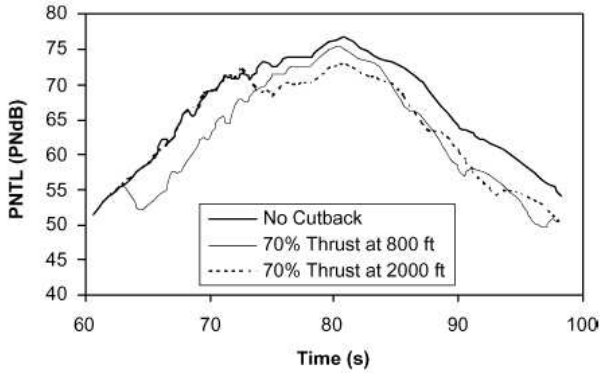

Figure 7: Example of Cutback for Two Different Cutback Altitudes [10]

minimizing flyover (and hence cumulative) noise margins during the noise certification process, and secondly, during engine preliminary design wherein several engine geometries are studied and optimized for noise, weight, and fuel burn. Each of these aspects is discussed in the sub-sections below.

2.3.1 Dynamic Cutback for Noise Certification

The standard takeoff flight profile for noise certification as per ICAO Annex 16 and FAR Part 36 is shown in Figure 8 *(permission to reproduce this figure has been granted by ICAO.)* The aircraft begins the takeoff roll at point A, lifts off at point B, and begins climbing at point C with a constant flight path angle. The thrust cutback is initiated at point D, and completed at point E where the engine has spooled down to the desired power setting. A second constant climb begins at an angle γ, and is continued at least till point F, which represents a ground distance of 11 km.

The takeoff noise monitor is located at point K, which is 6.5 km from the brake release point A. The general trend of the noise history for the above flight path is shown in Figure 9 *(permission to reproduce this figure has been granted by ICAO.)*

There are 3 curves that can be observed in this figure. The first dotted curve represents the noise history for a full power takeoff scenario, while the second dotted curve corresponds to a flight path flown at constant cutback power. The resultant noise history for the flight path with dynamic cutback contains portions of the full power and cutback noise histories, and also the spool down noise history.

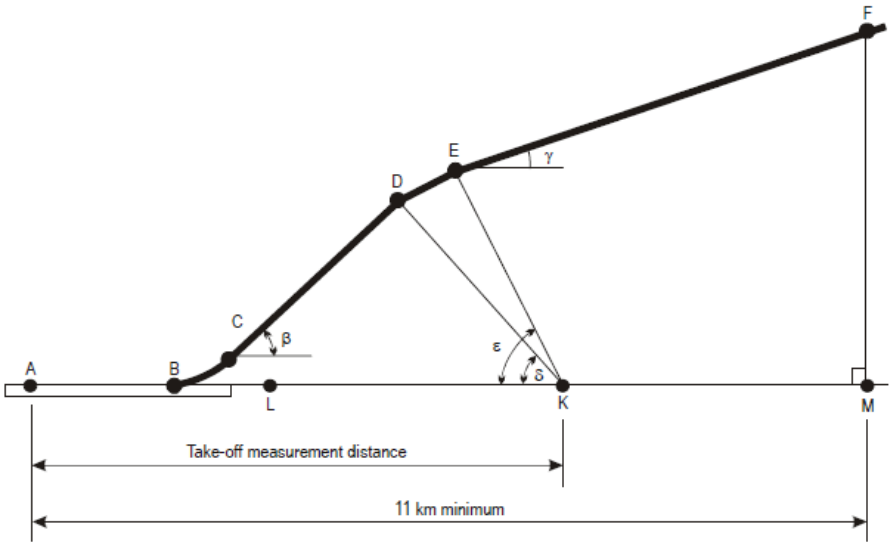

Figure 8: Standard Takeoff Profile as per ICAO for Noise Measurement [5]

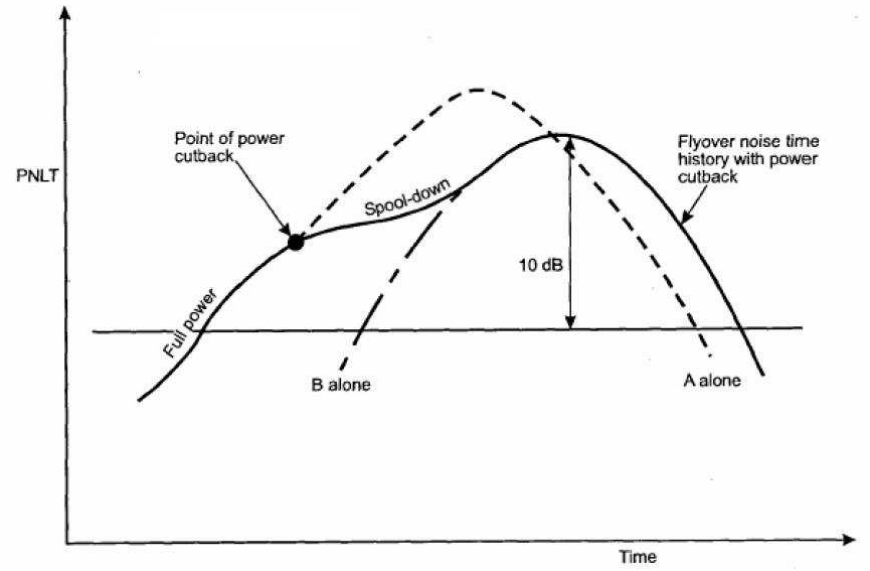

Figure 9: PNLT-Time History for Dynamic Cutback [6]

In practice, airframers adopt "equivalent procedures" for noise certification, instead of following the exact flight path procedure as described in ICAO's Annex 16, Volume 1. An equivalent procedure is one that leads to the same noise levels as the specified procedure. Such procedures are preferred as they allow the use of previously acquired certification data, and also minimize costs by reducing testing time and airfield usage.

Figure 10 *(permission to reproduce this figure has been granted by ICAO)* shows a flight

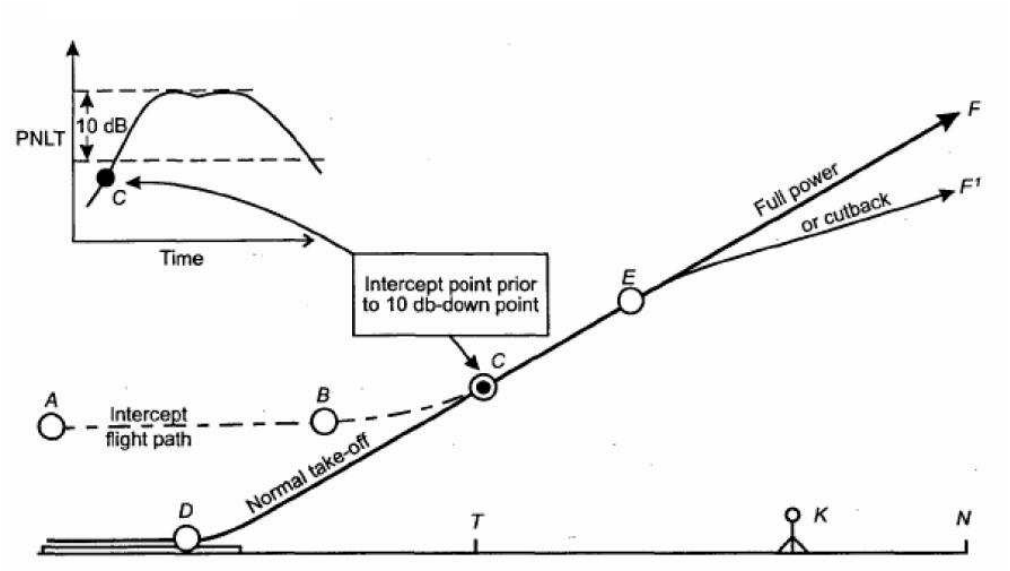

Figure 10: Flight Path Intercept Procedure for Flyover Noise Certification [6]

path intercept procedure - an equivalent procedure in lieu of the standard takeoff procedure shown in Figure 8 - for takeoff noise certification. Here, the airplane is stabilized in level flight at point A and continues to point B where take-off power is selected. The airplane then starts climbing, and intercepts the predetermined reference flight path at point C. If thrust cutback is employed, the point of application of the thrust reduction is point E.

This procedure is typically flown for a range of takeoff and cutback power settings over the flyover and lateral microphones to establish a noise database called the Noise-Power-Distance (NPD) plot. The NPD plot, shown in Figure 11, presents EPNL values for a range of distances and engine noise performance parameters. The performance parameter typically used is the corrected fan speed or the corrected net thrust.

These NPD curves are used for noise certification for the baseline or "datum" aircraft. The NPD data is also useful for certifying derivative aircraft when used along with analytical procedures, static testing of the engine and nacelle, or additional limited flight tests. The ICAO's "Environmental Technical Manual on the Use of Procedures in the Noise Certification of Aircraft" [6] provides guidance on these procedures.

In the flyover noise certification process, the aircraft manufacturer initially builds an NPD database for the baseline aircraft configuration based on noise measurements taken

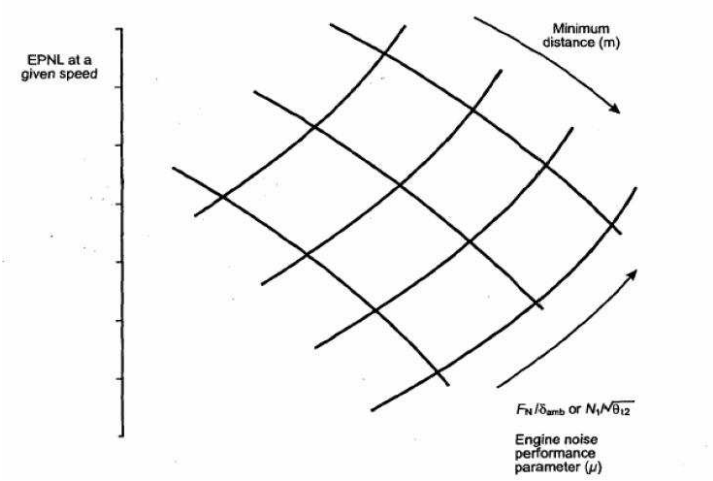

Figure 11: Noise-Power-Distance (NPD) Curve [6]

during flight tests. Typically, there are configuration changes made to both the airframe and the engine before entry-into-service. If there is a major change in the engine configuration, a static engine test is carried out to determine changes in noise spectra for the different engine components. The manufacturer may use this static engine test data in predicting flyover noise levels by analytical means only if certain conditions specified in the Environmental Technical Manual are satisfied.

These analytical methods (referred to as "analytical equivalent procedures") are proprietary methods that allow the aircraft manufacturer to perform a simulated flyover with thrust reduction. The procedures make use of the datum NPD database, speed adjustment procedures defined in Annex 16 Volume 1, and certificated airplane aerodynamic performance data to determine noise levels for the derivative configuration.

Dynamic cutback optimization allows the aircraft manufacturer to estimate the optimal conditions for a thrust reduction so that flyover noise is minimized. These conditions may include the fan speeds at takeoff and after cutback, cutback initiation altitude, rate of change of engine thrust, takeoff weight, flap settings, etc. The analytical equivalent procedures may make use of such optimal conditions to demonstrate compliance with ICAO Annex 16 regulations.

NPD databases for the derivative configuration determined based on the analytical procedures, as well as those determined based on actual noise measurements can be used in

conjunction to establish certification noise levels.

Previous research on certification flyover noise optimization shows that the cutback location is a very important factor in flyover noise certification. Grantham and Smith, in their paper [11] on the development of takeoff and landing procedures for a supersonic cruise research (SCR) aircraft, describe noise abatement simulations conducted using NASA's Visual Motion Simulator. It is shown that flyover EPNL can be significantly reduced by employing thrust cutback at appropriate altitudes and speeds. The variation of flyover noise with cutback altitude is shown in Figure 12 for two different climb speeds. It is seen that in both cases, the EPNL curve dips with increase in cutback altitude, then increases after hitting an optimum.

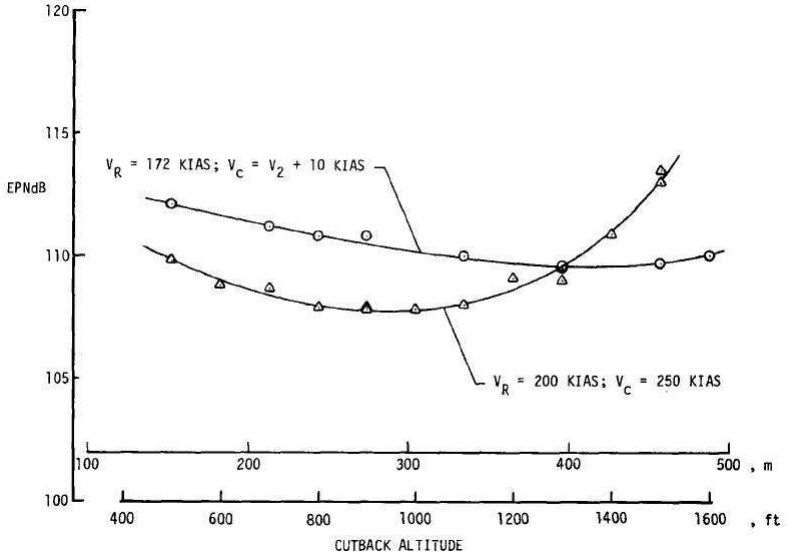

Figure 12: Variation of EPNL vs Cutback Altitude [11]

The flight parameters for the optimal cases are shown in Figure 13. It is observed from the noise plot that due to the cutback procedure, the overall 10 dB-down area is decreased, and this leads to low EPNL values. It is also noted that the PNLT points during engine spool down are also included in the 10 dB-down window. The authors note that the regulations require a constant climb speed to be maintained, and mention that the rate of thrust cutback and the rate of climb gradient change are very important parameters to achieve a constant speed.

In this thesis, the takeoff simulation model developed (described in Section 4.2.2) maintains a constant speed during the engine spool down by varying the angle of attack. It is also ensured that the climb speed does not exceed $V_2 + 20$ kts as per current ICAO requirements.

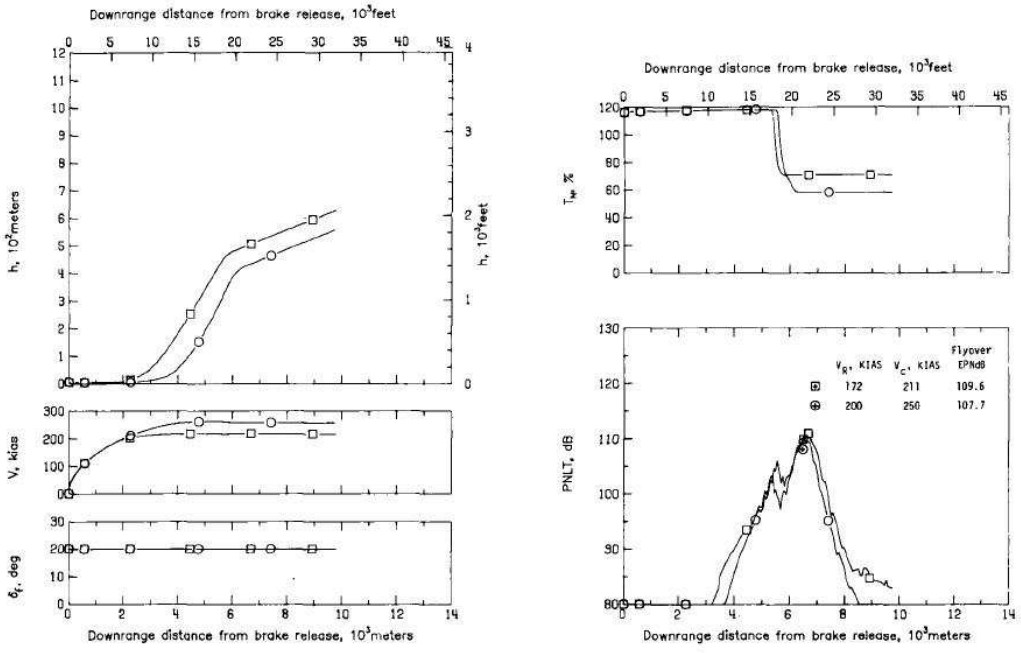

Figure 13: Flight Path Information and Noise History from NASA Cutback Study [11]

Apart from the cutback altitude, the fan speed is another critical parameter that affects flyover noise. With reductions in fan speed during cutback, engine thrust decreases, leading to fan and jet noise reduction. In a paper on ultra low noise takeoff for the Silent Aircraft Initiative concept aircraft [12], Crichton et. al. describe an optimization process to determine the optimal takeoff profile for reduced flyover noise levels. Two cases are analyzed - one where jet noise is minimized, and the other where overall noise is minimized. When fan speed is reduced from 87% to 70%, net thrust reduces by around 85,000 N, as shown in the plots in Figure 14 *(permission to reproduce this figure has been granted by Dr. J. I. Hileman.)*

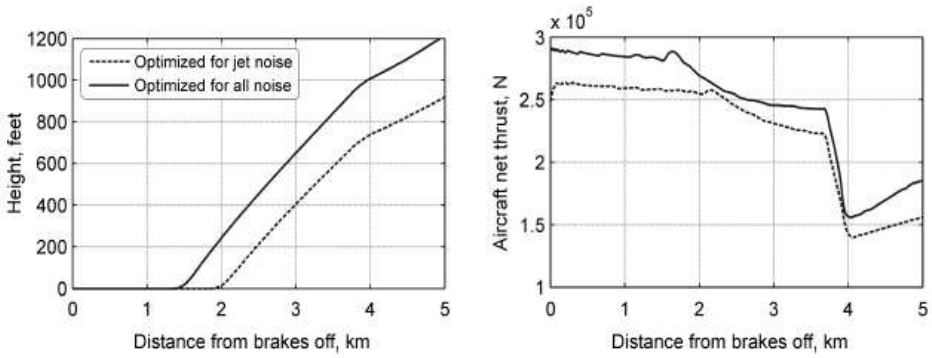

Figure 14: Flight Path and Thrust Variation from Silent Aircraft Cutback Study [12]

2.3.2 Dynamic Cutback in the Engine Preliminary Design Process

Dynamic cutback plays an important role during engine preliminary design as well. Due to increasingly stringent regulations being imposed to minimize aircraft noise and emissions, airframers and engine manufacturers are striving to improve design processes in the conceptual and preliminary design stages using enhanced acoustics and emissions modeling and simulation techniques In the recent past, there has been a lot of work carried out in assessing tradeoffs between noise and emissions in the preliminary design stage.

As far as acoustics is concerned, it is important to improve the cumulative noise margin with respect to Chapter 4 noise limits. Modeling thrust cutback in the preliminary design stages can improve this margin as this procedure leads to lower flyover noise levels. Typically, propulsion engineers assume an instantaneous thrust reduction in the cutback procedure while estimating flyover noise. It is generally understood that modeling engine spool down during the cutback for acoustic evaluation has the potential to reduce the flyover EPNL. A part of this research effort's goals is to quantify the noise benefit due to modeling the spool down.

The difference between a cutback procedure with instantaneous power reduction and one with spool down is depicted in Figure 15 below. While dynamic cutback involves a spool down region, instantaneous thrust cutback can be modeled in two ways.

In Case A, it is assumed that the cutback initiation point for instantaneous cutback is the same as that for dynamic cutback. In this scenario, modeling dynamic cutback has the

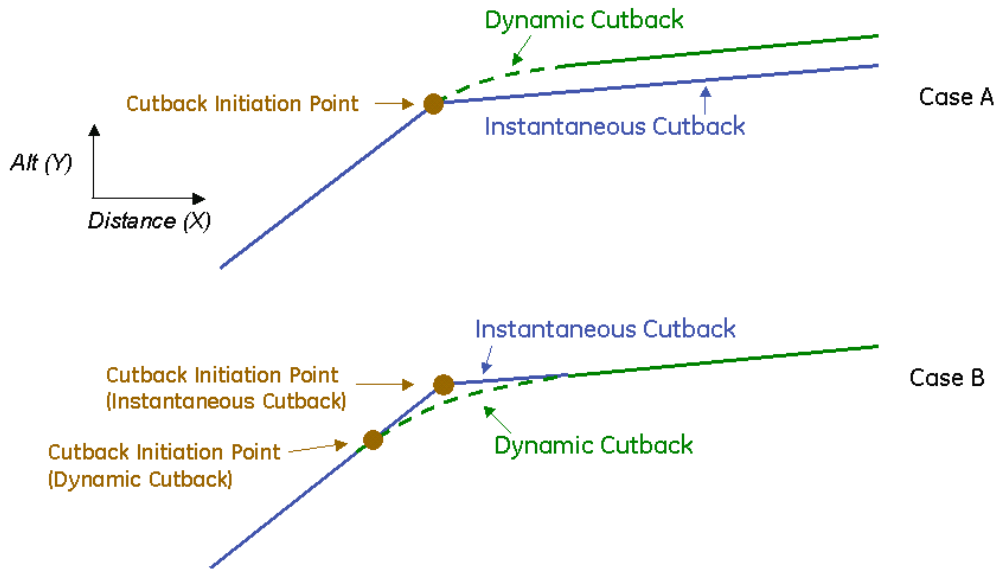

Figure 15: Instantaneous vs. Dynamic Cutback

advantage that there is a small increase in altitude, which leads to lower noise levels on the ground. In Case B, the flight path segments corresponding to full power and post-cutback are the same for both instantaneous and dynamic cutback. Even here, dynamic cutback is important as noise levels are reduced due to modeling of the engine spool down. With the help of an optimization procedure, it will be possible to determine the optimal cutback initiation altitude, spool down rate, and percentage reduction in thrust for minimum flyover noise.

During preliminary engine design, several customer requirements need to be satisfied. For noise, increased bypass ratio (BPR) for a given thrust is beneficial [13][14], as depicted in Figure 16 (derived from [13]), but engine drag/weight goes up which may lead to a higher fuel burn if increased beyond an optimum value. A dynamic cutback optimization procedure has the potential to generate a slightly higher noise margin for flyover noise and cumulative margin, relative to non-dynamic cutback. For a given noise requirement, this small benefit can be traded against a slightly smaller BPR to achieve a lower fuel burn. A smaller BPR for a given core size results in fan diameter reduction. This in turn reduces overall engine weight, fuel burn, and cost.

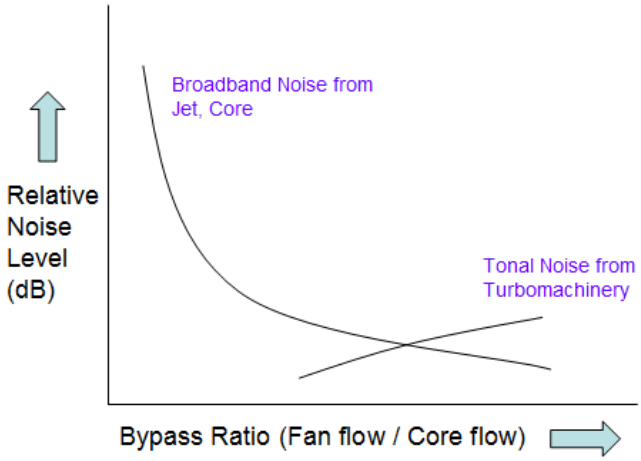

Figure 16: Effect of Bypass Ratio on Noise

There exist several multi-disciplinary tools and methodologies for carrying out tradeoff studies between noise, emissions, performance, cost, and other quantities. While this thesis makes use of a proprietary integrated framework, the process that was developed for dynamic cutback optimization (described in Section 4.2) could be incorporated into some of the tools and frameworks discussed below in brief.

Caffe Design Framework

Antoine and Kroo [10] describe a design tool illustrated in Figure 17 to estimate the tradeoff between operating cost and certification noise.

This tool consists of a library of routines for aircraft design and performance estimates, NASA's Aircraft Noise Prediction Program (ANOPP) for noise modeling, and NASA's Engine Performance Code (NEPP). These programs are integrated in a multi-disciplinary framework called Caffe. The design variables in the optimization process include aircraft performance, engine performance, and mission profile parameters.

The ANOPP code, whose structure is shown in Figure 18 *(permission to reproduce this figure has been granted by Dr. M. D. Dahl)*, contains several empirical-based programs for engine and airframe source noise prediction [15]. The combined noise source representation of the aircraft is then projected on to a flight path (either generated within the program or provided externally) to obtain noise levels at different observation points on the ground.

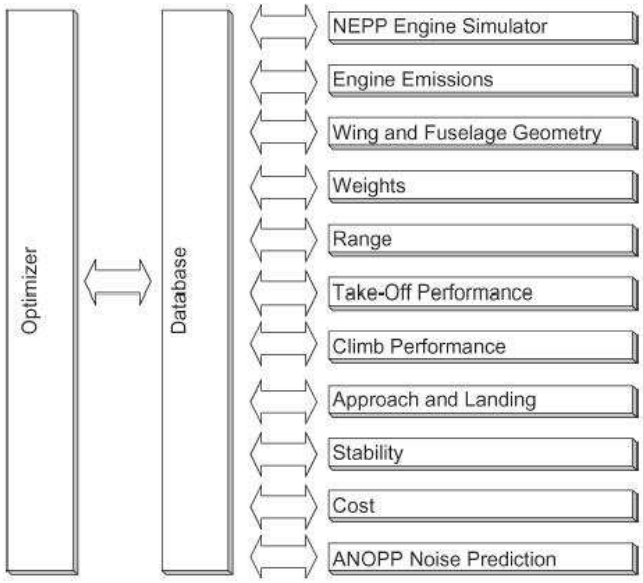

Figure 17: Caffe Design Framework [10]

The authors describe a thrust cutback study using this design tool, and note that "the greatest gain involves cutting thrust as much as allowable to maintain the minimum climb gradient, which should be done close to but before the flyover noise measurement point for maximum beneficial effect."

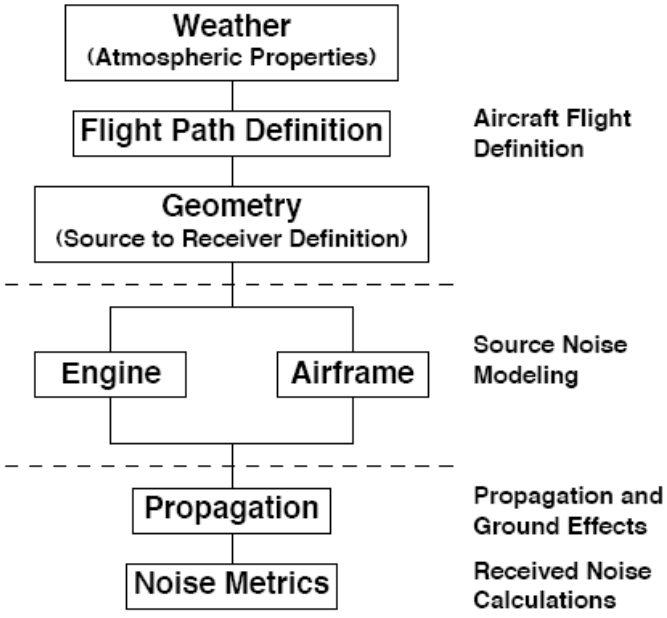

Figure 18: ANOPP Framework [15]

Environmental Design Space Tool

The Environmental Design Space (EDS) tool is a physics-based numerical simulation program [16] consisting of several modules that allow for a thorough assessment of the environmental effects of aviation. EDS provides the capability to estimate source noise, emissions, performance, and economics for existing and future aircraft, and also enables the study of interdependencies. This tool, in conjunction with the Aviation Environmental Portfolio Management Tool (APMT) and the Aviation Environmental Design Tool (AEDT), will also allow for the assessment of operational and market scenarios.

The EDS architecture, with examples of its usage, is described in detail by Kirby and Mavris [16]. The noise analysis module used in the framework is ANOPP, which has the capability to predict certification noise levels for user-defined flight paths.

PREDATER

PREDATER [17][18], which stands for Preliminary Robust Engine Design Analysis Tool for Evaluating Return is GE's proprietary MDO tool that allows propulsion engineers to understand in the preliminary design stage which engine parameters have the biggest impact on engineering design decisions. The design framework includes multiple modules including engine design and performance, acoustics, aircraft performance, and cost. The dynamic cutback optimization model could be incorporated into PREDATER to estimate and minimize flyover noise for different engine configurations.

2.3.3 Dynamic Cutback in Noise Abatement Departure Procedures

The ICAO's PAN-OPS Volume 1 and the FAA's advisory circular AC91-53A [19] provide details of two standardized noise abatement departure procedures (NADPs), which serve as guidelines for airlines in the development of customized procedures. While the study of NADPs is not the goal of this thesis, the extensive literature available on this subject provides a knowledge base in understanding the concept of thrust cutback and its potential to significantly reduce flyover noise levels.

The first procedure called NADP1 is used for noise mitigation close to the airport, while the second one - NADP2 - is applicable for noise reduction further out along the departure

path. Both NADP1 and NADP2 involve a thrust cutback soon after takeoff.

Figure 19 below illustrates the difference in noise benefits of NADP1 (shown in red) and NADP2 (shown in blue). While thrust cutback is initiated at 800 ft in both procedures, the acceleration phase in NADP1 is at 3,000 ft as compared to 800 ft for NADP2. Thus, the relatively steeper flight path in NADP1 between 800 ft and 3,000 ft leads to lower noise on the ground. This noise benefit is depicted as the (orange) shaded area between the two flight paths. There is a "cross-over" point where the benefits of NADP1 due to delayed acceleration are overtaken by the benefits of NADP2. Beyond this point, the climb in NADP2 is steeper, leading to lower noise as shown by the (orange) shaded area.

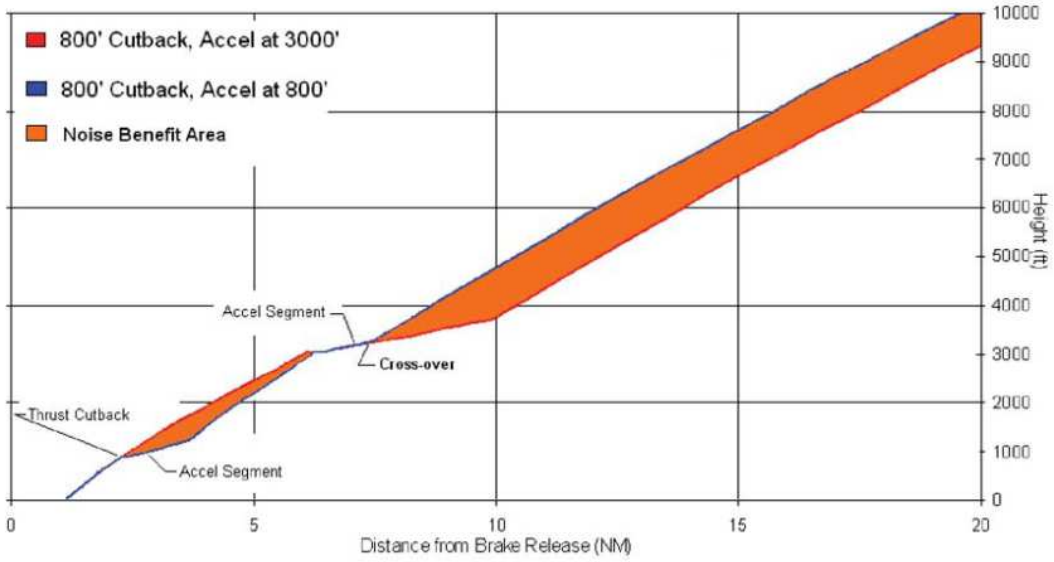

Figure 19: Noise Benefits due to Noise Abatement Departure Procedures [1]

In takeoff procedures at many airports, thrust cutback is used to reduce community noise levels. In a study [20] that dealt with assessing departure noise levels at Heathrow, Stansted and Gatwick airports, it was found that the operating procedure was a key factor in governing departure noise levels, including the variation of engine thrust and flap settings along the flight track. The report discusses in detail the effects of various cutback heights and power settings in minimizing noise. The FAA's Integrated Noise Model (INM) [21] and the CAA's ANCON model are used in determining noise contours around the airports.

Various modeling and optimization techniques have been developed to determine noise-abatement operational procedures. Hebly and Visser [22] describe a concept for custom optimized departure profiles, wherein a trajectory optimization tool is used by the airline in determining the most optimal profile. An in-house developed tool called NOISHHH is used to generate departure flight paths while satisfying operational and safety constraints. The optimization process has the capability to simultaneously minimize both fuel burn and noise exposure.

Clarke [23] describes a systems analysis tool called NOISIM that combines a flight simulator, a noise model, and a geographic information system to create an environment in which the user can simulate an aircraft's operation and evaluate the noise impact. A comparison of different departure procedures involving thrust cutback is made, and the tradeoffs involved is selecting these procedures are discussed.

Visser and Wijnen [24] describe the development of noise abatement departure trajectories using a similar tool that combines a noise model, geographic information system, and a dynamic trajectory optimization algorithm. The optimization algorithm - based on a collocation technique - modifies flight paths to minimize community noise impact, while satisfying all operational and safety constraints. Numerical examples are provided for departure trajectories from Amsterdam Airport, Schiphol.

CHAPTER III

APPROACH

3.1 Assumptions

In developing a process and framework for minimizing flyover EPNL by means of dynamic cutback, a few assumptions were made. These are listed below.

(a) Aircraft Configuration

The thesis focuses on dynamic cutback modeling and optimization for subsonic commercial aircraft with modern turbofan engines which are either in operation currently or which will enter service in the next 10-15 years.

(b) Certification Noise

The dynamic cutback procedure primarily affects the flyover noise. Therefore, the scope of the research was restricted to evaluating and minimizing certification noise levels at the flyover point alone.

(c) Modeling Environment and Design Variables

There are a number of factors that affect flyover certification noise levels. These include airplane and engine configuration and source noise characteristics, the flight path geometry, operational scenario, and atmospheric conditions. While estimating flyover noise using simulation models, certification noise levels are established by projecting static engine noise to flight conditions under acoustic standard day (ISA+18F, 70% humidity) conditions. Several correction factors are used in this projection of noise spectra, including atmospheric attenuation and Doppler shifting. Figure 20 shows the key parameters involved in estimating flyover noise, including the ones that were used in the modeling environment developed in this thesis.

The overall noise model considered includes source noise models for the fan inlet and exit, combustor, and jet, and a model that performs static-to-flight projections of

noise spectra to predict flyover noise. An airframe noise model, although capable of being added to the overall noise model, was not considered while studying dynamic cutback optimization for the two configurations discussed. As airframe noise is not a major contributor during takeoff [15], it is not included in this study.

In the takeoff flight path modeling, velocity is held constant during the engine spool down. This is discussed in detail in Section 4.2.2. The flight profile generated for reference conditions compared well with flight data from actual noise certification flight tests.

With regard to the optimization process, only three important design variables were considered - the cutback initiation altitude, the corrected fan speed after cutback, and the fan spool down rate during cutback. These parameters have a significant impact on flyover noise as discussed in Section 2.3.1 and are of interest to the propulsion engineer studying dynamic cutback. However, the optimization framework can readily incorporate additional design variables including the aircraft takeoff gross weight, rotation speed, gear retraction schedule, and others as required.

(d) Aircraft Model

The aircraft is modeled as a point mass that is equivalent in weight to the real aircraft, with all forces acting at this point as shown in Figure 21. The aerodynamic characteristics are defined by means of a drag polar and lift-slope curve. A set of standard differential equations (shown in Figure 21) integrated with respect to time determines the aircraft's flight path. Apart from the landing gear retraction, the aircraft configuration is assumed to be constant, including the fuel load. The fuel fraction for the takeoff and initial climb for commercial aircraft is very small, and therefore, this assumption is justifiable.

(e) Engine Model

The engine model is assumed to be a matrix of cycle parameter values for different combinations of altitude, Mach number, and corrected fan speed. For a given dynamic cutback study, cycle data for specific conditions are obtained by interpolating on this

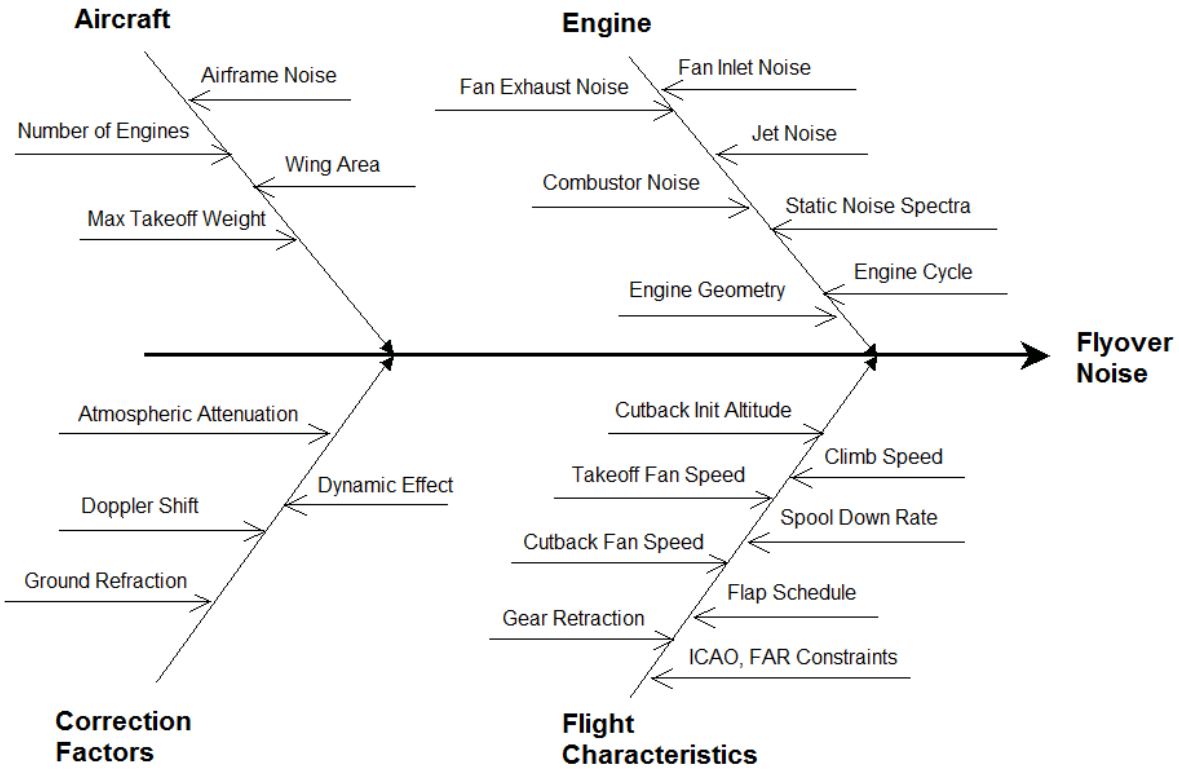

Figure 20: Factors Affecting Flyover Noise in a Modeling Environment

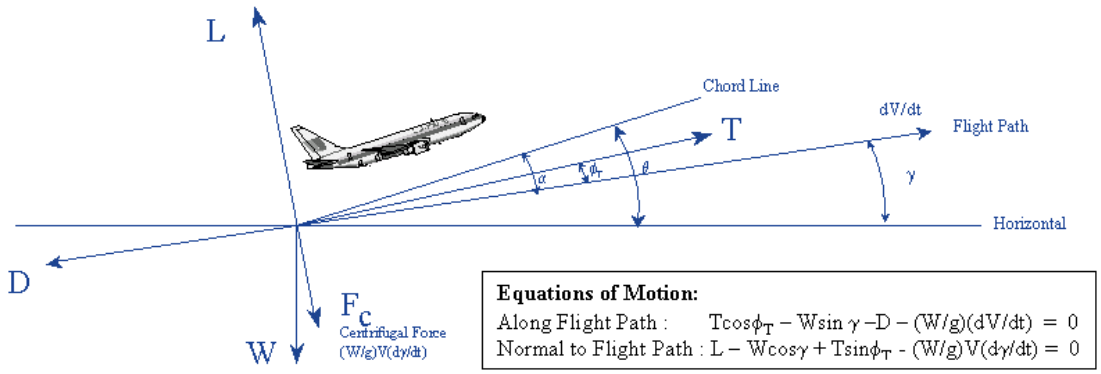

Figure 21: Aircraft Flight Path Model

cycle matrix. As the noise calculation process makes use of a flight path consisting of a series of linear segments with each segment corresponding to a constant fan speed (described in Section 4.2.6), the use of this quasi-steady state model is warranted, as opposed to using a transient cycle model.

Combined equations of motion for ground roll and airborne phase

$$\frac{dV}{dt} = g\left((T/W)\cos\phi_T - \frac{(C_{Do} + kC_L^2)\rho V^2}{2(W/S)} - \sin\gamma - \left(\mu\left(\cos\phi_G - \left(\frac{C_L \rho V^2}{2(W/S)} \right) \right) \right) \right)$$

$$\frac{d\gamma}{dt} = \frac{g}{V}\left((T/W)\sin\phi_T + \frac{C_L \rho V^2}{2(W/S)} - \cos\gamma \right)$$

$$V = \sqrt{V_x^2 + V_y^2} \quad V_x = dx/dt \quad V_y = dy/dt$$

$$C_L = C_{L_o} + \left(\frac{dC_L}{d\alpha} \right)\alpha$$

Figure 22: Aircraft Equations of Motion

3.2 Overall Procedure

The research effort was divided into several sub-tasks as listed below.

(a) Instantaneous cutback modeling and optimization

(b) Process for dynamic cutback

(c) Flight path for dynamic cutback

(d) Dynamic cutback optimization framework

(e) Parametric studies

(f) Optimization studies

(g) Robust optimization

Initially, the focus was to develop a model to perform instantaneous cutback optimization. The goal of this sub-task was to understand the noise benefit gained by the cutback procedure as opposed to a full power takeoff. A simple optimization framework was developed to minimize flyover EPNL while varying cutback altitude.

The next sub-task was to develop a process for modeling thrust cutback while considering engine spool down. This process, described in Section 4.2.7, calculates the noise emission points on the flight path at 0.5-second intervals for which PNLT is determined. These PNLT

values are then used for computing the EPNL. This process extended the methodology used by the instantaneous cutback modeling for determining PNLT values.

Flight path modeling was required to generate a flight trajectory for takeoff and initial climb, with cutback initiated at a specified altitude. The intent was to provide this trajectory as input to the acoustic evaluation process for estimating the EPNL.

To estimate flyover EPNL with dynamic cutback, several acoustic tools were required, and these were integrated into the optimization framework along with the takeoff simulation model. Section 4.2 describes the entire dynamic cutback optimization framework and process.

After the design framework was developed, parametric studies were carried out to understand the effect of the design variables of flyover noise. The importance of modeling engine spool down is also highlighted.

Following this, optimization studies were carried out to determine the optimal design points for a four-engine and two-engine commercial transport aircraft. The results from these studies are discussed in Sections 5.1 and 5.2.

Lastly, a robust optimization study is performed for the four-engine configuration to determine a robust optimum, if any, at which the objective function is relatively insensitive to perturbations in the design variables.

CHAPTER IV

ANALYSIS PROCESS AND FRAMEWORK

4.1 Instantaneous Cutback Modeling

The first step in the analysis process was to simulate a takeoff with instantaneous power reduction, and to evaluate the flyover noise for this profile. The idea of using this "instantaneous cutback" approach was to understand the trend of EPNL variation with cutback altitude, and to compare this trend with that seen in the literature [11]. Moreover, the process for estimating the flyover noise level could be extended to a dynamic cutback that involves the engine spool down.

4.1.1 Flight Path for Instantaneous Cutback

Figure 23 below shows a takeoff flight path with instantaneous power reduction. There are two linear segments, one corresponding to the full power region and the other for the cutback power region. Due to the power reduction, the flight path angle of the cutback region of the flight path has a reduced flight path angle. This simple model was used initially in studying the effect of thrust cutback on flyover noise.

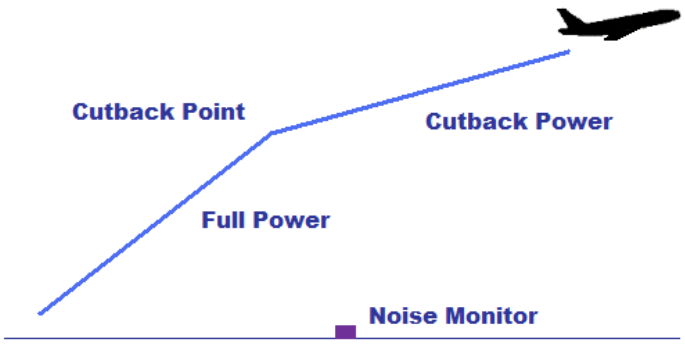

Figure 23: Instantaneous Cutback Simulation

4.1.2 Flight Path Noise Model (FLIGHTNOISE[1])

FLIGHTNOISE, depicted in Figure 24 below, is the Acoustics Model used for computing the noise history for a specified flight path segment. This model accepts engine component noise spectra that are determined for a specific corrected fan speed, and flight path parameters including flight path co-ordinates (X, Y), flight path angle (FPA), and angle of attack (AoA).

Figure 24: Flight Noise Model

The output of this model is the PNLT-Time history for the flight path flown at a constant corrected fan speed, as shown in Figure 25. The (X,Y) co-ordinates on the flight path at which source noise is emitted (i.e. "noise emission" points) are also generated, using which flyover observer angles can be calculated. Noise history shown as a function of observer angle is more useful for comparison studies, and is used in the Results and Analysis discussion in Chapter 5.

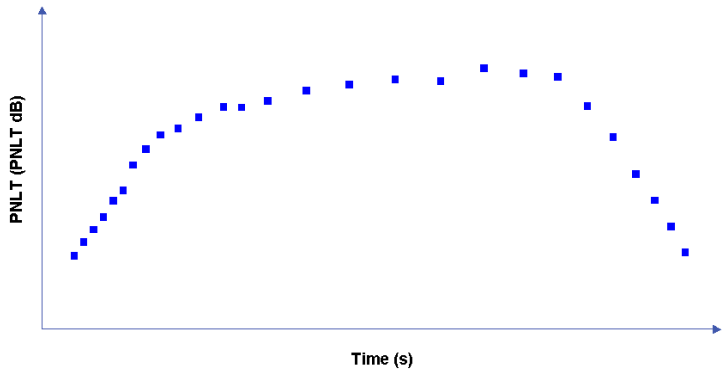

Figure 25: Noise History Output of FLIGHTNOISE Model

[1]This is a representative model name used for the purpose of this thesis.

4.1.3 EPNL Calculation

For instantaneous cutback, since there are two flight path segments, the Acoustics model FLIGHTNOISE needs to be run for both these segments in succession. This results in two PNLT-Time plots that are combined to produce a single PNLT-Time plot for the flight path as a whole. This plot in turn is used to compute the flyover EPNL.

Given two aircraft positions on a linear flight path as shown in Figure 26, the time elapsed between measurements of noise emitted from these positions is given by the equation:

$$t = \frac{P_2 - P_1}{V} + \frac{d_2 - d_1}{c}$$

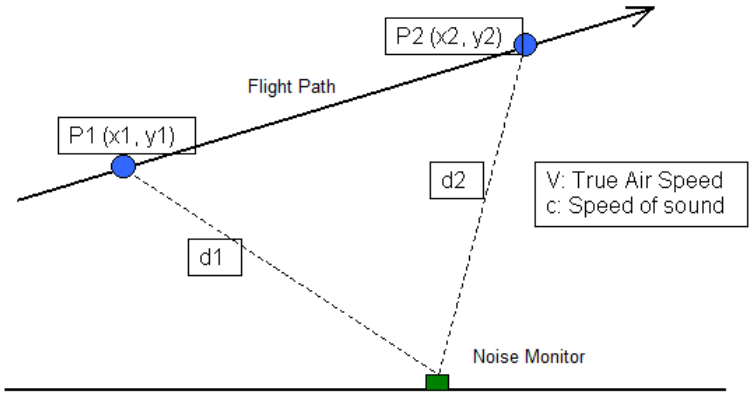

Figure 26: Flight Path Geometry for Noise Measurements

This principle is applied while computing the PNLT values for a two-segment instantaneous cutback, and is described below.

In Figure 27, there are two line segments, A-B and C-D, representing full power and cutback flight paths respectively. The cutback point is the intersection of the two segments, indicated by X. In the instantaneous cutback model, the aircraft flies along A-X, and then along X-D.

As shown in Figure 28, flight paths A-B and C-D yield two different PNLT-Time curves, where the 0.5-second PNLT points are represented by blue circles for A-B and pink circles for C-D. The maximum value of PNLT ($PNLT_M$) of the noise history for C-D is assumed to correspond to a time of 0 seconds. The noise history for the flight path with instantaneous cutback (i.e. A-X-D) is then computed as follows.

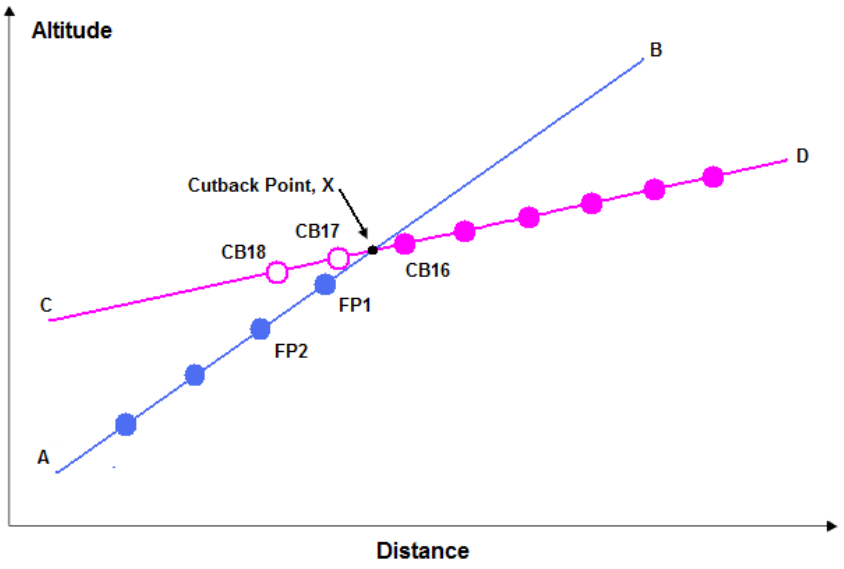

Figure 27: Noise Emission Points on Flight Path with Instantaneous Cutback

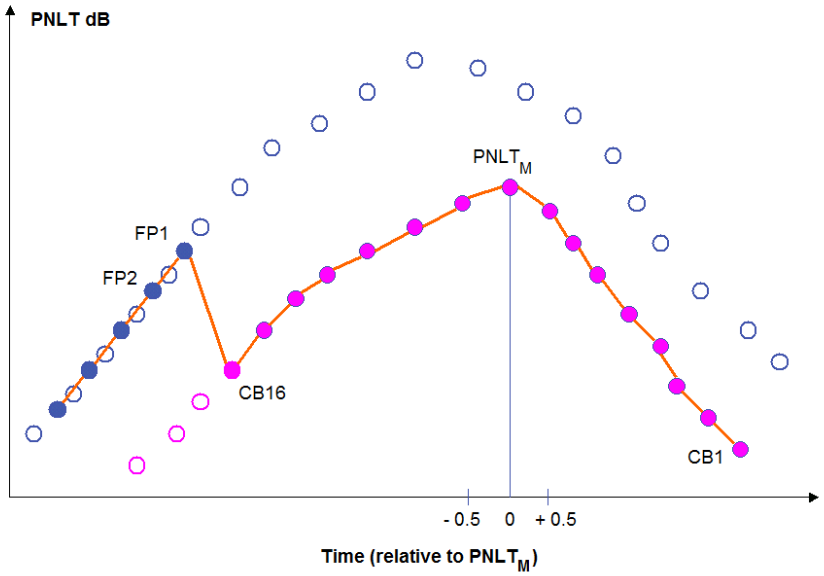

Figure 28: Calculating PNLT Values for Instantaneous Cutback

(a) Select all the 0.5-second PNLT points for the flight path segment X-D in reverse, i.e. beginning from point CB1 (which represents a 10 dB drop from $PNLT_M$).

(b) Find the time elapsed between the CB16 (the last point on X-D, as shown in Figure 27) and the cutback point X. This time, say t_{seg}, is less than 0.5 seconds since the previous 0.5-second point on segment C-D is CB17, which is to the left of X.

(c) Determine the co-ordinates of point FP1 on flight path segment A-B such that the time elapsed in noise measurement between FP1 and X is (0.5 - t_{seg}) seconds. This is done using the geometry described in Figure 26.

(d) Determine the PNLT value at FP1 by interpolating between the PNLT values bounding FP1 on the full power curve.

(e) Find the remaining points on A-B in reverse by calculating the position every 0.5 second back in time, and then interpolating to find the required PNLT value.

(f) From the set of PNLT values determined from steps (a) to (e), find the maximum PNLT value. In most cases, $PNLT_M$ of the cutback segment C-D shown in Figure 28 will be the overall maximum as well. However, it may happen that a point of the full power curve has a higher PNLT value. In either case, find the PNLT values that fall within a 10 dB-down window of the overall maximum PNLT, and finally compute the EPNL using these values.

This process was extended to compute the EPNL for a dynamic cutback as well, and is described in Section 4.2.

4.1.4 Instantaneous Cutback Optimization

In order to understand the effect of the cutback procedure in reducing flyover noise, a simple optimization framework was built, and the only design variable considered was the cutback initiation altitude. The framework was designed such that it could later incorporate a flight path model and other acoustics tools.

For this simple optimization model, it was assumed that cycle conditions for the full power and cutback flight segments are constant. The optimization problem formulation for instantaneous cutback is as follows.

Minimize: Flyover EPNL

Varying: Cutback Initiation Altitude

The optimization results are shown in Figure 29 below.

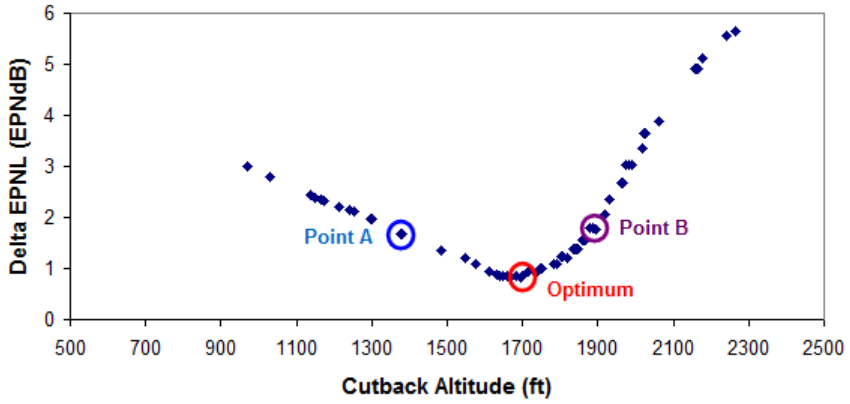

Figure 29: Instantaneous Cutback: EPNL vs Cutback Altitude

To understand why such a trend is observed, three points on the curve are considered - Point A, Point B, and the Optimum. At point A, the cutback altitude is 1,350 ft, at B, it is 1,900 ft, and at the optimum, it is 1,700 ft. Let the corresponding EPNL values be $EPNL_A$, $EPNL_B$, and $EPNL_{OPT}$.

The flight path for each of these points and the corresponding noise history are shown in Figure 30 and Figure 31 below.

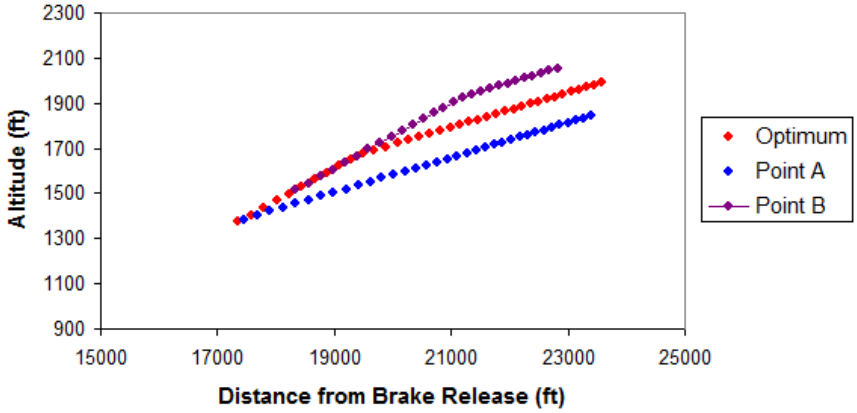

Figure 30: Instantaneous Cutback: Noise Emission for Different Cutback Altitudes

It is observed that for point A, cutback is initiated too far ahead of the noise monitor, and therefore the aircraft's altitude over the monitor is low as most of the climb segment is using reduced thrust. Therefore, the EPNL is relatively high in this case. On the other hand, for point B, although cutback occurs at a high altitude, most of the time history is at

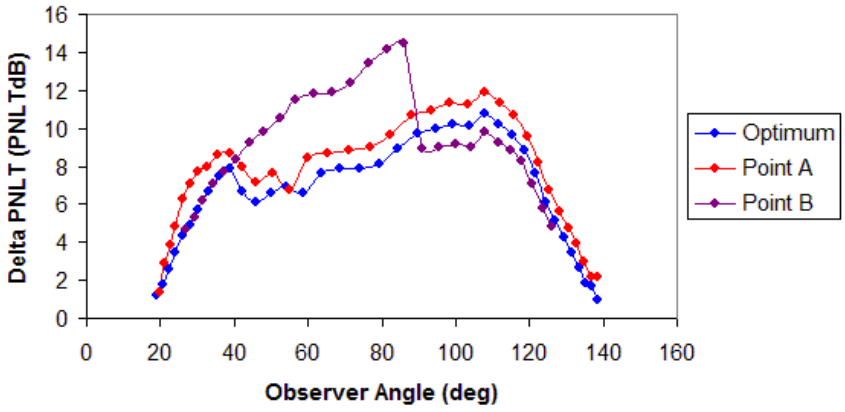

Figure 31: Instantaneous Cutback: Noise History for Three Cases

full power and reduced thrust impact on time history is relatively minor leading to a high EPNL. There is an optimum altitude to perform cutback that minimizes the EPNL.

4.2 Dynamic Cutback Modeling and Optimization

This section describes the design process and tools used for modeling dynamic cutback. The optimization problem formulation and framework is then discussed.

4.2.1 Modeling Environment

In order to verify the hypotheses stated in Chapter 3 and understand the effect of engine spool down in a cutback procedure, a multi-disciplinary framework was built incorporating a takeoff simulation model, a suite of acoustics tools, and a quasi-transient engine cycle model. The framework is shown in Figure 32 below, and the individual tools are described in subsequent sections.

4.2.2 Takeoff Simulation Model (TAKEOFF[2])

This model simulates an aircraft takeoff with dynamic cutback. The aircraft is considered to be a point mass, while the flight trajectory is computed by time-integrating a set of differential equations. The inputs to the Takeoff Simulation Model include:

(a) Aircraft gross weight at takeoff

(b) Wing area

[2]This is a representative model name used for the purpose of this thesis.

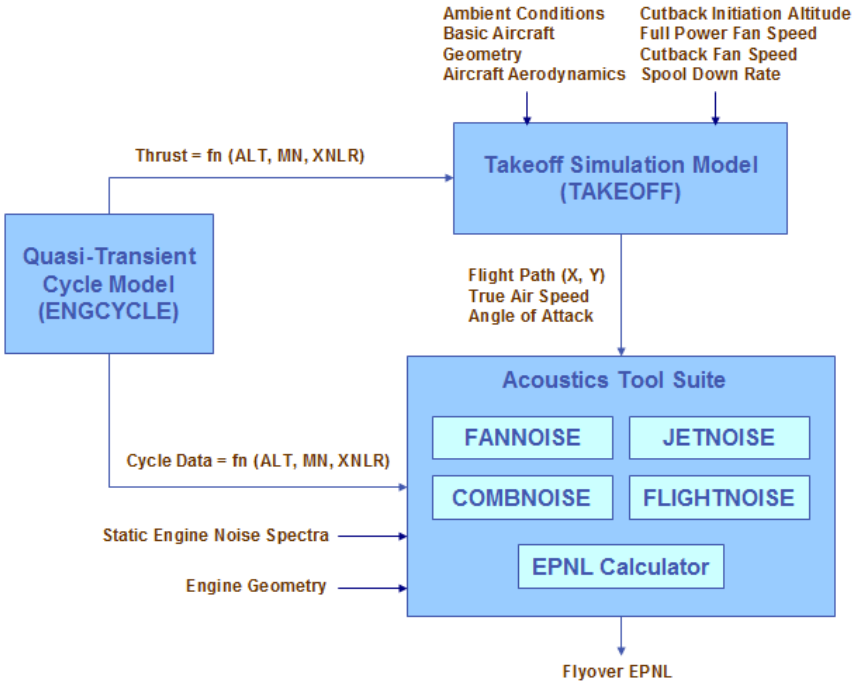

Figure 32: Integrated Dynamic Cutback Model

(c) Number of engines

(d) Drag polar

(e) Thrust per engine as a function of altitude, Mach number, and corrected fan speed

(f) Rotation velocity, V_R

(g) Rotation rate

(h) Cutback initiation altitude

(i) Corrected fan speed at takeoff power

(j) Corrected fan speed at cutback power

(k) Spool down rate

The flight path is computed for different segments, where each segment has specific initial and termination conditions. A typical flight path generated by this model is shown in Figure 33. The flight path segments are defined as follows.

Segment 1: V_0 to V_R (Start of takeoff roll to Rotation speed)

Segment 2: V_R to V_{LOF} (Rotation speed to Liftoff speed)

Segment 3: V_{LOF} to V_{CLIMB} (Liftoff speed to All-engines climb speed)

Segment 4: V_{CLIMB} to ALT_{CB_INIT} (All-engines climb speed to Cutback Init Altitude)

Segment 5: ALT_{CB_INIT} to ALT_{CB_END} (Cutback Init Altitude to Cutback End Altitude)

Segment 6: ALT_{CB_END} to ALT_{FLT_END} (Cutback End Altitude to Flight Path End Altitude)

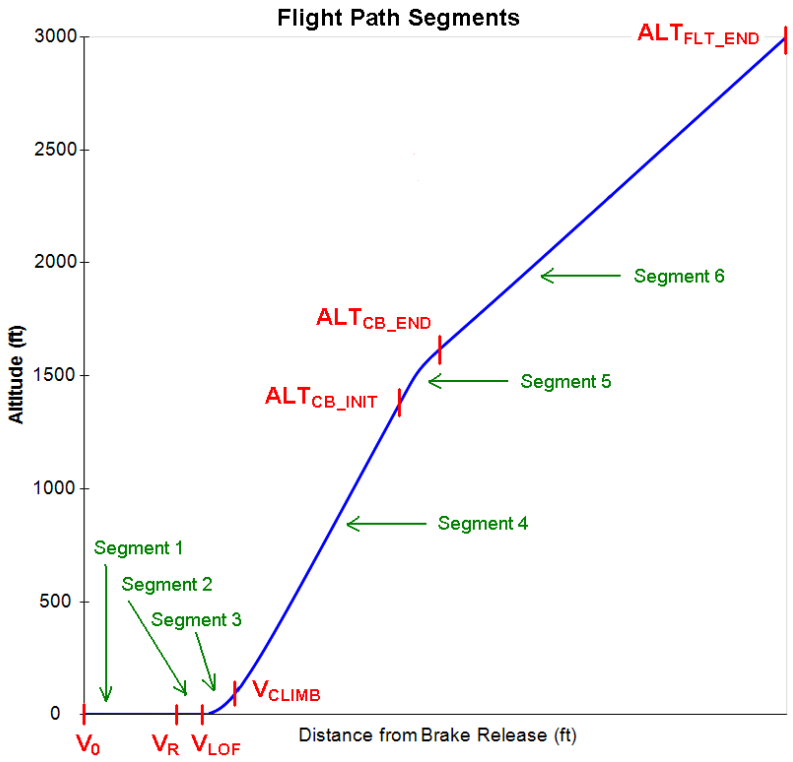

Figure 33: Flight Path Segments in Takeoff Simulation Model

Segment 1 corresponds to the takeoff run from brake release to the point where the specified rotation speed is attained. In this segment, angle of attack is constant. Segment 2 starts as soon as Segment 1 ends. Here, the angle of attack is increased at a constant rate of 3 deg/s (assumed) until the point where enough lift is generated to make the aircraft airborne. The speed at this point is designated as V_{LOF}. Segment 3 then begins where Perry's Control Law (described in the following section) is applied to smoothly bring the aircraft into a climb mode at the obstacle reference height of 35 ft.

The speed at the end of this segment is V_{CLIMB}, which corresponds to the all-engines screen speed, also referred to as V_3 [25]. The takeoff safety speed V_2 is the airspeed obtained at a height of 35 ft with one-engine-inoperative. For the purpose of verifying if the climb

speed constraint as per ICAO Annex 16 Volume 1 is satisfied, V_2 is computed as:

$V_2 = V_{CLIMB} - 10\,kts$, as per Torenbeek [25].

The takeoff climb then continues in Segment 4 until the specified cutback initiation altitude is reached. At this point, Segment 5 begins wherein the engine spools down to the required corrected fan speed. The duration of this segment is decided by the specified spool down rate. The final segment, Segment 6 starts from the point where spool down ends to an altitude of 3,000 ft, which represents the termination point of the noise certification flight.

Perry's Control Law for Rotation Phase

Perry's Control Law [26] assumes that the aircraft is rotated at a constant rate of pitch from the moment of lift-off to the point at which it attains a steady climb path. This assumption (described in detail in [26]) was based on the following findings by Perry:

(a) "Data from real and simulated takeoffs suggests that the rotation technique actually used by pilots resembles one with constant rate of pitch."

(b) "Rate of pitch and pitch attitude can be directly sensed and controlled by the pilot, unlike other variables such as the lift coefficient."

This law can be represented by the equation:

$\frac{d\gamma}{dt} + \frac{d\alpha}{dt} = C(constant)$

It is observed that modeling Perry's Control Law results in a smooth transition from liftoff to climb, as shown in the plots in the next section.

Modeling Dynamic Cutback

Modeling dynamic cutback in the flight path model requires an appropriate control mechanism such that the flight path is stabilized both during and after the cutback. Different control mechanisms were applied to obtain a flight path trajectory that best matched flight data points from actual flight tests. Some observations with different control techniques are illustrated in Figures 34, 35 and 36.

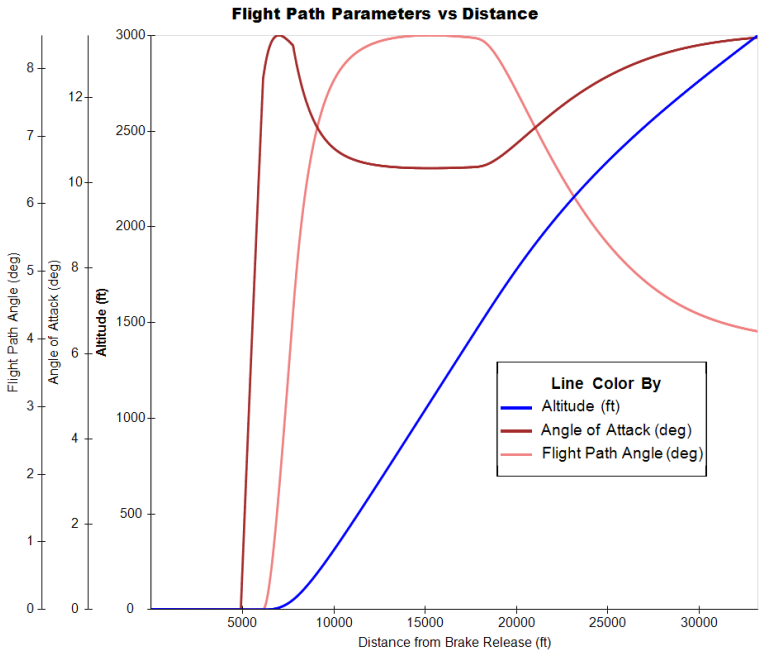

Figure 34: Flight Path Parameters for Control Logic A

Figure 34 shows the flight path, and variation of the angle of attack and the flight path angle when the same control logic for the initial climb is applied to the spool-down and post-cutback regions (Case A). It is seen that the flight path angle continues to decrease gradually even after the cutback procedure has ended. This is not acceptable, as the flight path angle should remain more-or-less constant after engine spool down has been completed. Also, the flight path curvature spans a large altitude range, which is unlike flight paths observed for actual noise certification tests.

Figure 35 shows the same flight parameters for the case when angle of attack is held constant during the takeoff climb (Case B). In this scenario, the resultant flight path enters into a phugoid mode, with flight path angle varying as a damped oscillation. Therefore, this control technique was ruled out as well.

The control logic for the spool down region that resulted in the most favorable flight path was when net acceleration dV/dt during the spool down region was zero (Case C). The corresponding flight parameters are shown in Figure 36. In this scheme, the angle of attack is computed at each time step in the spool down region. It is observed that the angle of attack decreases linearly while thrust is decreased. In the flight segment following the

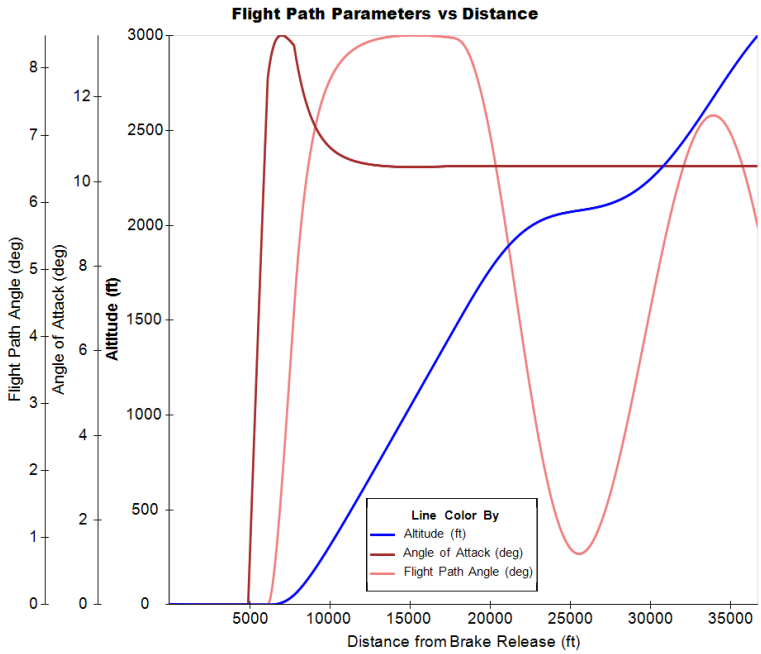

Figure 35: Flight Path Parameters for Control Logic B

end of spool down, a variant of Perry's Control Law is applied to stabilize the flight path angle and angle of attack. The resultant flight path closely matched actual flight path data points.

Therefore, the third approach ($dV/dt = 0$ during spool down) was selected as the control logic for the spool down region. This was found to give satisfactory results for a range of cutback initiation altitudes and spool down conditions.

4.2.3 Fan Noise Model (FANNOISE[3])

The Engine Fan Noise Model FANNOISE uses fan noise spectra from static engine testing for specific fan speeds, cycle data for both static and target flight conditions (altitude, Mach number, corrected fan speed), and certain engine geometry parameters to determine the acoustic spectra (Sound Pressure Level values) for the fan for the target conditions. The noise spectra are predicted separately for the fan inlet and the fan exhaust, which are used as inputs to the FLIGHTNOISE module. Figure 37 illustrates the FANNOISE model.

[3]This is a representative model name used for the purpose of this thesis.

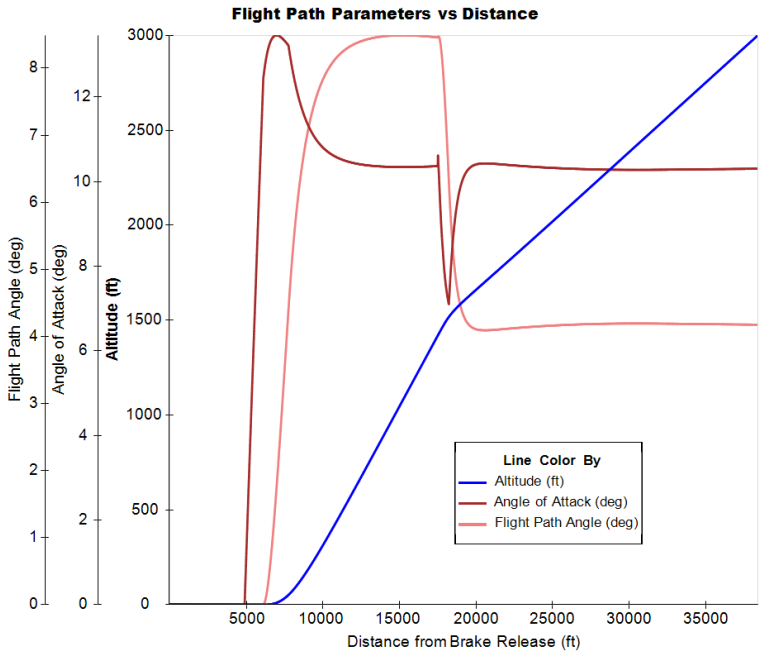

Figure 36: Flight Path Parameters for Control Logic C

Figure 37: Fan Noise Model

4.2.4 Jet Noise Model (JETNOISE[4])

The Jet Noise Model JETNOISE accepts jet noise spectra from static engine testing for specific corrected fan speeds, cycle data for these fan speeds, and cycle data for the target conditions (altitude, Mach number, corrected fan speed). Appropriate scaling parameters are used to determine the acoustic spectra for the jet for the target conditions. The output noise spectral data is used by the FLIGHTNOISE module. Figure 38 illustrates the JETNOISE model.

[4]This is a representative model name used for the purpose of this thesis.

Figure 38: Jet Noise Model

4.2.5 Combustor Noise Model (COMBNOISE[5])

The Combustor Noise Model COMBNOISE accepts combustor noise spectra determined from overall static engine spectra, and also accepts cycle data for the target conditions (altitude, Mach number, corrected fan speed). Again, scaling techniques are used to determine the acoustic spectra for the combustor for the target conditions. This output spectra is used as input to the FLIGHTNOISE module. Figure 39 illustrates the COMBNOISE model.

Figure 39: Combustor Noise Model

4.2.6 Engine Cycle Model (ENGCYCLE[6])

The Engine Cycle Model is a quasi-transient model that contains cycle parameter values for a range of altitudes, Mach numbers, and corrected fan speeds for the acoustic standard day, i.e. ISA+18F and 70% humidity. This range of parameters covers all possible conditions under which dynamic cutback can be performed, and is illustrated in Figure 40. Linear interpolation is used to determine cycle data for specific target conditions.

Table 1 below lists the cycle parameters used by the engine component acoustic models.

[5]This is a representative model name used for the purpose of this thesis.
[6]This is a representative model name used for the purpose of this thesis.

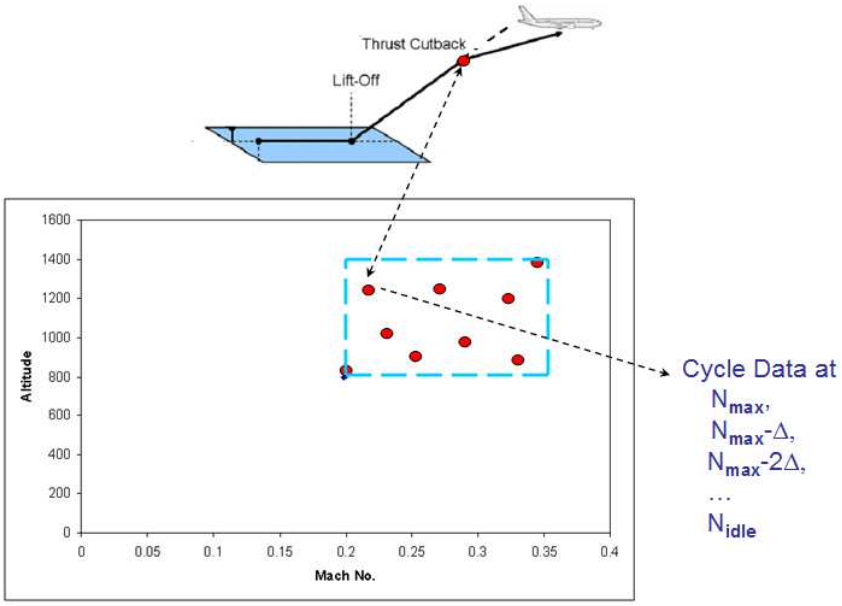

Figure 40: Engine Cycle Model

4.2.7 Process to Model Dynamic Cutback

The modeling of dynamic cutback and flyover noise prediction was done by integrating the takeoff simulation model and the acoustic tools described in the previous section. A process was developed to divide the spool down region of the flight path into multiple linear segments. This division enables the acoustic evaluation for the entire flight path to be carried out, considering varying cycle conditions during the power reduction.

The process for computing flyover EPNL is described as follows.

1. Run takeoff simulation model for given inputs of full power corrected fan speed, cutback initiation altitude, cutback corrected fan speed, and spool down rate.

2. Calculate the total number of linear flight path segment divisions based on the fan speeds and spool down rate.

$$SegmentCount = \frac{(FullPowerRPM - CutbackRPM)}{SpoolDownRate} \times 2$$

(This equation generates an adequate number of segments that capture the spool down region accurately.)

3. With the assumption that each linear segment represents a fraction of the flight path

Table 1: Cycle Parameters used by Acoustics Model

Cycle Parameter Name	Description	Units
JETFNV	Fan nozzle velocity	ft/s
JETFA	Fan area	sq.ft
JETFWF	Fan weight flow	lb/s
JETCNV	Core nozzle velocity	ft/s
JETCA	Core area	sq.ft
JETCPR	Core nozzle pressure ratio	-
JETCWF	Core weight flow	lb/s
JETCT	Core temperature	deg R
COMITT	Combustor inlet total temperature	deg R
COMITP	Combustor inlet total pressure	lb/sq.in
COMIWF	Combustor inlet weight flow	lb/s
COMETT	Combustor exit total temperature	deg R
COMDTT	Turbine inlet total temperature at takeoff power minus turbine exit total temperature at takeoff power	deg R
VMIX	Jet mixing velocity	ft/s
W2ARE	Corrected inlet mass flow	lb/s
W18E	Fan exhaust mass flow	lb/s
P1312E	Fan pressure ratio	-
RPME	Physical fan speed	rpm
RPMCE	Corrected fan speed	rpm
VELJET	Core velocity	ft/s

flown at constant power, calculate the corrected fan speeds for the linear segments.

4. Determine the co-ordinates of these linear segments by analyzing the continuous flight path data and determining exactly where the above fan speeds are attained.

5. For each linear segment, perform the following.

(a) Determine the flight path parameters (true air speed, flight path angle, and aircraft angle of attack), and engine cycle conditions.

(b) Run the acoustic tools FANNOISE, COMBNOISE, JETNOISE to compute the engine component noise spectra at the corrected fan speed assumed to be constant for the segment.

(c) Run the acoustic tool FLIGHTNOISE to compute the noise history (PNLT vs Time) for the segment.

6. After the noise history for each flight path segment has been determined, compute the resultant noise history for the flight path as a whole using the technique described in Section 4.1.3, and finally compute the EPNL.

Figure 41 below shows the spool down region of the flight path divided into three segments A-B, B-C and C-D with corresponding constant fan speeds RPM1, RPM2 and RPM3. The points marked in red are the noise emission points on the flight path that yield 0.5 second PNLT measurements.

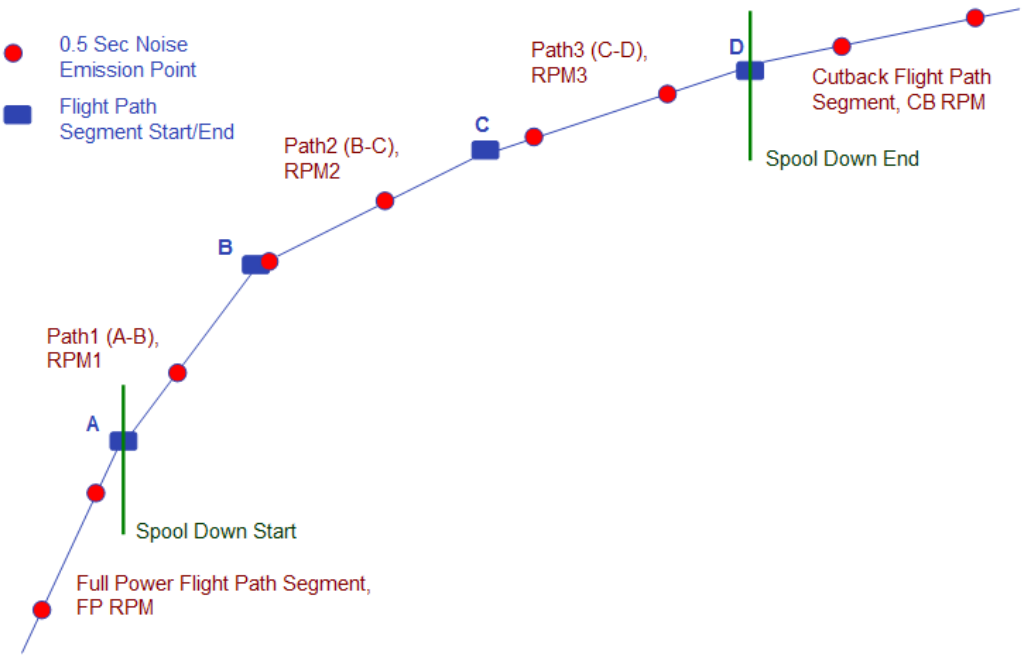

Figure 41: Determining Noise Emission Points on Flight Path

These emission points are calculated in reverse - starting from the cutback segment, through the spool down segments, and finally the full power segment. When the cutback flight path segment ends (at point D), the previous emission point (on the final spool down segment) should be determined such that 0.5 sec have elapsed in the noise measurement.

The remaining 0.5-second noise emission points are calculated in a similar manner. If the number of spool down segments is large, there is a possibility that no emission point will be found on a given segment (as the duration of the segment itself is less than 0.5 seconds). In this case, this segment will need to be skipped, and the previous emission point will be

found on the segment preceding this one.

4.2.8 Dynamic Cutback Optimization Problem Formulation

The Dynamic Cutback optimization problem can be formulated as follows.

Minimize: Flyover Certification EPNL

Varying: Cutback initiation altitude, Cutback corrected fan speed, Fan spool-down rate

Subject to: ICAO Annex 16 Vol 1 constraints

The integrated framework consisting of all the above models and the FLIGHTNOISE (described in Section 4.1.2) module is shown in Figure 42.

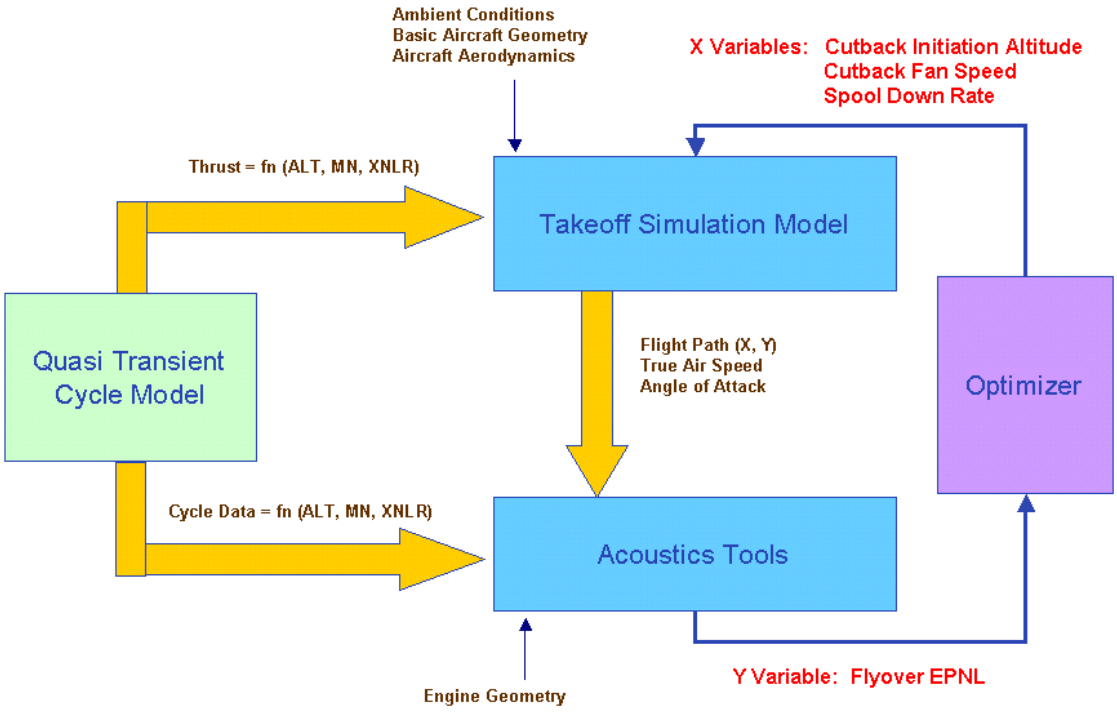

Figure 42: Dynamic Cutback Optimization Framework

The Takeoff Simulation Model TAKEOFF generates the required takeoff profile based on input design variable values provided by the optimizer. The takeoff path is then used for performing acoustic evaluation, and determining the objective function value, which is the flyover EPNL.

This framework allows the user to easily perform dynamic cutback optimization studies for different airframe/engine configurations. It also enables the user to assess the shift in the optimum design point due to changes in airframe/engine configuration or cycle conditions.

The optimization framework also allows other variables to be used as optimization design variables. However, for the purpose of this research effort, only three key variables pertaining to dynamic cutback were used.

4.2.9 Constraints

Section 3.6.2 of the ICAO Annex 16 Volume 1 [5] specifies constraints that need to be satisfied by the takeoff flight procedure for noise certification. These include a minimum cutback initiation altitude depending on the number of engines, a minimum climb gradient after reduction in power, constraints on the climb speed, and maintaining a constant takeoff configuration except for landing gear retraction. These constraints are discussed below.

Cutback Initiation Altitude

As per the ICAO, thrust reduction for a cutback procedure can begin only when the following height is reached:

(a) Aircraft with two engines or less - 984 ft

(b) Aircraft with three engines - 853 ft

(c) Aircraft with four engines or more - 689 ft

At the beginning of the optimization process, the lower bound for the cutback initiation altitude is checked against these minimum altitudes, based on the number of engines selected.

Climb Gradient

The constraint on climb gradient states that the thrust during the cutback procedure should not be reduced below that required to maintain:

(a) a climb gradient of 4%, or

(b) in the case of multi-engined aircraft, level flight with one engine inoperative

whichever thrust is greater.

Thus, the optimizer needs to check if the all-engines-operating and one-engine-inoperative

climb gradients are least 0.04 and 0 respectively, from the initiation of cutback till the end of the noise certification flight path.

The climb gradient is a measure of climb performance, and is defined as the ratio of climb rate to forward speed (Figure 43). For a constant speed climb, the climb gradient can also be expressed as the ratio of (Net Thrust - Drag) and aircraft weight [27].

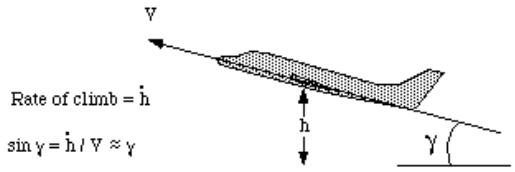

Figure 43: Climb Gradient

All-engines Climb Gradient: $Grad_{OEI} = \frac{((ThrustPerEngine \times N) - Drag)}{Weight}$

where N is the number of engines on the aircraft.

In the takeoff simulation model, the all-engines climb gradient is calculated as per the equation above at each time step starting from the point of cutback initiation to the end of the flight path. For the one-engine case, the equation below was assumed to hold good, instead of simulating an engine failure during the cutback and calculating the OEI gradient.

One-engine-inoperative Climb Gradient: $Grad_{OEI} = \frac{((ThrustPerEngine \times (N-1)) - Drag)}{Weight}$

Also, it is reasonable for the purpose of this thesis to assume that the additional drag due to the failed engine is negligible.

Climb gradient plots are shown in Chapter 5 for a four-engine and twin-engine commercial aircraft. For any iteration in the optimization process, if the flight path generated by the takeoff simulation model violates these climb gradient requirements, subsequent acoustic evaluation of the flight path is not performed. The objective function (EPNL) is set to a high value indicating to the optimizer that this is not a feasible run.

Climb Speed

The ICAO states that the climb speed for the noise certification test should be the all-engines operating takeoff climb speed, which should be at least $V_2 + 10kt$, but not greater than $V_2 + 20kt$. Moreover, the climb speed should be attained as soon as possible after

liftoff, and maintained throughout the flight test.

As discussed in Section 4.2.2, the velocity during engine spool down was held constant in the takeoff simulation, so as to generate an accurate flight path that closely matched real flight test data. However, it was observed that in general, for high spool down rates, the angle of attack variation was high, leading to an increase in speed that violated the maximum climb speed constraint. Optimization results in Chapter 5 show that the climb speed constraint is satisfied for moderate spool down rates.

Constant Takeoff Configuration

It is required that the aircraft configuration be held constant for the entire noise certification test, except for the landing gear which may be retracted. In the dynamic cutback optimization process, the landing gear retraction may be optionally modeled, in which case a small drag penalty is added.

4.2.10 Choice of Optimizer

The dynamic cutback optimization problem may be solved by a number of optimizers, either gradient-based optimizers like CONMIN [28] and SQP, or heuristic optimizers like Genetic Algorithms (GA) [29]. However, GA was selected for the purpose of this thesis for the following reasons.

(a) The Genetic Algorithm does not require an initial guess of the design variables (viz. cutback initiation altitude, cutback fan speed, and spool down rate), unlike traditional optimizers. This is a big advantage especially when the designer does not know the region of the design space where the global optimum might lie.

(b) GA-based optimization can automatically result in multiple solutions, if these exist. Different optimal solutions could be found by gradient-based optimizers too, but only for different initial guesses. As one of the research questions in this thesis asks if multiple global optima exist, it was decided to apply GA to locate these optima automatically.

(c) Due to its exploratory nature, the Genetic Algorithm surveys the entire design space

in search of the global optimum. As the number of generations increases, the concentration of points in the region around the global optimum increases. This trend may be very useful in understanding the nature of the problem, and may give insights into the design space being considered. Such trends are plotted in Chapter 5.

A disadvantage of GA's is that it is computationally expensive due to the fact that a large number of runs are required. For the dynamic cutback optimization problem, the number of runs could be 200 or more, with each run taking 2 minutes on average to complete.

CHAPTER V

RESULTS AND ANALYSIS

This chapter discusses results from various studies performed using the integrated framework described in the previous chapter. These results are used to prove or disprove the hypotheses stated in Section 1.3.

5.1 Dynamic Cutback Study for a Four-Engine Aircraft

This section discusses results from different dynamic cutback studies carried out for a four-engine commercial transport aircraft.

5.1.1 Effect of Cutback Initiation Altitude

A simple DOE study was carried out to analyze the effect of the dynamic cutback procedure for different cutback initiation altitudes. In this study, the cutback fan speed was set to 88% of the full power fan speed (leading to a thrust reduction of around 35%), and the spool down rate was held constant as well. The flyover delta EPNL values are plotted against the cutback initiation altitude in Figure 44 below.

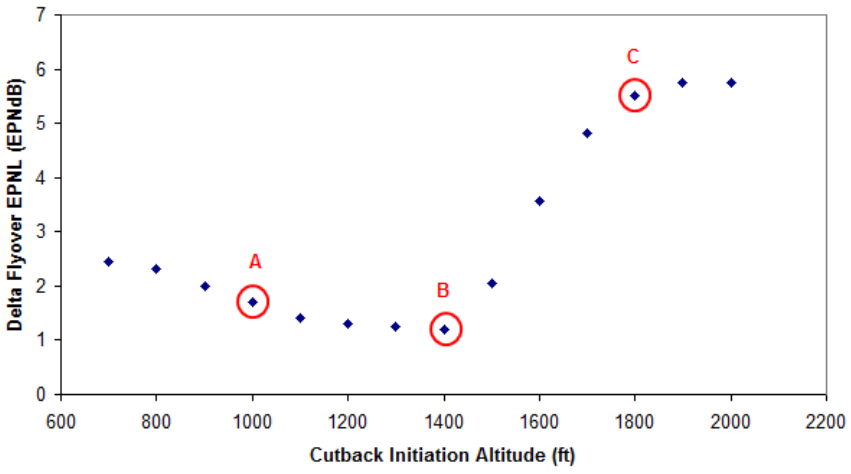

Figure 44: Flyover EPNL vs Cutback Initiation Altitude for Four-Engine Aircraft

Similar to the analysis carried out for the "instantaneous" cutback simulation, three

points are considered in this plot at which the flight trajectory and noise history are analyzed. This helps in understanding the effect of dynamic cutback on flyover noise.

In Case A, cutback is initiated at an altitude of 1,000 ft, case B at 1,400 ft, and case C at 1,800 ft. The flight paths for the three cases are plotted in Figure 45, along with the corresponding noise emission co-ordinates that are responsible for the overall flyover noise. The delta EPNL values for the three cases are 1.71, 1.2, and 5.51 EPNdB respectively.

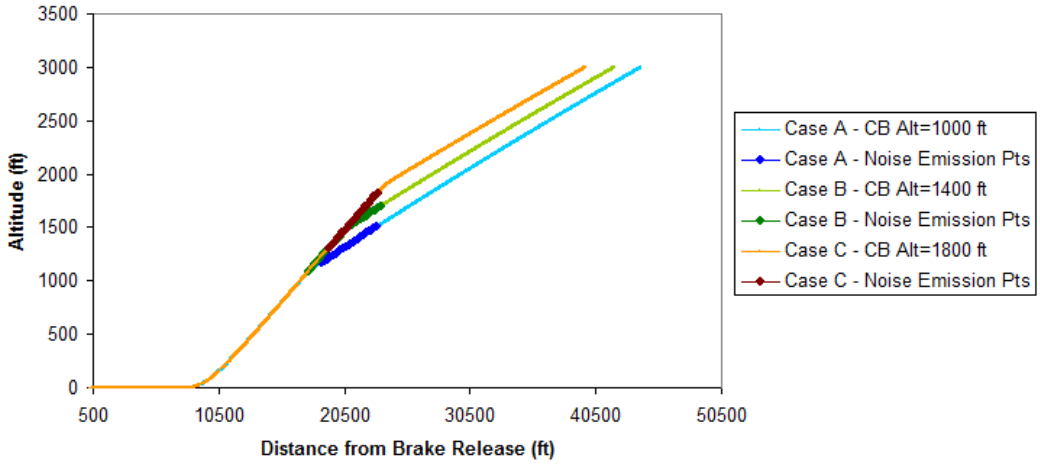

Figure 45: Flight Paths for Different Cutback Altitudes for Four-Engine Aircraft

As can be seen in the figure, in Case A, as cutback is initiated relatively early, the noise emission from the flight path after cutback is responsible for certification noise at the flyover microphone. Although the aircraft is at reduced power in this region, the noise emission points are at relatively lower altitudes resulting in higher PNLT values, and consequently a high EPNL value. In Case C, cutback is initiated at a relatively high altitude (1,800 ft), but the advantage of the altitude increase is offset by the noise being primarily produced from the full power region of the flight path. The PNLT values again are relatively higher, leading to a high EPNL.

The optimal case for this study is Case B, wherein cutback is initiated at 1,400 ft. This altitude produces the lowest EPNL, as there is a good balance between altitude gain and reduced noise emission. The noise emission points are from all three regions of the flight path, viz. full power, spool down, and post-cutback regions. This is highlighted in Figure 46.

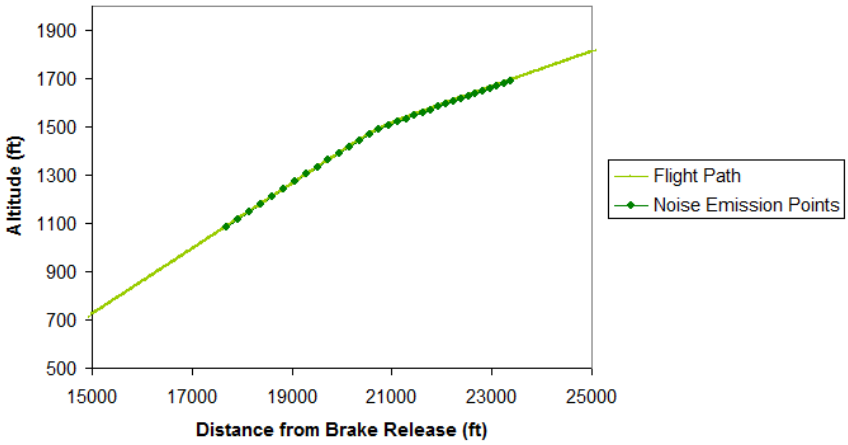

Figure 46: Noise Emission Points on Flight Path with Cutback at 1,400 ft for Four-Engine Aircraft

The flight path parameters for the optimal case, i.e. Case B are plotted in Figure 47. It is seen that the aircraft maintains a constant climb and angle of attack after the end of the cutback procedure.

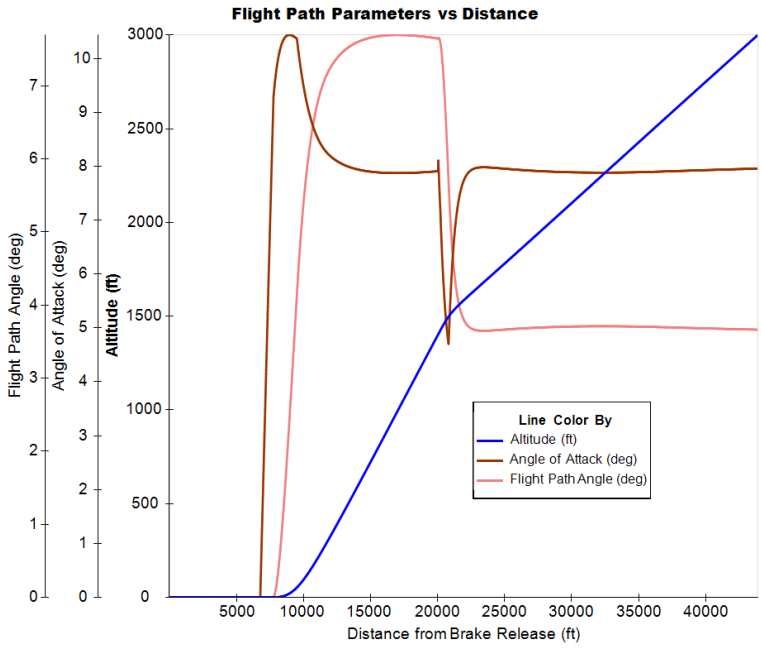

Figure 47: Flight Path Parameters vs Distance for Four-Engine Aircraft

The all-engines-operating (AEO) and one-engine-inoperative (OEI) climb gradients as a function of distance are shown in Figure 48. The minimum stipulated AEO and OEI gradient requirements of 0.04 and 0 respectively are satisfied. However, the climb speed,

which should be contained within a band of $V_2 + 10\ kts$ and $V_2 + 20\ kts$ as per ICAO requirements, is not satisfied (Figure 49). This constraint is built into the optimization process, and discussed in Section 5.1.4.

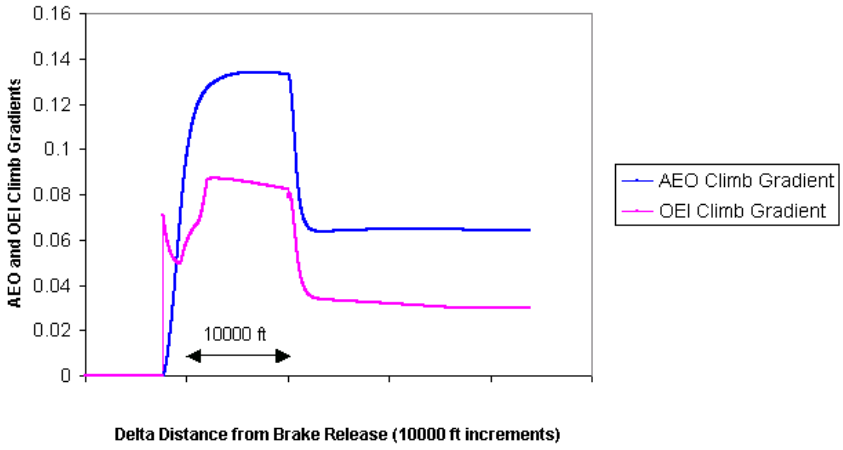

Figure 48: Climb Gradients for Four-Engine Aircraft

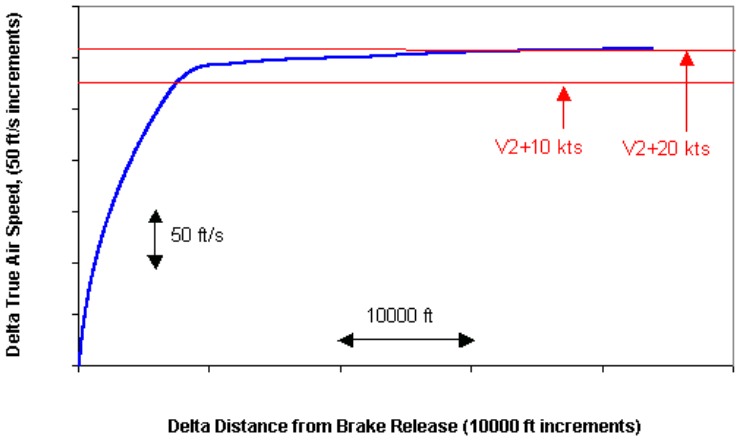

Figure 49: Climb Speed for Four-Engine Aircraft

The noise histories for the three cases (Case A, Case B, Case C) are plotted in Figure 50. For Case A, the maximum PNLT value $PNLT_M$ is recorded at an observer angle of around 110 degrees. All the PNLT values are from the post-cutback region of the flight path. For Case C, only the final PNLT value is from the spool down region, while all the other points are from the full power region of the flight path. Due to the full power operation, it is seen that PNLT values (including $PNLT_M$) for this case are significantly higher than in

the other two cases, leading to a high EPNL value. For the optimum case, i.e. Case B, the entire spool down region contributes to the overall noise. For all observer angles up to around 35 degrees, the PNLT values are higher than in Case A, due to noise from the full power region. The spooling down of the engine causes a decrease in PNLT values, leading to a lower $PNLT_M$, and also a lower integrated noise value.

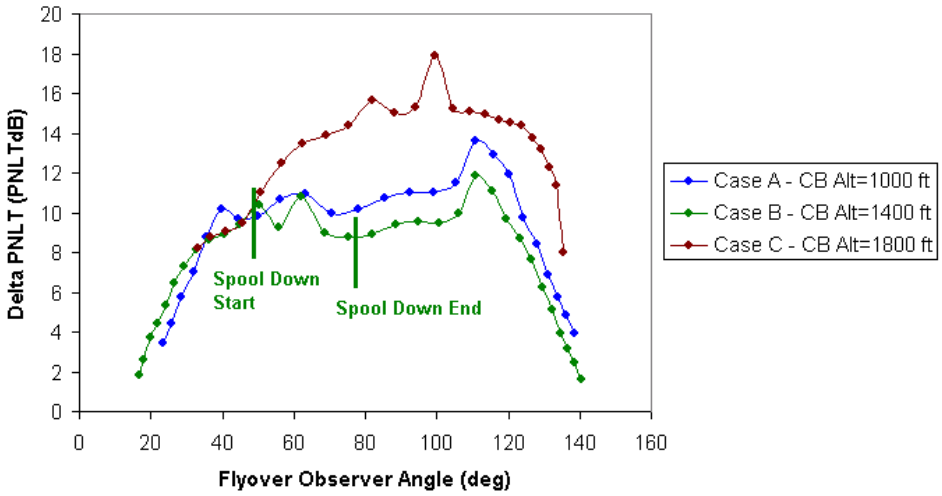

Figure 50: Noise History for Different Cutback Altitudes for Four-Engine Aircraft

5.1.2 Effect of Spool Down Rate

In this section, the effect of fan spool down rate is studied for the same four-engine aircraft configuration as in the previous section. In this study, the cutback initiation altitude is fixed at 1,100 ft, and the cutback corrected fan speed is fixed at 88% of the full power corrected fan speed. Figure 51 shows the variation of flyover EPNL with spool down rate for a cutback initiation altitude of 1,100 ft. It is observed that a delta spool down rate of 50 rpm/s gives a noise benefit of 0.5 EPNdB compared to a delta spool down rate of 500 rpm/s, which is close to an instantaneous cutback.

This clearly demonstrates the fact that modeling engine spool down has the potential to reduce flyover noise.

The noise emission points on the flight paths for three cases A, B, and C (with delta spool down rates of 0, 40, and 160 rpm/s) are shown in Figure 52, and the PNLT noise history for these cases is plotted in Figure 53. The delta EPNL values for the three cases

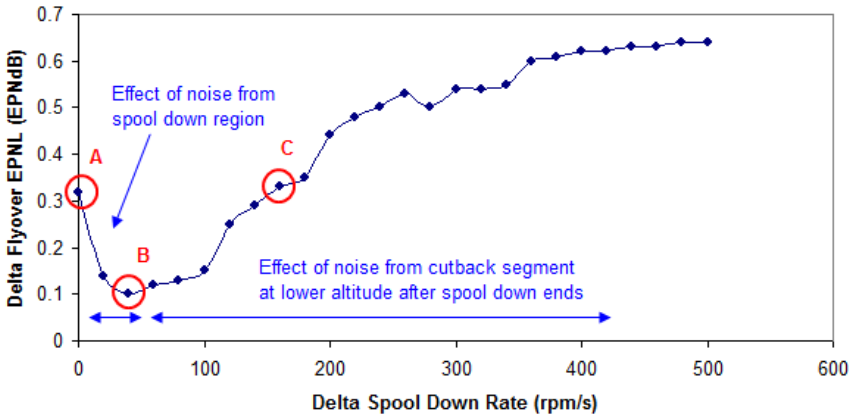

Figure 51: Effect of Modeling Spool Down for Four-Engine Aircraft

are 0.31, 0.1, and 0.33 EPNdB.

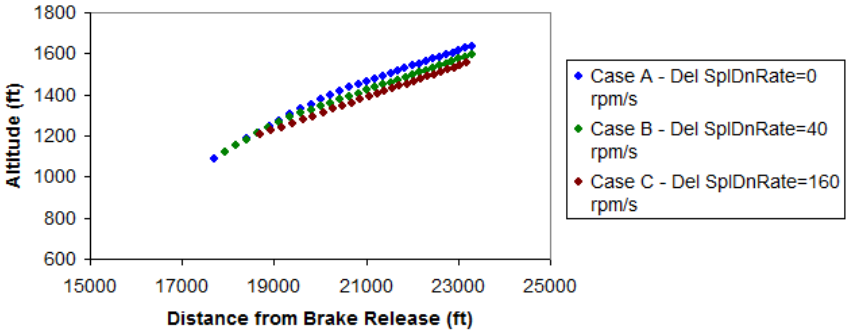

Figure 52: Noise Emission Points for Different Spool Down Rates for Four-Engine Aircraft

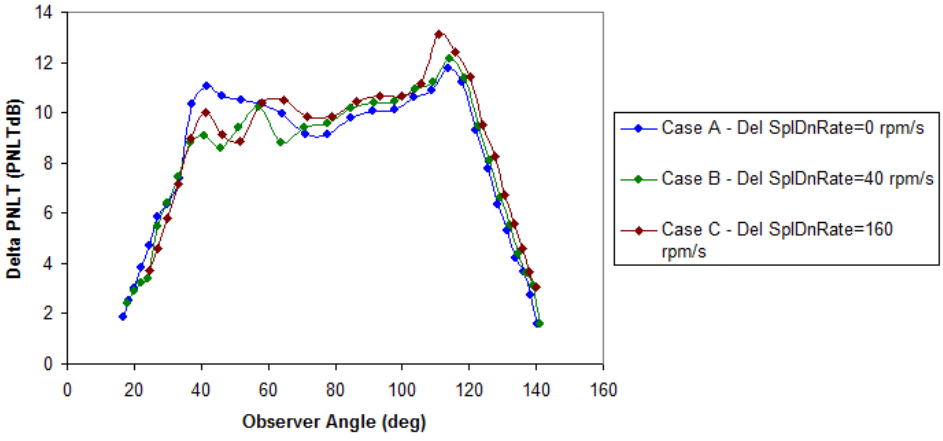

Figure 53: Noise History for Different Spool Down Rates for Four-Engine Aircraft

Case A has a relatively slow spool down rate compared to the other cases, leading to

a flight trajectory at a higher altitude. However, the PNLT values are still higher than the other cases up to an observer angle of about 60 degrees due to the fact that this noise emission is for relatively higher fan speeds. The EPNL is thus relatively high in Case A. For Case C, the spool down occurs very rapidly, and the noise is primarily from the cutback region (after spool down ends) at a low altitude, leading to a relatively high EPNL. Case B leads to the lowest EPNL due to lower PNLT values because of a moderate spool down rate.

5.1.3 Effect of Cutback Fan Speed

The degree of thrust reduction and its impact on flyover EPNL is studied in this section for a four-engine commercial transport. In general, lowering the cutback thrust rating lowers noise. This is justified in Figure 54.

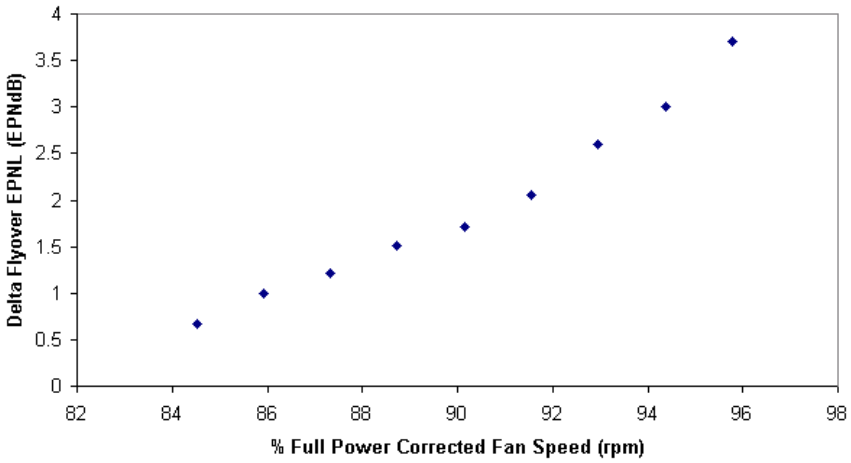

Figure 54: Flyover Noise vs Cutback Fan Speed for Four-Engine Aircraft

5.1.4 Dynamic Cutback Optimization

After understanding the variation of flyover noise with individual design variables for the four-engine aircraft discussed in the previous sections, a dynamic cutback optimization was carried out, varying all the three design variables.

The optimization problem formulation is:

Minimize:	Flyover EPNL	
Varying:	(a) Cutback Initiation Altitude	[689 - 2,000 ft]
	(b) Cutback Corrected Fan Speed	[80% - 100% Full Power Corrected Fan Speed]
	(c) Spool Down Rate	[Delta 0 - 250 rpm/s]
Subject To:	ICAO Annex 16 Volume 1 constraints:	
	(a) Climb Speed:	$(V_2 + 10)\ kts < V_{CLIMB} < (V_2 + 20)\ kts$
	(b) Climb Gradient after Cutback:	$Grad_{AEO} \geq 0.04, Grad_{OEI} \geq 0$

The optimization iteration history is shown below in Figures 55 - 57. The number of GA Generations used was 10, with a GA Population size (runs per Generation) of 20.

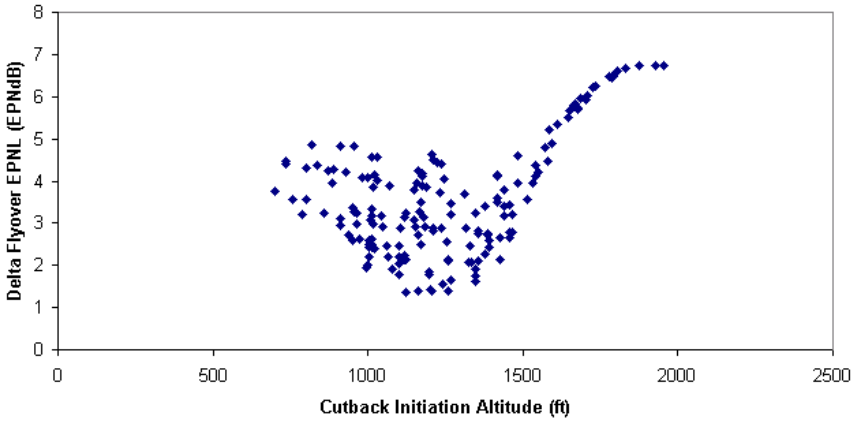

Figure 55: GA Iteration History of Flyover Noise vs Cutback Altitude for Four-Engine Aircraft

From the above graphs, several observations are made:

(a) The Genetic Algorithm optimizer explores the entire design space in search of the global optimum. This is evident from the iteration history graphs, where the flyover EPNL range is around 6 EPNdB. The iteration history for each design variable reveals a similar trend in flyover EPNL variation when compared to the variation seen in the DOE studies. The plot for cutback fan speed reveals a distinct trend - in general, as cutback fan speed decreases (higher thrust reduction), the flyover noise decreases.

(b) The exact optimum in this optimization study is for a cutback initiation altitude of 1,123.84 ft, a corrected cutback fan speed of 83.51% of full power fan speed, and

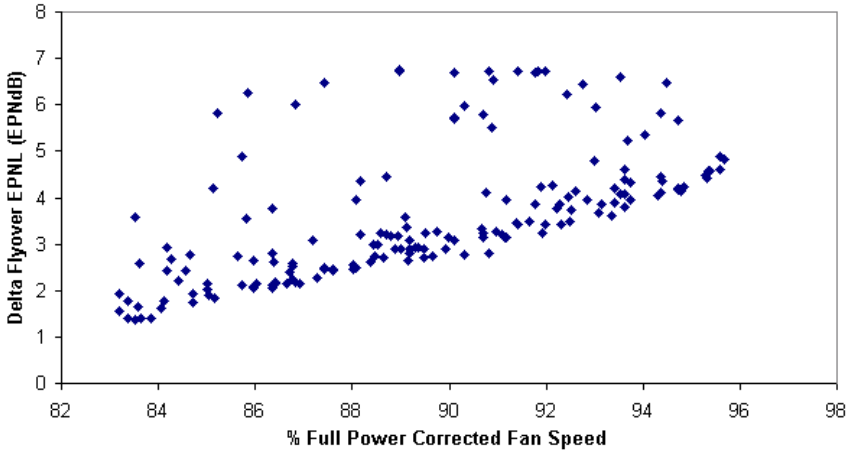

Figure 56: GA Iteration History of Flyover Noise vs Cutback Fan Speed for Four-Engine Aircraft

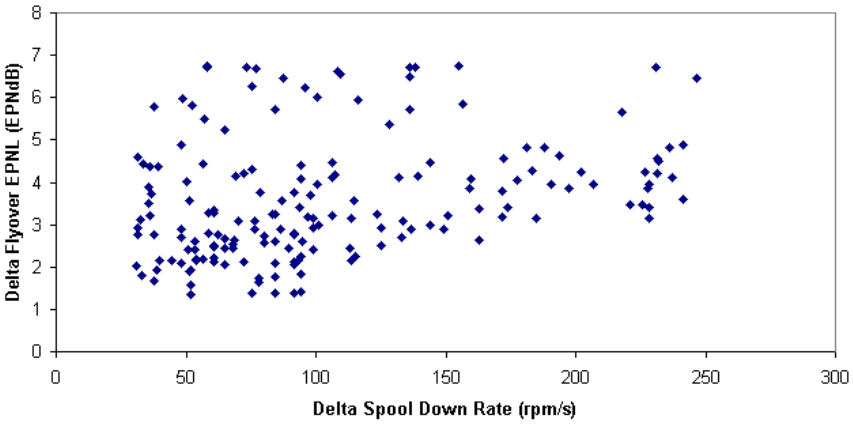

Figure 57: GA Iteration History of Flyover Noise vs Spool Down Rate for Four-Engine Aircraft

a delta spool down rate of 51.81 rpm/s. However, if a tolerance of 0.05 EPNdB is considered (approximately equal to the error in the calculation process), there are multiple optimum points found. The plots suggest that the optimum cutback initiation altitude lies between 1,000 and 1,400 ft, the optimum cutback corrected fan speed between 83% and 84% of full power fan speed, and the optimum delta spool down rate between 50 and 100 rpm/s. During the engine preliminary design process, the designer may wish to analyze these optimum points in detail by studying the acoustic spectra for each case. The selection might depend on other criteria too, such as FAR Part 25 constraints [30], emissions requirements, etc.

(c) In Figure 55, it is seen that when cutback is initiated above 1,850 ft, the flyover EPNL is constant, implying that the noise from the full power region of the flight path alone is responsible for the flyover noise. In other words, the cutback procedure has no effect in mitigating flyover noise.

(d) In Figure 56, it is seen that there are no points for a cutback fan speed less than 83%. This is because the climb gradient constraint is being violated due to a large percentage reduction in engine thrust. An example of a situation where this constraint was violated is shown in Figure 58.

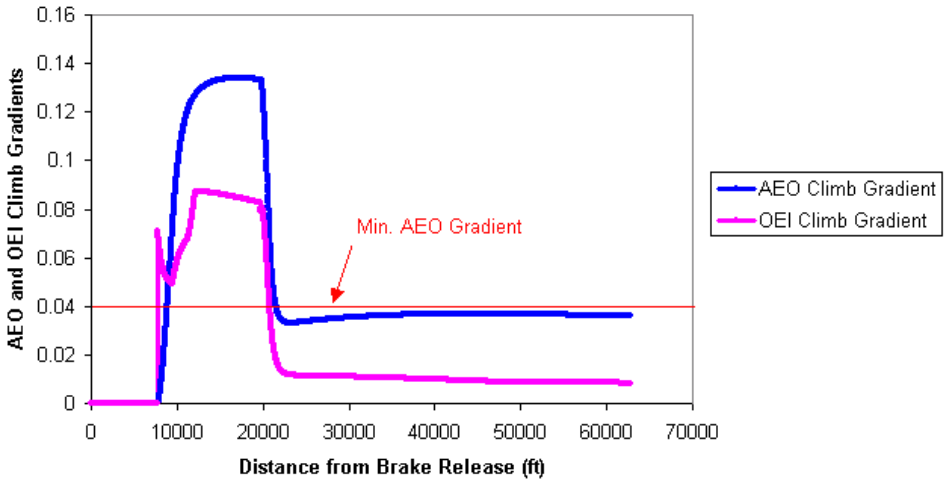

Figure 58: Climb Gradient Not Satisfied for Cutback Fan Speed of 82% for Four-Engine Aircraft

(e) In Figure 57, it is observed that there are relatively a fewer number of points for delta spool down rates in excess of 150 rpm/s. On analyzing the flight path data for cases with high spool down rates, it was seen that the climb velocity constraint was being violated. Thus, acoustic evaluation was not performed for these cases.

The convergence of the GA optimization as a function of Generation count is shown in Figure 59. It is seen that the flyover EPNL does not vary significantly as the generations increase, implying that a near-optimum point was located in the first generation itself.

The optimization process was then carried out with the number of GA Generations

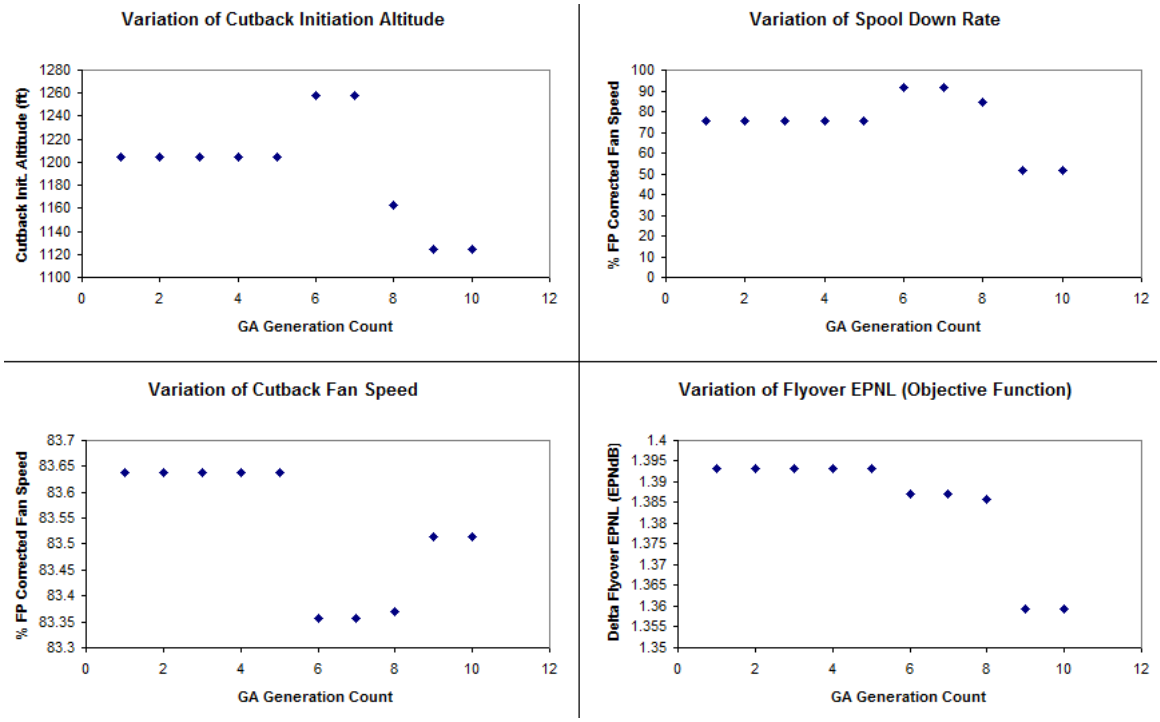

Figure 59: GA Generation History (10 Generations) for Four-Engine Aircraft

increased to 25 and GA Population size reduced to 10 to determine if a lower optimum could be found. The results from this study are shown in Figures 60 - 63.

It is observed that with an increase in the number of generations, the convergence trend of the GA optimizer is well defined. The plots show that the density of points in the optimum region increases as the number of iterations increase.

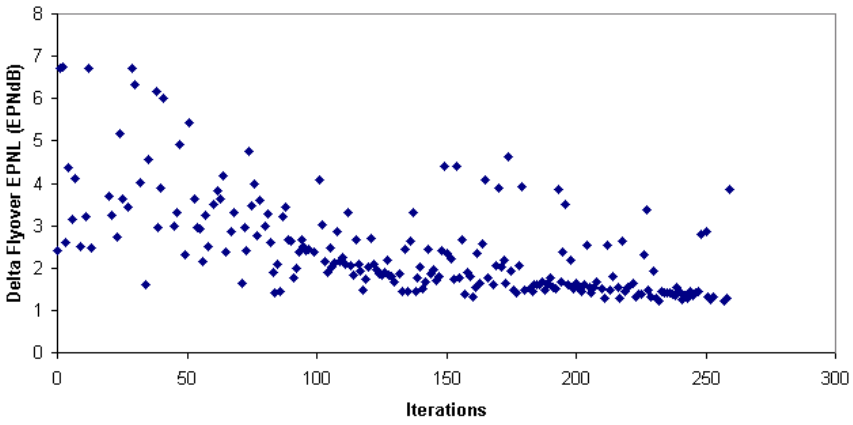

Figure 60: GA (with Increased Generations) Convergence History for Four-Engine Aircraft

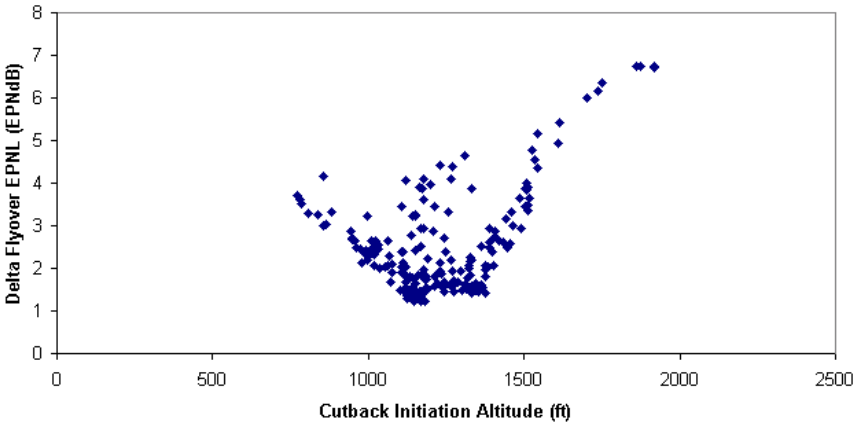

Figure 61: GA (with Increased Generations) Iteration History of Flyover Noise vs Cutback Altitude for Four-Engine Aircraft

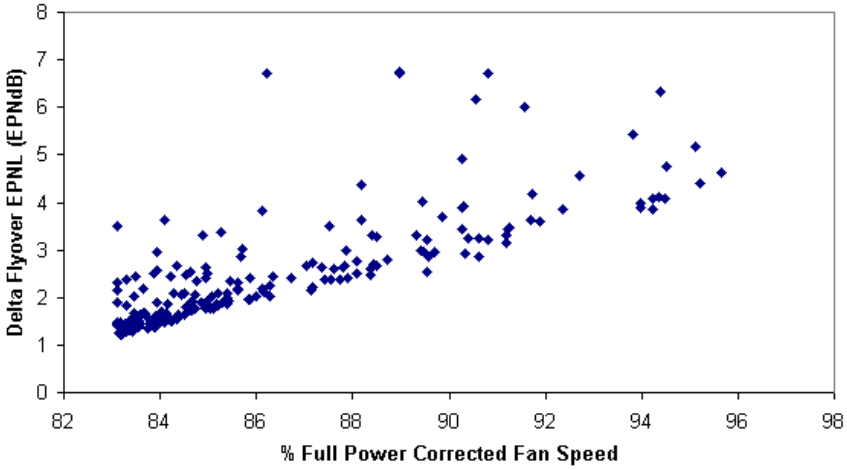

Figure 62: GA (with Increased Generations) Iteration History of Flyover Noise vs Cutback Fan Speed for Four-Engine Aircraft

Figure 64 shows the values of the design variables and the flyover EPNL as a function of GA Generation count in the optimization process. The flyover EPNL decreases significantly in the third Generation, then further decreases in subsequent Generations.

It is seen that the exact optimum is now 0.13 EPNdB less than in the previous case (i.e. with 10 Generations). This new optimum occurs for the following values of the design variables:

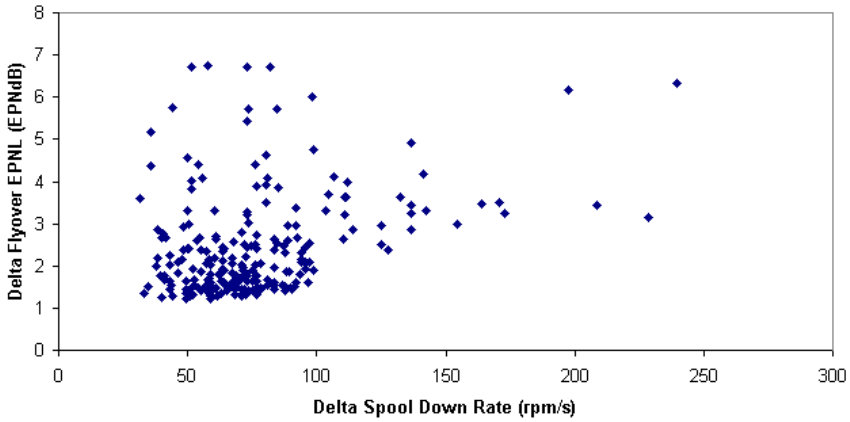

Figure 63: GA (with Increased Generations) Iteration History of Flyover Noise vs Spool Down Rate for Four-Engine Aircraft

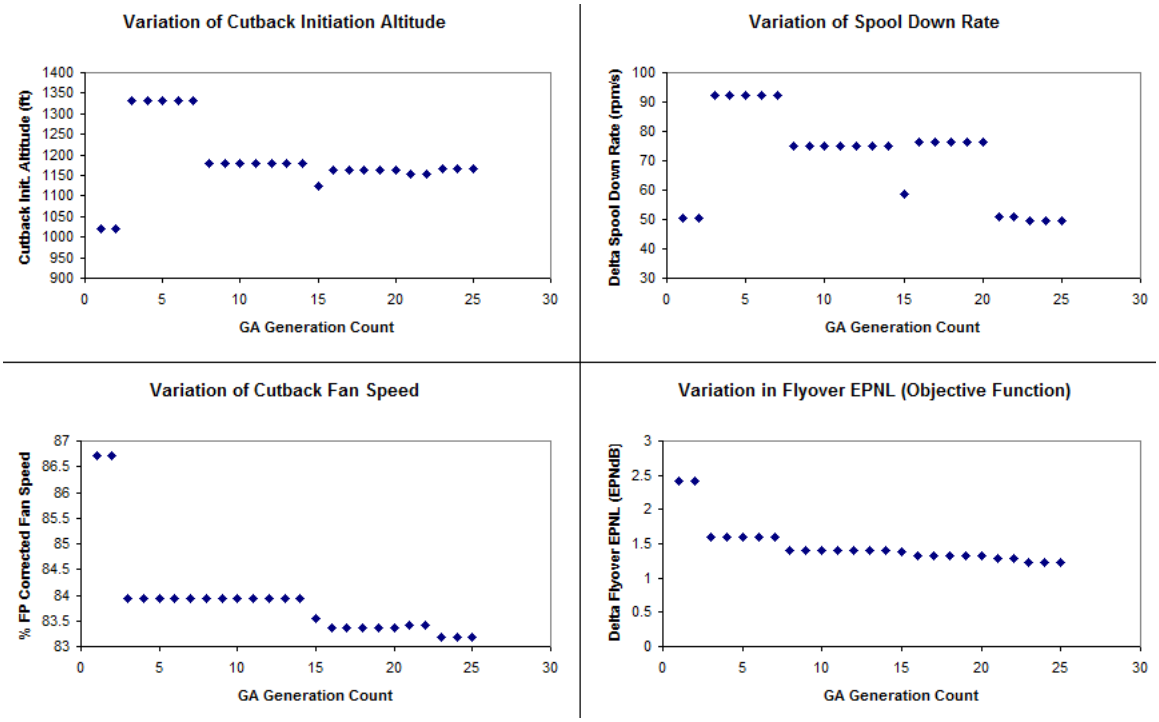

Figure 64: GA Generation History (25 Generations) for Four-Engine Aircraft

Cutback Initiation Altitude: 1,166.7 ft

Corrected Cutback Fan Speed: 83.2% of Full Power Fan Speed

Delta Spool Down Rate: 49.33 rpm/s

However, several optimum points can be found (Table 2) within a small tolerance of 0.05 EPNdB, which is approximately equal to the error in the calculation process. In other

words, different combinations of design variable values can result in the same flyover EPNL, making these design points equally significant or optimal.

Table 2: Multiple Optima for Four-Engine Dynamic Cutback Optimization

S.No.	Cutback Corrected Fan Speed (% Full Power rpm)	Cutback Initiation Altitude (ft)	Delta Spool Down Rate (rpm/s)	Delta EPNL w.r.t. Exact Optimum
1	83.19	1166.7	49.33	0.000
2	83.21	1183.0	58.72	0.007
3	83.13	1146.1	40.18	0.012
4	83.21	1177.7	49.76	0.033
5	83.42	1124.1	44.07	0.047
6	83.42	1152.3	51.04	0.049

The effect of modeling engine spool down is now considered at the exact optimum found. For the same flight path, three cases are considered, each with a different number of linear segments to represent the flight path, and each segment corresponding to a constant fan speed. The noise history for these cases is shown in Figure 65.

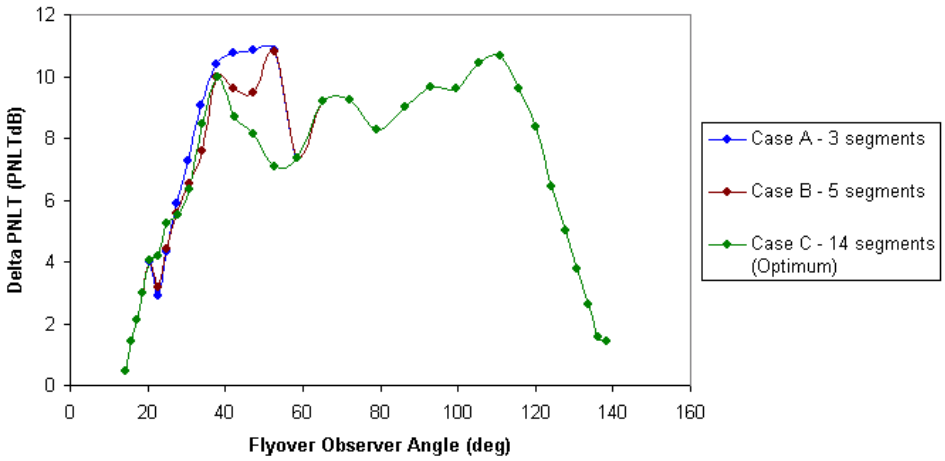

Figure 65: Effect of Modeling Spool Down at Optimum for Four-Engine Aircraft

In Case A, three segments (and therefore three speeds) are considered, where the middle segment represents the spool down region. As the noise from the entire spool down region is now evaluated at a single fan speed, the PNLT values are relatively high as seen in the blue curve. As the number of segments representing spool down increase, lower fan speeds

result in lower PNLT values (Case B, brown curve).

In Case C, with 14 segments as determined automatically in the optimization process based on the spool down rate, the PNLT values in the spool down region are lower, thus leading to a relatively low EPNL. In fact, the EPNL benefit due to modeling spool down at the optimum location is 0.48 EPNdB (+/- 0.05 EPNdB), which is a significant reduction.

It was observed that at the optimum design point, modeling more than 12 flight path segments saw noise reduction leveling off (i.e. within error tolerance of 0.05 EPNdB), as shown in Figure 66. This justifies the selection of 14 segments to model the flight path at the optimum.

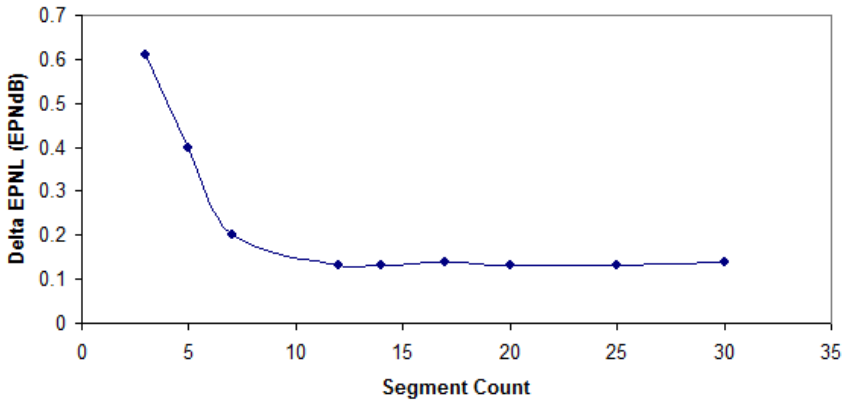

Figure 66: Effect of Segment Count at Optimum for Four-Engine Aircraft

5.2 Dynamic Cutback Study for a Two-Engine Aircraft

Dynamic cutback studies, similar to those in the Section 5.1, were performed for a twin-engine commercial transport in order to compare the effect of dynamic cutback for both configurations.

5.2.1 Effect of Cutback Initiation Altitude

In this study, the cutback initiation altitude is varied between 1,000 and 2,000 ft, while keeping other parameters constant. Thrust is reduced by around 30% during the cutback procedure. The trend observed (shown in Figure 67) is similar to the one seen for the four-engine configuration.

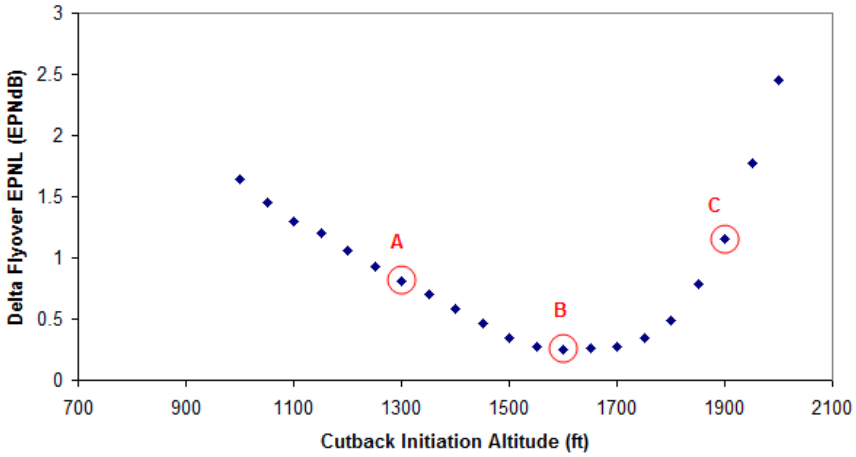

Figure 67: Flyover EPNL vs Cutback Initiation Altitude for Two-Engine Aircraft

As before, three cases - A, B, and C - in the above figure are analyzed. The cutback initiation altitudes for these points are 1,300 ft, 1,600 ft, and 1,900 ft. It can be observed that Case B gives the lowest EPNL. The flight trajectories for these points, along with the corresponding noise emission points are shown in Figure 68. The noise emission points plotted are used in the EPNL computation for each case. As observed for the four-engine aircraft, Case B produces the least flyover EPNL as the noise history comprises of noise emission from the full power, spool down, and cutback flight path regions.

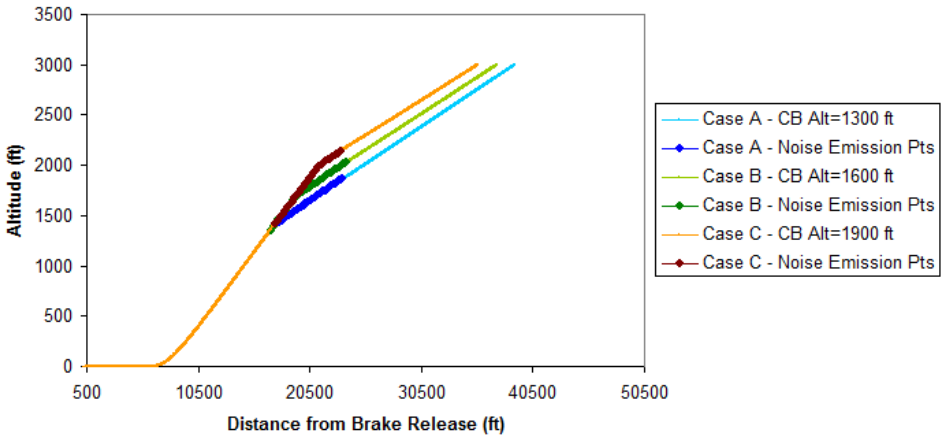

Figure 68: Flight Paths for Different Cutback Altitudes for Two-Engine Aircraft

The noise histories for the three cases, along with that for the full power takeoff are shown in Figure 69. For Case A, the noise emission points that lie within the 10 dB band

below $PNLT_M$ are primarily on the cutback segment of the flight path. This is seen clearly in Figure 68, where the first 10 dB-down PNLT point is from an altitude of 1,411 ft, more than 100 ft above the point where cutback was initiated.

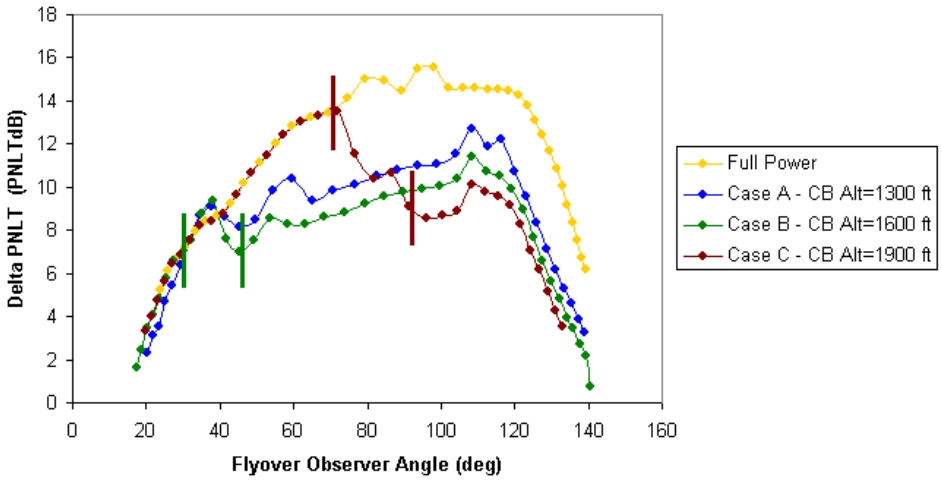

Figure 69: Noise History for Different Cutback Altitudes for Two-Engine Aircraft

Beyond an observer angle of around 40 deg, the PNLT values are higher than those for the optimal case, viz. Case B. This is because the aircraft's flight path post-cutback is closer to the flyover microphone. Consequently, Case A results in a higher flyover EPNL.

In case C, where cutback is initiated at 1,900 ft, the noise within the 10dB-down band is from partly from different regions of the flight path - the full power segment, the spool down region, and the segment after cutback ends. In Figure 68, we see that the noise history for this case coincides with that of the full power takeoff until the cutback initiation point, which is indicated by a vertical bar. The next few PNLT points are from the spool down region, which ends at the second vertical bar. The subsequent PNLT points at the tail end are from the flight path post-cutback. Although the PNLT values at the tail end are lower than those in the optimal case (case B), the initial PNLT values including $PNLT_M$ are significantly higher, and this leads to a higher integrated noise value.

It is observed that even in the optimal case (case B), the noise history contains components from the full power, spool down, and post-cutback flight path regions. However, as cutback is initiated relatively early (at 1,600 ft), the bulk of the noise is from the segment

post-cutback, leading to the lowest integrated noise.

5.2.2 Effect of Spool Down Rate

In this study, the cutback initiation altitude and cutback fan speed are held constant, while the engine spool down rate is varied between a range of 450 rpm/s. The variation of flyover EPNL with spool down rate is shown in Figure 70.

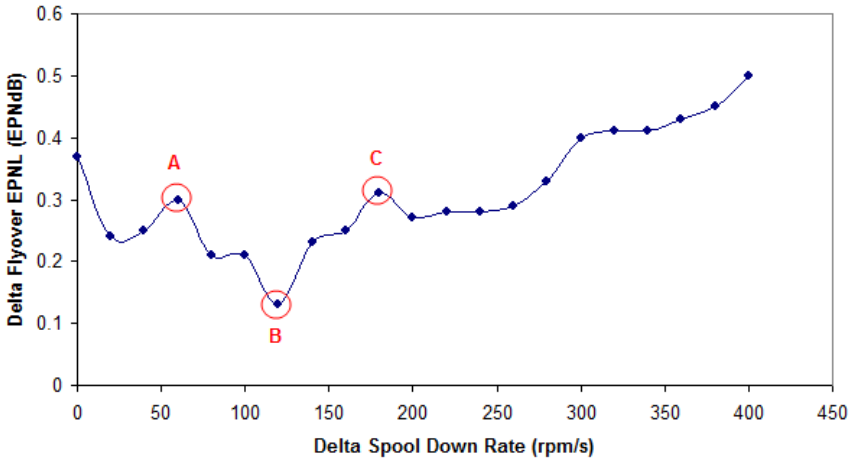

Figure 70: Effect of Modeling Spool Down for Two-Engine Aircraft

It is seen that for delta spool down rates of 60 rpm/s (Case A) and 180 rpm/s (Case C), the EPNL tends to suddenly increase, while on the other hand, there is a drop of about 0.1 EPNdB when the delta spool down rate is increased to 120 rpm/s (Case B). The noise histories for the three cases are analyzed in Figure 53.

For Case A, there is a sharp increase in PNLT values in the spool down region, and this leads to a higher EPNL. While Case B and Case C have similar trends in PNLT variation, Case C has slightly higher PNLT values in the spool down and cutback regions, and this leads to a slightly higher EPNL.

5.2.3 Effect of Cutback Fan Speed

In this study, the effect of corrected cutback fan speed on flyover EPNL is analyzed. Here, the cutback initiation altitude and spool down rate are assumed to be constant. The plot in Figure 72 shows the variation of flyover EPNL.

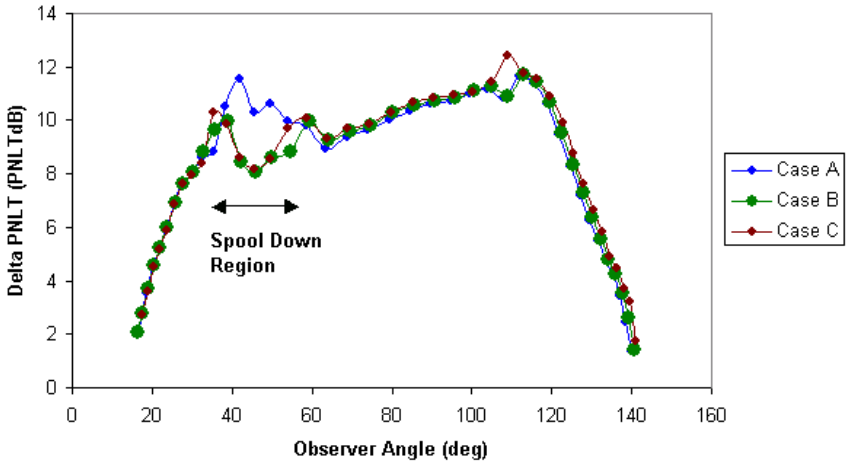

Figure 71: Noise History for Different Spool Down Rates for Two-Engine Aircraft

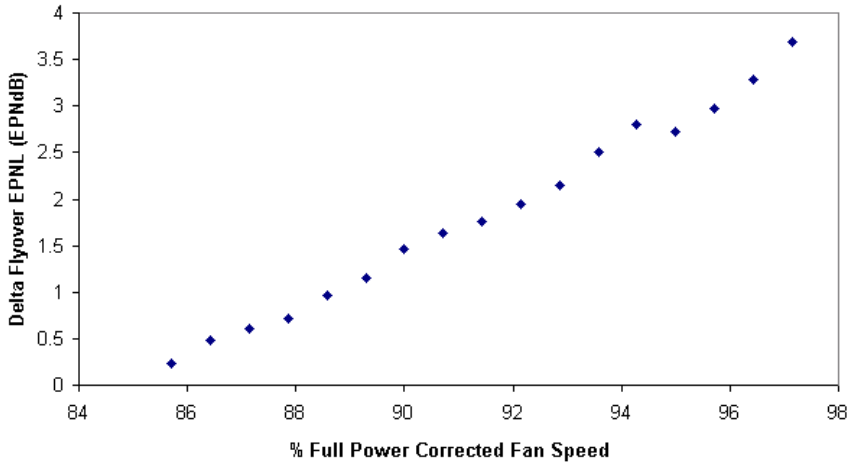

Figure 72: Flyover Noise vs Cutback Fan Speed for Two-Engine Aircraft

This trend is fairly linear, indicating that reducing fan speed can reduce flyover EPNL. A similar trend is observed for the four-engine case (Figure 54).

5.2.4 Dynamic Cutback Optimization

A dynamic cutback optimization is carried out for the two-engine configuration. The optimization problem formulation is:

Minimize:	Flyover EPNL	
Varying:	(a) Cutback Initiation Altitude	[689 - 2,000 ft]
	(b) Cutback Corrected Fan Speed	[85% - 100% Full Power Corrected Fan Speed]

(c) Spool Down Rate [Delta 0 - 450 rpm/s]

Subject To: ICAO Annex 16 Volume 1 constraints:

(a) Climb Speed: $(V_2 + 10)\ kts < V_{CLIMB} < (V_2 + 20)\ kts$

(b) Climb Gradient after Cutback: $Grad_{AEO} \geq 0.04, Grad_{OEI} \geq 0$

The optimization iteration history is shown below in Figures 74 - 76.

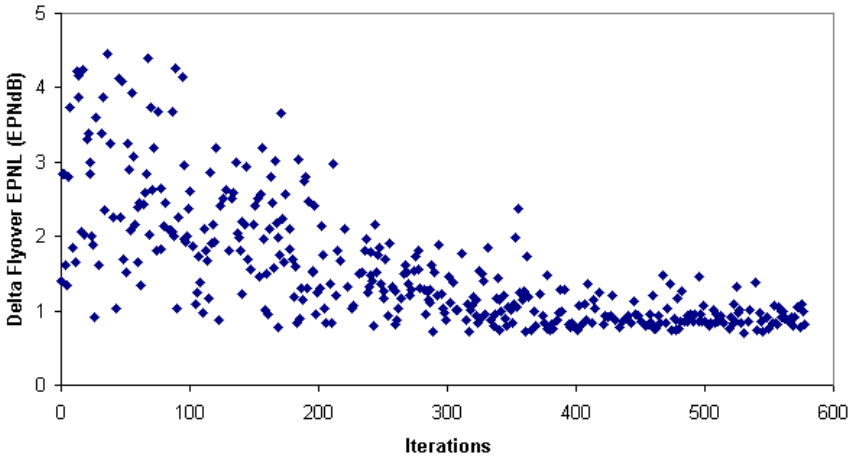

Figure 73: GA Convergence History for Two-Engine Aircraft

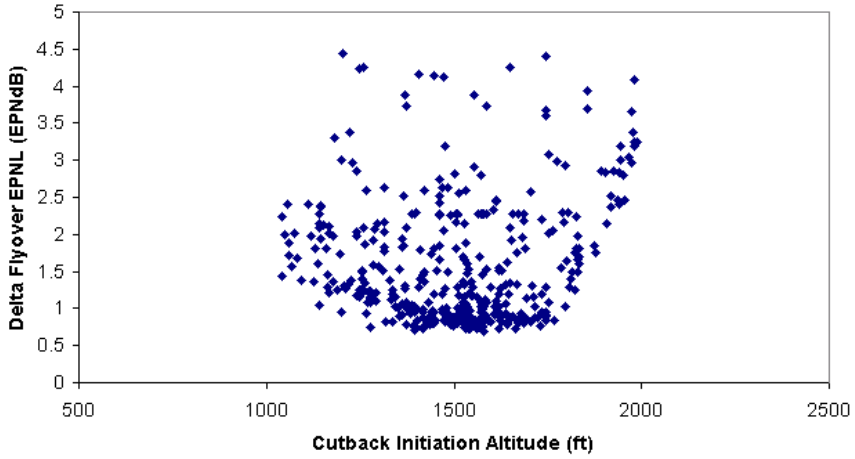

Figure 74: GA Iteration History of Flyover Noise vs Cutback Altitude for Two-Engine Aircraft

The GA optimization history as a function of Generation count for the two-engine dynamic cutback optimization is shown in Figure 77.

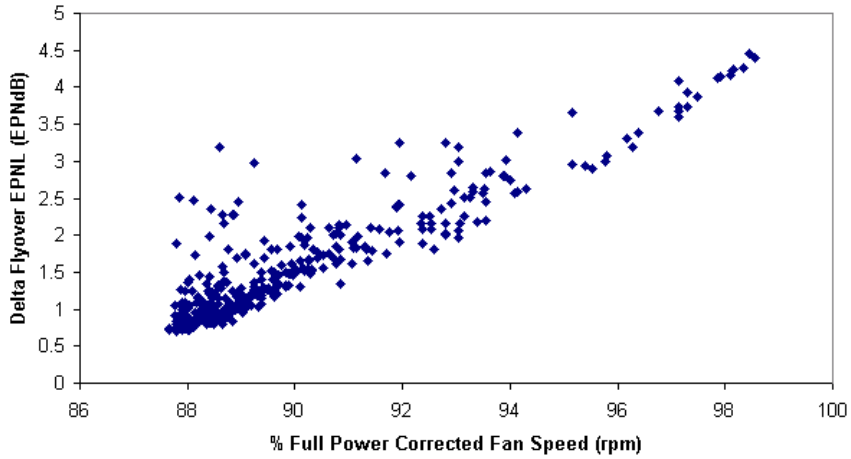

Figure 75: GA Iteration History of Flyover Noise vs Cutback Fan Speed for Two-Engine Aircraft

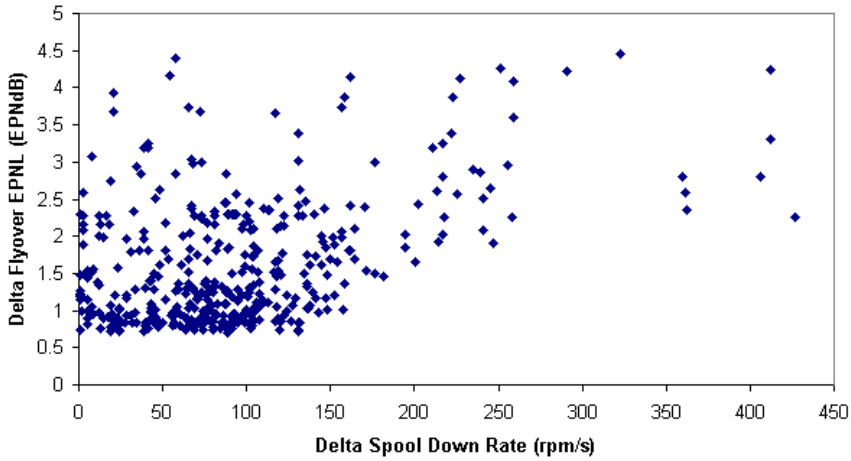

Figure 76: GA Iteration History of Flyover Noise vs Spool Down Rate for Two-Engine Aircraft

The exact optimum found for this two-engine optimization study was for the following values of the design variables:

Cutback Initiation Altitude: 1,579.1 ft

Corrected Cutback Fan Speed: 87.8% of Full Power Speed

Delta Spool Down Rate: 88.93 rpm/s

Again, if a small tolerance of 0.05 EPNdB is considered, there were a total of 11 optima found for different values of the design variables as shown in Table 3.

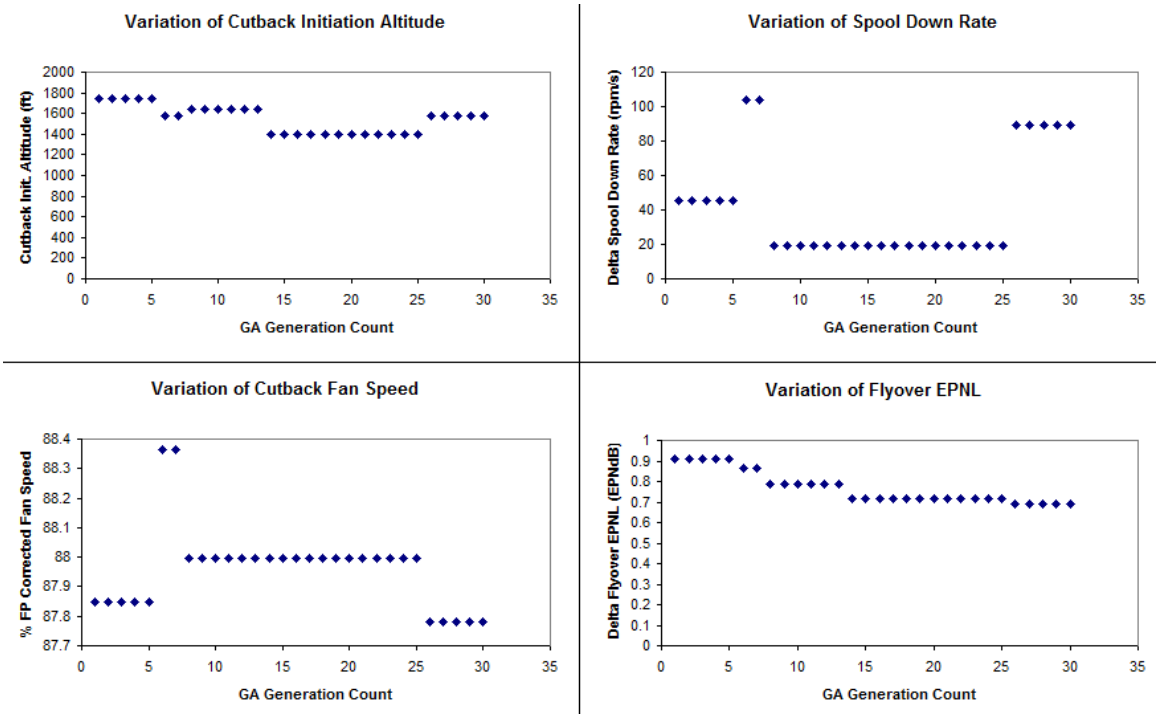

Figure 77: GA Generation History for Two-Engine Aircraft

Table 3: Multiple Optima for Two-Engine Dynamic Cutback Optimization

S.No.	Cutback Corrected Fan Speed (% Full Power rpm)	Cutback Initiation Altitude (ft)	Delta Spool Down Rate (rpm/s)	Delta EPNL w.r.t. Exact Optimum
1	87.78	1579.1	88.93	0.000
2	88.00	1396.8	19.01	0.027
3	88.03	1663.9	39.07	0.034
4	87.89	1416.3	24.17	0.036
5	87.66	1543.0	131.17	0.038
6	87.66	1619.8	131.17	0.039
7	87.98	1530.1	80.42	0.041
8	87.88	1562.1	63.39	0.043
9	87.94	1539.8	69.24	0.044
10	88.03	1276.8	0.63	0.047
11	87.76	1529.1	120.03	0.048

If the flight path determined at the optimum is evaluated with a different number of segments (as done for the four-engine study), it is seen that the 10-segment case (Case C in Figure 78) gives the lowest EPNL, a benefit of 0.22 EPNdB (+/- 0.05 EPNdB) over the

3-segment case.

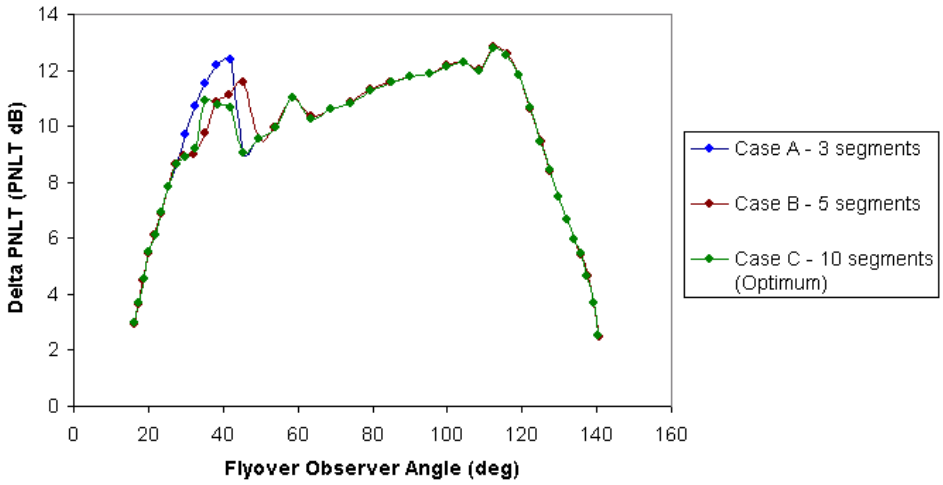

Figure 78: Effect of Modeling Spool Down at Optimum for Two-Engine Aircraft

It is seen that at the design optimum, the noise reduction levels off for segment counts of 7 or more. That is, no significant noise reduction (greater than 0.05 EPNdB) is seen. The selection of 10 segments by the optimizer for minimum noise is thus justified. This trend, shown in Figure 79, is similar to that of the four-engine case.

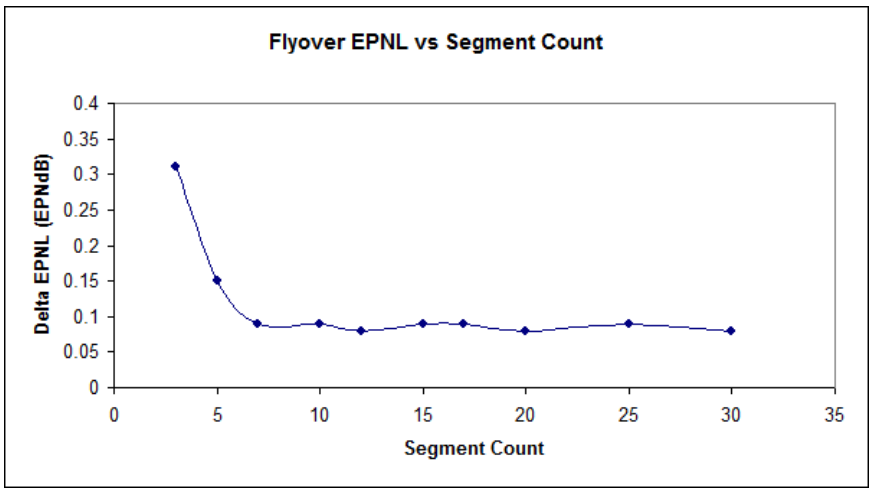

Figure 79: Effect of Segment Count at Optimum for Two-Engine Aircraft

Based on the dynamic cutback optimization studies carried out two configurations, the following comparison (Table 4) can be made.

Table 4: Comparison of Dynamic Cutback Optimization Results

S.No.	Quantity / Parameter	Four-Engine Aircraft	Two-Engine Aircraft
1	Cutback initiation altitude	Global optimum at 1,166.7 ft	Global optimum higher by more than 400 ft, at 1,579.1 ft
2	Cutback fan speed	17% of full power rpm at optimum	12% of full power rpm at optimum (lower degree of cutback)
3	Spool down rate	Relatively lower delta value of 50 rpm/s	Relatively higher delta value of 90 rpm/s
4	Climb gradients	Satisfied, min. AEO gradient constraint of 0.04 more prohibitive that min. OEI gradient constraint of 0 during optimization	Satisifed, OEI gradient constraint more prohibitive
5	Climb velocity	Satisfied, within $V_2 + 10$ and $V_2 + 20kt$	Satisfied, within $V_2 + 10$ and $V_2 + 20kt$
6	Max EPNL reduction due to spool down	0.5 EPNdB	0.35 EPNdB
7	EPNL reduction due to spool down at optimum	0.48 EPNdB	0.22 EPNdB
8	EPNL reduction w.r.t full power takeoff	5.51 EPNdB	4.52 EPNdB

The flyover noise reduction due to dynamic cutback optimization for both the four-engine and two-engine configurations was compared against real test results, and found to be accurate.

5.3 Robust Optimization

From the optimization studies in Sections 5.1.4 and 5.2.4, it is seen that the deterministic optimum lies at the boundary of the constraint corresponding to minimum cutback fan speed. Below this fan speed, the aircraft will not have enough power to satisfy the ICAO Annex 16 climb requirements. Therefore, any perturbation in cutback fan speed at the optimum has a 50% probability of violating this requirement.

A probabilistic analysis or uncertainty assessment was carried out at the deterministic optimum by performing a DOE sampling (with 50 DOE points) using the Optimal Latin

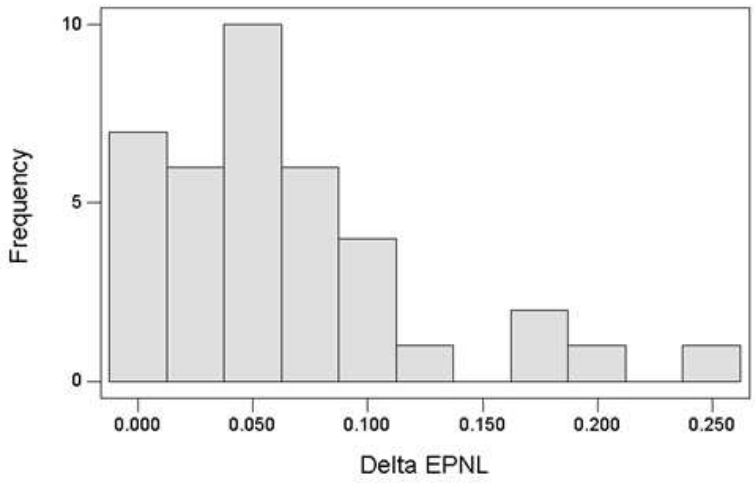

Figure 80: Flyover EPNL Histogram at Deterministic Optimum

Hypercube (OLH) technique. The OLH technique ensures a uniform sampling across the region of interest, with a user-specified number of DOE points. The EPNL was then evaluated at these DOE points provided the climb gradient and velocity constraints were satisfied. This plot of delta EPNL values is shown in Figure 80. It is seen that the plot is skewed to the right as the EPNL was not evaluated at points to the left of 0.0 since the climb gradient constraint failed at these points. This means that perturbations in the cutback fan speed at the deterministic optimum will lead to an infeasible solution.

The objective of the robust optimization is to find that point in the design space where perturbations in the design variables do not violate constraints, and where the objective function value (flyover EPNL) is below a specified maximum limit. The robust optimizer used in this study is based on a genetic algorithm. The inputs to the optimizer include the standard deviation on the design variables, the lower and upper bounds of the variables, the upper bound on the objective function value, and a desired probability of defect, $p(d)$ on the objective function [31]. At each design point generated in the optimization process, the $p(d)$ is estimated by generating a normal distribution around this design point. The standard deviation assumed for each design variable in this problem is 0.5% of the deterministic optimum value. The optimizer ultimately locates the optimal design point that minimizes the objective function (flyover EPNL) and which also satisfies the specified $p(d)$.

For the four-engine configuration studied in Section 5.1, the exact deterministic global optimum occurs for a cutback initiation altitude of 1,166.74 ft, a corrected cutback fan speed of 83.2% of full power speed, and a delta spool down rate of 49.33 rpm/s.

The lower bound on the corrected fan speed for the robust optimization was set at a value of 84.4%, which corresponds to 3 standard deviations (3σ) away from the deterministic optimum value. This was done to minimize the chances of the climb gradient constraint being violated.

The robust optimization problem was formulated as follows.

Minimize: Flyover EPNL

Lower Spec Limit: None

Upper Spec Limit: (E_{DET} + 0.7) EPNdB

Varying: (a) Cutback Initiation Altitude [689 - 2,000 ft]

Std Dev: 5.8 ft

(b) Cutback Corrected Fan Speed [84.4% - 88% Full Power Corrected Fan Speed]

Std Dev: 0.4% Full Power Corrected Fan Speed

(c) Spool Down Rate [Delta 0 - 450 rpm/s]

Std Dev: 0.5% of Mean

Subject To: $p(d)$ of Flyover EPNL < 0.02

Here, E_{DET} is the value of the flyover EPNL at the deterministic optimum. The design space for robust optimization is shrunk based on the location of the deterministic optimum.

The iteration history of the robust optimization is shown in Figures 81 - 83.

The iteration history reveals that the robust optimizer explores the design space performing perturbations at various locations to quantity the probability of defect. A high penalty value is set if the specified upper bound on EPNL is not satisfied.

The robust optimum was found at the following design point:

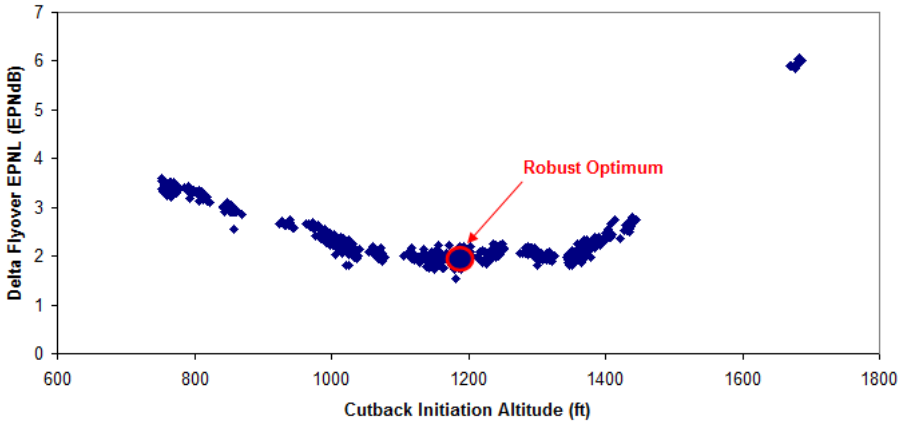

Figure 81: Robust GA Iteration History of Flyover Noise vs Cutback Altitude

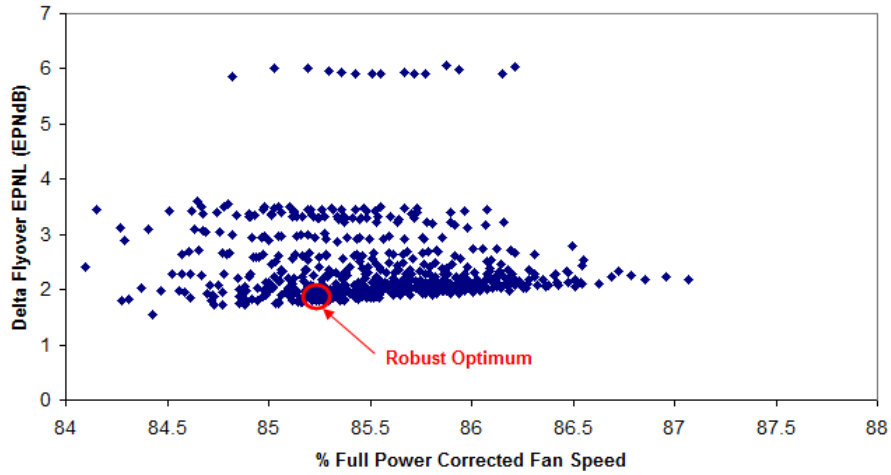

Figure 82: Robust GA Iteration History of Flyover Noise vs Cutback Fan Speed

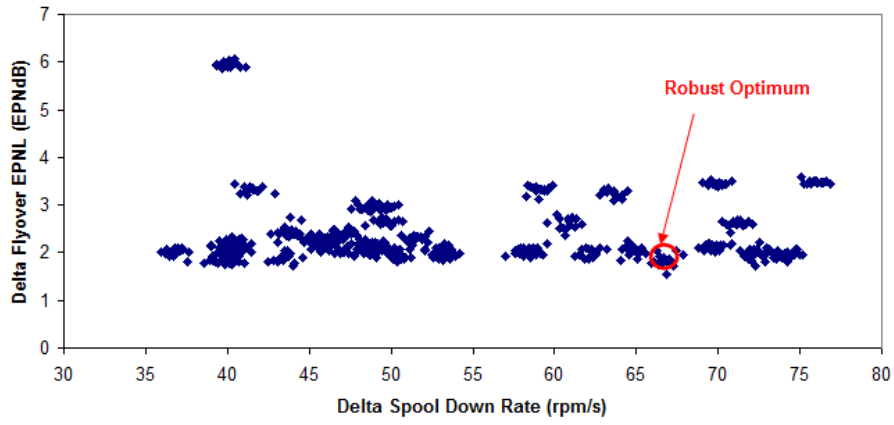

Figure 83: Robust GA Iteration History of Flyover Noise vs Spool Down Rate

Cutback Initiation Altitude = 1,188.11 ft

Corrected Cutback Fan Speed = 85.22% of Full Power Fan Speed

Spool Down Rate = Delta 66.8 rpm/s

It was observed that the flyover EPNL at this point was (E_{DET} + 0.54) EPNdB, less than the upper bound (E_{DET} + 0.7) EPNdB specified. However, the $p(d)$ was 0.06, 4% higher than the specified $p(d)$. Several sample points were generated around this robust optimum, and the EPNL was evaluated at these points. The histogram for this case is shown in Figure 84. It is seen that a normal distribution accurately captures the variation in EPNL.

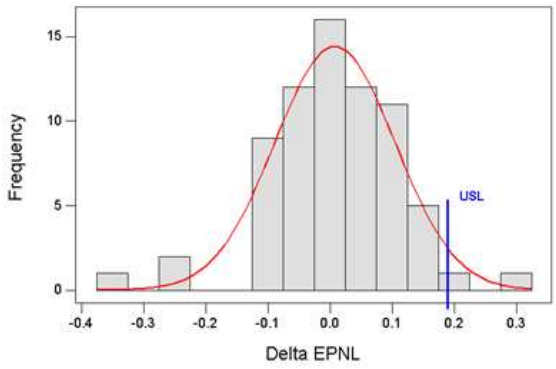

Figure 84: Flyover EPNL Histogram at Robust Optimum

The shift in the mean EPNL value from the deterministic to the robust optimum is 0.56 EPNdB, and is illustrated below in Figure 85. Peturbations in the design variables, especially the cutback fan speed, at the new optimum do not violate constraints, justifying that this is a "robust" optimum.

Similar probabilistic studies were carried out on the instantaneous cutback model. It was observed that the deterministic optimum was again on the constraint boundary corresponding to minimum climb gradient, with a failure probability of 50%. The robust optimization process was then applied as before to determine the optimum design point that is relatively insensitive to variations in design variables. The shift in the design optimum is shown in Figure 86.

The impact of robustness for the instantaneous cutback model is an increase of 0.59

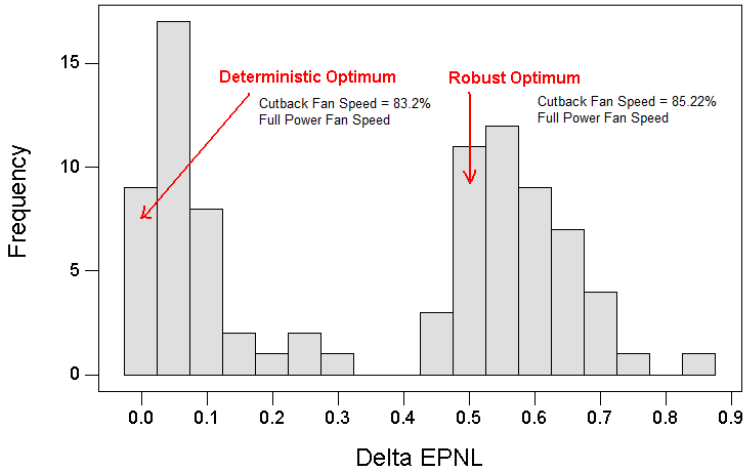

Figure 85: Shift in Mean EPNL as a Result of Robust Optimization on Dynamic Cutback Model

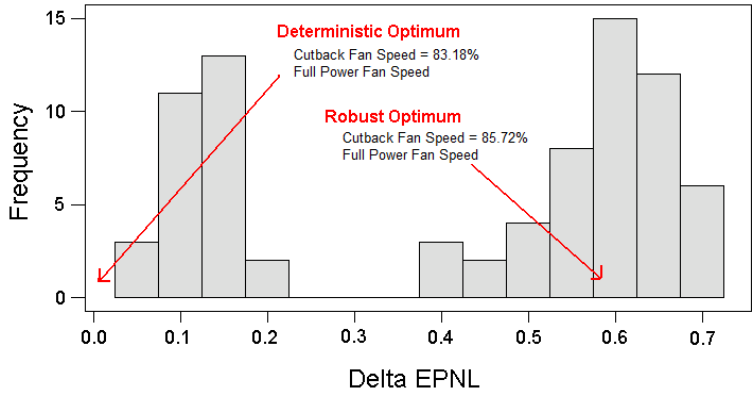

Figure 86: Shift in Mean EPNL as a Result of Robust Optimization on Instantaneous Cutback Model

EPNdB in the flyover EPNL. It is noted that this increase is comparable to the 0.54 EPNdB increase in EPNL for the dynamic cutback model. This shows that noise reduction due to dynamic cutback relative to instantaneous cutback (approx. 0.5 EPNdB for the four-engine configuration) is maintained whether deterministic or robust optimization is applied.

CHAPTER VI

CONCLUSIONS AND RECOMMENDATIONS

6.1 Conclusions

As seen in the literature survey, thrust cutback is a well-known procedure that has been used since the introduction of the turbojet for reducing community noise. With reduced thrust, fan and jet noise - which are the primary contributors to overall noise - are significantly reduced. During engine preliminary design, it is desired to minimize noise levels to improve the cumulative margin with respect to ICAO Chapter 4 (FAR Stage 4) limits. In this respect, the modeling and optimization of dynamic cutback plays an important role. While it was observed that several multi-disciplinary frameworks exist in industry and academia that make use of acoustic models to evaluate certification noise levels, very limited information regarding the modeling of the spool down was found.

One of the goals of this research work was to determine if this spool down modeling is advantageous or not, and a prediction model using proprietary acoustic tools was developed for this purpose. It is observed that the noise benefit compared to an instantaneous thrust cutback is between 0.3 and 0.5 EPNdB, which is important to consider during preliminary design of an engine.

The thesis also develops an optimization process to determine the ideal conditions for implementing a dynamic cutback for least flyover noise. This process was applied for a four-engine configuration, and it was observed that at the global minimum, the flyover EPNL is less by 5.51 EPNdB than the full power takeoff case without cutback.

This might be advantageous during a noise certification program where optimization studies can be performed to aid in the building or analysis of analytically derived Noise-Power-Distance (NPD) databases. The NPD data, along with noise data from actual flight tests, can be used for demonstrating compliance with Chapter 4 / Stage 4 regulations.

The hypotheses stated in Chapter 1 are now reexamined in order to determine their

validity, and to draw conclusions.

Hypothesis 1:

The modeling of engine spool down in a cutback simulation leads to a lower Effective Perceived Noise Level at the flyover certification point.

As seen in the parametric and optimization studies conducted for two different aircraft configurations, modeling of engine spool down during cutback does lower the EPNL at the flyover point. The exact reduction, however, depends on factors that include the cutback initiation altitude and the degree of cutback. It is noted that for the four-engine aircraft, the EPNL benefit was 0.5 EPNdB relative to instantaneous cutback for a cutback initiation altitude of 1,100 ft and a fan speed reduction of 88% corrected full power fan speed. At the optimum found from dynamic cutback optimization, a reduction of 0.48 EPNdB is seen when the number of spool down segments is high, further justifying the importance of modeling spool down.

For the two-engine configuration, though flyover EPNL reduced due to modeling the spool down, the reduction was less as compared to the four-engine case. The maximum reduction was 0.35 EPNdB, and 0.22 EPNdB at the optimum, both relative to instantaneous cutback.

Hypothesis 2:

There could be more than one combination of optimum cutback altitude and spool down behavior for a given aircraft that results in minimum flyover EPNL, while also satisfying the ICAO Annex 16 Volume 1 airworthiness requirements.

Dynamic cutback optimization results for the two configurations considered showed that although there is a single global optimum, there may be multiple optima when a small tolerance of 0.05 EPNdB (approximately equal to the modeling error) is considered. All these optima satisfied the ICAO Annex 16 Volume 1 requirements including the minimum cutback initiation altitude, and constraints on climb speed and climb gradients. The use of a genetic algorithm optimizer aided in the justification of this hypothesis.

Hypothesis 3:

The robust optimum has a higher flyover EPNL than the optimum found using regular

optimization techniques.

It was observed that the deterministic optimum found in the GA optimization was not robust as it was very close to the constraint boundary for minimum climb gradient. Chapter 5 discusses the robust optimization formulation that was applied to determine the robust optimum for the four-engine case. An increase of 0.54 EPNdB in the mean value of the optimum was seen, justifying the hypothesis. Moreover, robust optimization on the instantaneous cutback model showed a similar increase of 0.59 EPNdB.

6.2 Recommendations

The dynamic cutback optimization process described in this thesis demonstrates the fact the noise levels due to dynamic cutback can be significantly lowered when compared to a full power takeoff, and also the fact that modeling engine spool down leads to improved noise margins. Although only a few key variables were considered, the optimization framework can incorporate additional design variables as needed.

During the preliminary design stage, tradeoff studies between noise, emissions, fuel burn, weights, and performance are made while designing engine or airframe components. The simulation model developed as part of this study could be used as part of larger multi-disciplinary optimization frameworks as discussed to simultaneously optimize for one or more objectives.

The genetic algorithm optimization process can be quite time-consuming since many iterations are required before the algorithm converges to an optimum. One approach to mitigate this problem could be do a DOE sampling across the design space and determine the region where the optimum might exist. While the cutback fan speed should be as low as possible for minimum noise, this is not true for the cutback initiation altitude and spool down rate. Engineering judgment and prior knowledge of trends for similar configurations can be applied to shrink the design space.

Before beginning a dynamic cutback study, the flight path model would need to be validated; either based on flight test data, or based on FAR Part 25 performance requirements. The validation would involve checking the balanced field length, climb speed, and climb

gradients. From a pure acoustics perspective, these might not be important. However, if dynamic cutback optimization studies are being performed for a certification program, such validation would be essential. It is therefore recommended that the FAR Part 25 constraints [30] be considered along with the ICAO Annex 16 constraints.

As far as engine spool down simulation is concerned, alternate models for thrust reduction (such as a sine wave) could be considered depending on data from transient simulation runs to determine if any additional noise benefit can be gained. The transient cycle model itself could be used for more accurate predictions.

The robust optimization study showed that even though a robust optimum exists, the deviation from the deterministic mean offsets the small advantage gained by modeling the spool down. However, probabilistic analyses and robust optimization studies would typically be performed only in special cases.

The dynamic cutback optimization model offers the potential for the acoustics designer to better understand the design space and appreciate how flyover noise varies as a function of fan speeds, altitudes, and spool down rates. Detailed investigations into variations in engine component noise spectra during a dynamic cutback might be worth undertaking.

REFERENCES

[1] International Civil Aviation Organization (ICAO), *ICAO Environmental Report 2007.* [Online]. Available: `http://www.icao.int/env/pubs/Env_Report_07.pdf`. [Accessed Oct. 31, 2009].

[2] W. L. Willshire, Jr and D. G. Stephens, "Aircraft noise technology for the 21st century," in *NOISE-CON 98,* 1998, pp. 7-22.

[3] "National research and development plan for aviation safety, security, efficiency, and environmental compatibility," National Science and Technology Council Subcommittee on Transportation Research and Development, November 1999.

[4] D. L. McGregor, "Boeing Environmental Projects," March 22, 2007. [Online]. Available: `http://www.tailoredarrivals.com/Assets/tailored_assets/96308-07_mcgregor_001.ppt`. [Accessed: July 26, 2009].

[5] International Civil Aviation Organization (ICAO), *Aircraft Noise,* ICAO Annex 16, Environmental Protection, 5th ed., vol. 1. Effective 20 Nov. 2008.

[6] International Civil Aviation Organization (ICAO), *Environment Technical Manual on the Use of Procedures in the Noise Certification of Aircraft,* ICAO, Apr. 2007.

[7] Federal Aviation Administration. Department of Transportation, *Noise standards: Aircraft type and airworthiness certification,* Code of Federal Regulations, Title 14, Part 36.

[8] A. Depitre, "Aircraft Noise Certification: History/Development," presented at Noise Certification Workshop, Montreal, Oct. 2004. [Online]. Available: `http://www.icao.int/icao/en/env/NoiseCertification_04/BIPs/bip2_01.pdf`. [Accessed: Aug. 17, 2009].

[9] J. Friedrich, D. McGregor, and D. Weigold, "Quiet Climb System - Advanced Avionics for Quiet Operations,", Aero magazine, Jan. 2003. [Online]. Available: `http://www.britflight.com/wingfiles/performance/quietclimb.pdf`. [Accessed: Aug. 17, 2009].

[10] N. E. Antoine, I. M. Kroo, "Aircraft optimization for minimal environmental impact," *Journal of Aircraft,* vol. 41, no. 4, pp. 790-797, 2004.

[11] W. D. Grantham and P. M. Smith, "Development of SCR aircraft takeoff and landing procedures for community noise abatement and their impact on flight safety," NASA Technical Reports, March 1980. [Online]. Available: `http://ntrs.nasa.gov/archive/nasa/casi.ntrs.nasa.gov/19810009471_1981009471.pdf`. [Accessed: March 19, 2009].

[12] D. Crichton, E. de la Rosa Blanco, and T. R. Law, "Design and operation for ultra low noise take-off," in *45th AIAA Aerospace Sciences Meeting and Exhibit,* Reno, NV, Jan. 2007.

[13] M. J. T. Smith, *Aircraft Noise.* Cambridge, England: Cambridge University Press, 1989.

[14] N. E. Antoine and I. M. Kroo, "Optimizing aircraft and operations for minimum noise," in *AIAA Aircraft Technology, Integration, and Operations (ATIO) Technical Forum,* Los Angeles, CA, Oct. 2002.

[15] M. D. Dahl, "A process for assessing NASA's capability in aircraft noise prediction technology," in *14th AIAA/CEAS Aeroacoustics Conference,* Vancouver, British Columbia Canada, May 2008.

[16] M. R. Kirby and D. N. Mavris, "The Environmental Design Space," in *26th International Congress of the Aeronautical Sciences,* Anchorage, AK, Sep. 2008.

[17] J. L. Younghans, R. J. Luffy, J. T. Brewer, and D. R. Wallace, *14th International Symposium on Air Breathing Engines (ISABE),* Florence, Italy, Sep. 1999.

[18] General Electric (GE) Aircraft Engines, "System study - Technology assessment and prioritizing," NASA Technical Reports, Oct. 2005. [Online]. Available: `http://gltrs.grc.nasa.gov/reports/2005/CR-2005-213972.pdf`. [Accessed: Nov 23, 2009].

[19] Federal Aviation Administration (FAA). U.S. Department of Transportation, *Advisory Circular No. 91-53A, Noise Abatement Departure Profiles,* FAA, July 1993.

[20] J. B. Ollerhead, D. P. Rhodes, and D. J. Monkman, "Review of the departure noise limits at Heathrow, Gatwick and Stansted airports: Effects of take-off weight and operating procedure on noise displacement," R&D Report 9841, UK Civil Aviation Authority, March 1999. [Online]. Available: `http://www.caa.co.uk/docs/33/ercd9841.pdf`. [Accessed: June 4, 2009].

[21] J. Olmstead, G. Fleming, J. Gulding, C. Roof, P. Gerbi, and A. Rapoza, *Integrated Noise Model (INM) Version 6.0 Technical Manual,* No. FAA-AEE-02-01, Jan. 2002.

[22] S. J. Hebly and H. G. Visser, "Advanced noise abatement departure procedures: Custom optimized departure profiles," in *AIAA Guidance, Navigation and Control Conference and Exhibit,* Honolulu, HI, Aug. 2008.

[23] J. P. B. Clarke, "Systems Analysis of Noise Abatement Procedures Enabled by Advanced Flight Guidance Technology," *Journal of Aircraft*, vol. 37, no. 2, pp. 266-273, 2000.

[24] H. G. Visser and R. A. A. Wijnen, "Optimization of noise abatement departure trajectories," *Journal of Aircraft,* vol. 38, no. 4, pp. 620-627, 2001.

[25] E. Torenbeek, *Synthesis of Subsonic Airplane Design.* Delft, The Netherlands: Delft University Press and Kluwer Academic Publishers, 1982.

[26] D. H. Perry, *The Airborne Path During Take-off for Constant Rate-of-Pitch Manoeuvres,* vol. 1042, Aeronautical Research Council. London, England: Her Majesty's Stationery Office, 1969.

[27] D. P. Raymer, *Aircraft Design: A Conceptual Approach,* 3rd ed. Reston, VA: American Institute of Aeronautics and Astronautics, 2006, p. 541.

[28] G. N. Vanderplaats, *Numerical Optimization Techniques for Engineering Design,* 4th ed. Colorado Springs, CO: Vanderplaats Research and Development, Inc., 2005.

[29] D. E. Goldberg, *Genetic Algorithms in Search, Optimization and Machine Learning.* Reading, MA: Addison-Wesley, 1989.

[30] Federal Aviation Administration. Department of Transportation, *Airworthiness standards: Transport category airplanes,* Code of Federal Regulations, Title 14, Part 36.

[31] V. Ramanath and G. Wiggs, "DACE Based Probabilistic Optimization of Mechanical Components" in *ASME Turbo Expo,* Barcelona, Spain, May 2006.